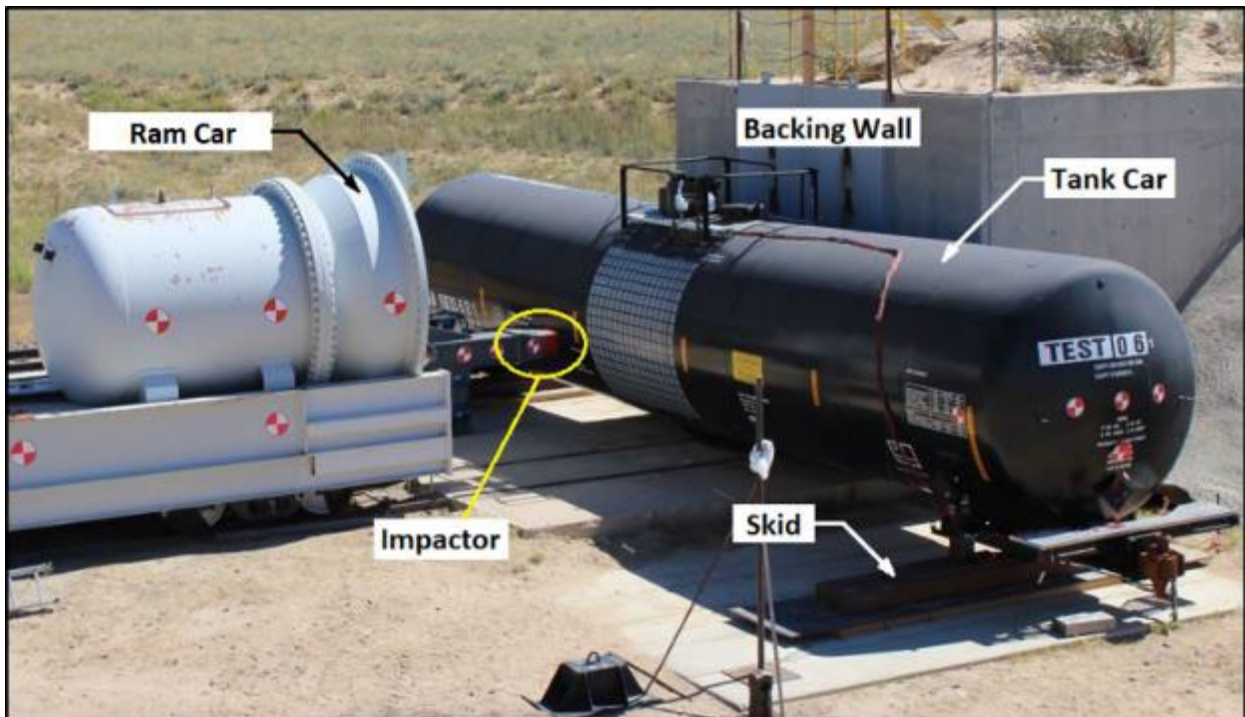




Review of Tank Car Side Impact Test Research and Analyses of 2007–2019



NOTICE

This document is disseminated under the sponsorship of the Department of Transportation in the interest of information exchange. The United States Government assumes no liability for its contents or use thereof. Any opinions, findings and conclusions, or recommendations expressed in this material do not necessarily reflect the views or policies of the United States Government, nor does mention of trade names, commercial products, or organizations imply endorsement by the United States Government. The United States Government assumes no liability for the content or use of the material contained in this document.

NOTICE

The United States Government does not endorse products or manufacturers. Trade or manufacturers' names appear herein solely because they are considered essential to the objective of this report.

REPORT DOCUMENTATION PAGE

*Form Approved
OMB No. 0704-0188*

The public reporting burden for this collection of information is estimated to average 1 hour per response, including the time for reviewing instructions, searching existing data sources, gathering and maintaining the data needed, and completing and reviewing the collection of information. Send comments regarding this burden estimate or any other aspect of this collection of information, including suggestions for reducing the burden, to Department of Defense, Washington Headquarters Services, Directorate for Information Operations and Reports (0704-0188), 1215 Jefferson Davis Highway, Suite 1204, Arlington, VA 22202-4302. Respondents should be aware that notwithstanding any other provision of law, no person shall be subject to any penalty for failing to comply with a collection of information if it does not display a currently valid OMB control number.
PLEASE DO NOT RETURN YOUR FORM TO THE ABOVE ADDRESS.

1. REPORT DATE (DD-MM-YYYY) March 2022		2. REPORT TYPE Technical Report		3. DATES COVERED (From - To) 2007 to 2019	
4. TITLE AND SUBTITLE Review of Tank Car Side Impact Test Research and Analyses of 2007–2019				5a. CONTRACT NUMBER DTFR53-11-D-00008	
				5b. GRANT NUMBER	
				5c. PROGRAM ELEMENT NUMBER	
6. AUTHOR(S) ² Aswani Krishnamurthy – 0000-0003-3116-7797 ; ¹ Shawn Trevithick – 0000-0001-6155-5526 ; ² Michael Carolan – 0000-0002-8758-5739 ; ¹ Ulrich Spangenberg – 0000-0003-2760-1394 ; ¹ Nicholas Wilson – 0000-0003-1140-7108 ; ² Shaun Eshraghi – 0000-0002-8152-0838 ; ³ Steve Kirkpatrick – 0000-0001-9590-7980				5d. PROJECT NUMBER	
				5e. TASK NUMBER 693JJ620F000040	
				5f. WORK UNIT NUMBER	
7. PERFORMING ORGANIZATION NAME(S) AND ADDRESS(ES) ¹ Transportation Technology Center, Inc. 55500 DOT Road PO BOX 11130 Pueblo, CO 81001-0130				8. PERFORMING ORGANIZATION REPORT NUMBER	
² Volpe National Transportation Systems Center 55 Broadway Cambridge, MA 02142					
³ Applied Research Associates, Inc. 95 1st Street, Suite 100 Los Altos, CA 94022					
9. SPONSORING/MONITORING AGENCY NAME(S) AND ADDRESS(ES) U.S. Department of Transportation Federal Railroad Administration Office of Railroad Policy and Development Office of Research, Development, and Technology Washington, DC 20590				10. SPONSOR/MONITOR'S ACRONYM(S)	
				11. SPONSOR/MONITOR'S REPORT NUMBER(S) DOT/FRA/ORD-22/14	
12. DISTRIBUTION/AVAILABILITY STATEMENT This document is available to the public through the FRA website .					
13. SUPPLEMENTARY NOTES COR: Francisco González, III					
14. ABSTRACT The Federal Railroad Administration (FRA) has a long-standing research program to examine the puncture resistance of railroad tank cars used in the transportation of hazardous materials within the U.S. Since 2007, FRA conducted 11 tank car shell impact tests at the Transportation Technology Center, Inc. (TTC) in Pueblo, CO, with the Volpe National Transportation Systems Center (Volpe) performing modeling and aiding with preparations for these tests. The objectives of the test program were to characterize the impact and puncture responses of tank cars and to support the development of finite element analysis (FEA) procedures to simulate tank car impacts and to evaluate the range of impact conditions under which various specification tank cars would puncture. Several FRA technical reports documented the results of these tests and the corresponding FEA over the course of this research program. This report contains a summary of the 11 tests and corresponding analyses, presents a discussion of numerous lessons learned over the course of the testing and analysis program, and includes comparisons of key results from the full-scale impact tests.					
15. SUBJECT TERMS Tank car, impact test, impact, finite element analysis, FEA, testing, hazardous materials, rolling stock					
16. SECURITY CLASSIFICATION OF:			17. LIMITATION OF ABSTRACT	18. NUMBER OF PAGES 145	19a. NAME OF RESPONSIBLE PERSON Francisco González, III
a. REPORT Unclassified	b. ABSTRACT Unclassified	c. THIS PAGE Unclassified			19b. TELEPHONE NUMBER (Include area code) 202-689-4316

METRIC/ENGLISH CONVERSION FACTORS

ENGLISH TO METRIC

LENGTH (APPROXIMATE)

- 1 inch (in) = 2.5 centimeters (cm)
- 1 foot (ft) = 30 centimeters (cm)
- 1 yard (yd) = 0.9 meter (m)
- 1 mile (mi) = 1.6 kilometers (km)

AREA (APPROXIMATE)

- 1 square inch (sq in, in²) = 6.5 square centimeters (cm²)
- 1 square foot (sq ft, ft²) = 0.09 square meter (m²)
- 1 square yard (sq yd, yd²) = 0.8 square meter (m²)
- 1 square mile (sq mi, mi²) = 2.6 square kilometers (km²)
- 1 acre = 0.4 hectare (he) = 4,000 square meters (m²)

MASS - WEIGHT (APPROXIMATE)

- 1 ounce (oz) = 28 grams (gm)
- 1 pound (lb) = 0.45 kilogram (kg)
- 1 short ton = 2,000 pounds (lb) = 0.9 tonne (t)

VOLUME (APPROXIMATE)

- 1 teaspoon (tsp) = 5 milliliters (ml)
- 1 tablespoon (tbsp) = 15 milliliters (ml)
- 1 fluid ounce (fl oz) = 30 milliliters (ml)
- 1 cup (c) = 0.24 liter (l)
- 1 pint (pt) = 0.47 liter (l)
- 1 quart (qt) = 0.96 liter (l)
- 1 gallon (gal) = 3.8 liters (l)
- 1 cubic foot (cu ft, ft³) = 0.03 cubic meter (m³)
- 1 cubic yard (cu yd, yd³) = 0.76 cubic meter (m³)

TEMPERATURE (EXACT)

$$[(x-32)(5/9)] \text{ } ^\circ\text{F} = y \text{ } ^\circ\text{C}$$

METRIC TO ENGLISH

LENGTH (APPROXIMATE)

- 1 millimeter (mm) = 0.04 inch (in)
- 1 centimeter (cm) = 0.4 inch (in)
- 1 meter (m) = 3.3 feet (ft)
- 1 meter (m) = 1.1 yards (yd)
- 1 kilometer (km) = 0.6 mile (mi)

AREA (APPROXIMATE)

- 1 square centimeter = 0.16 square inch (sq in, in²) (cm²)
- 1 square meter (m²) = 1.2 square yards (sq yd, yd²)
- 1 square kilometer (km²) = 0.4 square mile (sq mi, mi²)
- 10,000 square meters = 1 hectare (ha) = 2.5 acres (m²)

MASS - WEIGHT (APPROXIMATE)

- 1 gram (gm) = 0.036 ounce (oz)
- 1 kilogram (kg) = 2.2 pounds (lb)
- 1 tonne (t) = 1,000 kilograms (kg) = 1.1 short tons

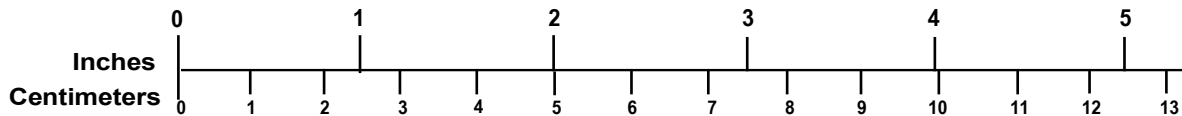
VOLUME (APPROXIMATE)

- 1 milliliter (ml) = 0.03 fluid ounce (fl oz)
- 1 liter (l) = 2.1 pints (pt)
- 1 liter (l) = 1.06 quarts (qt)
- 1 liter (l) = 0.26 gallon (gal)
- 1 cubic meter (m³) = 36 cubic feet (cu ft, ft³)
- 1 cubic meter (m³) = 1.3 cubic yards (cu yd, yd³)

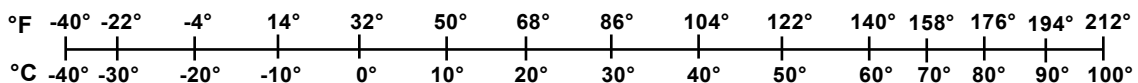
TEMPERATURE (EXACT)

$$[(9/5) y + 32] \text{ } ^\circ\text{C} = x \text{ } ^\circ\text{F}$$

QUICK INCH - CENTIMETER LENGTH CONVERSION



QUICK FAHRENHEIT - CELSIUS TEMPERATURE CONVERSION



For more exact and or other conversion factors, see NIST Miscellaneous Publication 286, Units of Weights and Measures. Price \$2.50 SD Catalog No. C13 10286

Updated 6/17/98

Acknowledgements

The authors acknowledge the Next Generation Rail Tank Car program for its role in initiating the first series of tank car shell puncture testing and modeling research. In addition, the authors acknowledge the contributions of the Advanced Tank Car Collaborative Research Program in supporting subsequent developments in tank car testing and modeling.

The authors acknowledge and appreciate the technical contributions of several Federal Railroad Administration (FRA) colleagues throughout the course of this testing program, especially Francisco González III, Program Manager of the Office of Research, Development and Technology, and Karl Alexy, Deputy Associate Administrator of FRA's Office of Railroad Safety.

The authors gratefully acknowledge the technical assistance of former Volpe National Transportation Systems Center colleagues Dr. Hailing Yu, Dr. David Jeong, and Mr. David Tyrell. The authors gratefully acknowledge the technical assistance of Anand Prabhakaran of Sharma & Associates. The authors would further like to acknowledge previous and current contributors to the test program including Ms. Satima Anankitpaiboon, Dr. Przemek Rakoczy, and Dr. Robert Fries.

Contents

Executive Summary	1
1. Introduction	3
1.1 Background	3
1.2 Objectives	6
1.3 Scope	7
1.4 Overall Approach	7
1.5 Organization of the Report	9
2. Summary of Shell Impact Tests and Analyses	10
2.1 Typical Test and Instrumentation Layout	11
2.2 Test Properties and Parameters	12
2.3 Summary of Analyses	19
3. Test 0 – DOT105A500W (April 11, 2007) Limited Instrumentation Test	22
3.1 Summary of Test 0	22
3.2 Summary of Analyses	25
3.3 Comparison of Test and Analysis Results	27
3.4 Summary of Lessons Learned	29
4. Test 1 – DOT105A500W (April 26, 2007)	30
4.1 Summary of Test 1	30
4.2 Summary of Analyses	33
4.3 Comparison of Test and Analysis Results	34
4.4 Summary of Lessons Learned	38
5. Test 2 – DOT105A500W (July 11, 2007)	40
5.1 Summary of Test 2	40
5.2 Summary of Analyses	42
5.3 Comparison of Test and Analysis Results	43
5.4 Summary of Lessons Learned	46
6. Test 3 – DOT105J500W with Protective Panel (May 18, 2011)	48
6.1 Summary of Test 3	49
6.2 Summary of Analyses	50
6.3 Comparison of Test and Analysis Results	51
6.4 Discussion and Lessons Learned	51
7. Test 4 – DOT111A100W (December 18, 2013)	53
7.1 Summary of Test 4	53
7.2 Summary of Analyses	56
7.3 Comparison of Test and Analysis Results	62
7.4 Summary of Lessons Learned	66
8. Test 5 – DOT112A340W (February 26, 2014)	68
8.1 Summary of Test 5	68
8.2 Summary of Analyses	70

8.3	Comparison of Test and Analysis Results.....	71
8.4	Discussion and Lessons Learned.....	71
9.	Test 6 – DOT105J500W (April 27, 2016)	73
9.1	Summary of Test 6	73
9.2	Summary of Analyses	75
9.3	Comparison of Test and Analysis Results.....	76
9.4	Summary of Lessons Learned	77
10.	Test 7 – DOT117J100W (September 28, 2016).....	78
10.1	Summary of Test 7	78
10.2	Summary of Analyses	80
10.3	Comparison of Test and Analysis Results.....	80
10.4	Discussion and Lessons Learned.....	80
11.	Test 8 – DOT105J500W (August 1, 2018)	82
11.1	Summary of Test 8	82
11.2	Summary of Analyses	84
11.3	Comparison of Test and Analysis Results.....	84
11.4	Discussion and Lessons Learned.....	85
12.	Test 9 – DOT111A100W (CPC-1232) (October 30, 2018).....	86
12.1	Summary of Test 9	87
12.2	Summary of Analyses	88
12.3	Comparison of Test and Analysis Results.....	89
12.4	Discussion and Lessons Learned.....	90
13.	Test 10 – DOT113C120W (November 19, 2019).....	92
13.1	Summary of Test 10	92
13.2	Summary of Analyses	94
13.3	Comparison of Test and Analysis Results.....	95
13.4	Discussion and Lessons Learned.....	95
14.	Discussion Across Multiple Tests	97
14.1	Tests of Pressurized Tank Cars	98
14.2	Tests of Tank Cars Not Initially Pressurized.....	104
14.3	Puncture Outcomes.....	106
14.4	Non-puncture Outcomes.....	111
14.5	Comparison at Peak Force.....	116
14.6	Discussion of Results Only Obtainable from FE Results.....	121
15.	Conclusion.....	127
16.	References	130
	Abbreviations and Acronyms	132

Illustrations

Figure 1. Timeline of Shell Impact Tests (2007–2019).....	5
Figure 2. Railroad Tank Car Marking System.....	6
Figure 3. Flowchart Showing Typical FEA Modeling Approach.....	7
Figure 4. Flowchart Showing Typical Testing Approach.....	8
Figure 5. Typical Test Setup.....	11
Figure 6. Impactor Energy as a Function of Speed for all Tests.....	17
Figure 7. Peak of Energy Transferred to Tank Car vs. Impactor Energy	18
Figure 8. Test 0 – Test Setup Showing DOT105 Tank Car and Impactor.....	22
Figure 9. Test 0 – Impact Response.....	24
Figure 10. Test 0 – Impact Damage to the Inner Tank Shell.....	24
Figure 11. Test 0 – Updated Model Generated for a DOT105J500W Pressure Tank Car	25
Figure 12. Test 0 – ARA Test 0 Impact Model	26
Figure 13. Test 0 – Volpe Test 0 Impact Model.....	27
Figure 14. Test 0 – Comparison of Test 0 and ARA Post-Test Analyses	28
Figure 15. Test 0 – Comparison of Test 0 and Volpe Post-Test Analyses	28
Figure 16. Test 1 – Test Setup Showing Tank Car.....	30
Figure 17. Test 1 – Shell Side Impact Behavior in Test 1 for Tank Car 3069	32
Figure 18. Test 1 – Post-Test Dents in the Jacket and Shell of Tank Car 3069	32
Figure 19. Test 1 – Updated Model Generated for a DOT105J500W Pressurized Tank Car	33
Figure 20. Test 1 – Calculated Test 1 Impact Response with Cutaway Showing Lading.....	34
Figure 21. Test 1 – Comparison of the Measured and ARA’s Predicted Impactor Car Accelerations.....	35
Figure 22. Test 1 – Comparison of the Measured and ARA’s Predicted Test 1 Tank Displacements.....	36
Figure 23. Test 1 – Comparison of Test 1 and Volpe Post-test Analyses	37
Figure 24. Test 1 – Test vs. Analysis Comparison of Force-Displacement Plot.....	37
Figure 25. Test 2 – Tank Car 3074 Mounted on Support Skids.....	40
Figure 26. Test 2 – Modified Impactor Car and Impactor Head Used in Test 2	41
Figure 27. Test 2 – Puncture Response Observed in the Full-Scale Impact Test 2.....	42
Figure 28. Test 2 – Updated Tank Car and Impactor Car Models for Test 2.....	43
Figure 29. Test 2 – ARA’s Predicted Tank Damage for the Impact Conditions	44

Figure 30. Test 2 – Comparison of Measured and ARA’s Predicted Force-Displacement Response	45
Figure 31. Test 2 – Test vs. ARA’s Post-Test Analysis Comparison of Force-Displacement Plot	45
Figure 32. Test 3 – Test Setup Showing Tank Car and Impactor.....	48
Figure 33. Test 3 – Damage to Protective Panel.....	50
Figure 34. Test 3 – Deformation to Jacket and Tank.....	50
Figure 35. Test 3 – Test vs. Analysis Comparison for Force-Displacement Plot.....	51
Figure 36. Test 4 – Target Tank Car Mounted on Support Skids.....	53
Figure 37. Test 4 – Test Setup Showing Tank Car and Impactor.....	54
Figure 38. Test 4 – Impactor Car Configuration Before Test.....	54
Figure 39. Test 4 – Post-test Puncture Response of the Tank Car.....	56
Figure 40. Test 4 – Post-test Puncture Damage of the Tank Car.....	56
Figure 41. Test 4 – Global Response Model of DOT111 Tank Car Side Impact Test.....	57
Figure 42. Test 4 – Skid Mounted DOT111 Tank Car Model Used in Global Response Model.	58
Figure 43. Test 4 – Impact Zone of Shell-Based Tank in Global Response Model	59
Figure 44. Test 4 – P-V Curve for an Unpressurized Tank with 3 Percent Outage.....	60
Figure 45. Test 4 – Puncture Model Overview.....	60
Figure 46. Test 4 – Close-up of Impact Patch in Detailed Puncture Model	61
Figure 47. Test 4 – Comparison of ARA’s Predicted and Measured Force-Displacement and Impact Energy	62
Figure 48. Test 4 – Effect of Outage Volume on Impact Force: 2 to 3 Percent Outage Range ...	63
Figure 49. Test 4 – ALE Lading Mesh Added to the Global Response Model.....	64
Figure 50. Test 4 – ARA’s Predicted Force and Energy Response With Explicit Lading Model	65
Figure 51. Test 4 – ARA’s Predicted Tank Pressure with Explicit Lading Model	66
Figure 52. Test 5 – Test Setup Showing DOT112 Tank Car and Impactor.....	68
Figure 53. Test 5 – Deformation of the (left) Jacket and (right) Tank Shell Due to Impact	70
Figure 54. Test 5 – Test vs. Analysis Comparison of Force and Energy vs. Displacement Plot .	71
Figure 55. Test 6 – Test Setup Showing DOT105 Tank Car and Impactor.....	73
Figure 56. Test 6 – Impact Zone Post-testing (left) With and (right) Without Jacket.....	75
Figure 57. Test 6 – Test vs. Analysis Comparison of Force/Energy-Displacement Plot	76
Figure 58. Test 7 – Test Setup Showing DOT117 Tank Car and Impactor.....	78
Figure 59. Test 7 – Post-test Images of (left) the Tank Car with Jacket and (right) Tank Inner Shell	79

Figure 60. Test 7 – Test vs. Analysis Comparison of Impactor Force-Travel Plot	80
Figure 61. Test 8 – Test Setup Showing DOT105 Tank Car and Impactor.....	82
Figure 62. Test 8 – Post-test Images (left) Tank and Jacket and (right) Tank Shell	84
Figure 63. Test 8 - Test vs. Analysis Comparison of Force and Energy vs. Displacement Plot ..	85
Figure 64. Test 9 – Test Setup Showing DOT111 Tank Car.....	86
Figure 65. Test 9 – Post-test Image of the Tank.....	88
Figure 66. Test 9 – Test vs. Analysis Comparison of Impactor Force-Travel Plot	90
Figure 67. Test 10 – Test Setup Showing DOT113 Tank Car and Impactor.....	92
Figure 68. Test 10 – Test vs. Analysis Comparison of Impactor Force-Travel Plot	95
Figure 69. Naming Convention Used to Distinguish Tests	97
Figure 70. Force vs. Time for all Initially Pressurized Tank Cars.....	98
Figure 71. Force vs. Displacement for all Initially Pressurized Tank Cars	99
Figure 72. Force vs. Displacement – Tests 2, 6, and 8	100
Figure 73. Force vs. Speed – Tests 2, 6, and 8	102
Figure 74. Speed Normalized Force vs. Normalized Speed – Tests 2, 6, and 8.....	103
Figure 75. Speed Normalized Force vs. Normalized Speed – All DOT105 Tank Cars	103
Figure 76. Force vs. Time – Unpressurized Tank Cars	104
Figure 77. Force vs. Displacement – Unpressurized Tank Cars.....	105
Figure 78. Force vs. Speed – Unpressurized Tank Cars.....	106
Figure 79. Speed Normalized Force vs. Normalized Speed – Unpressurized Tank Cars	106
Figure 80. Photographs of Puncture Zone in All Tests with Puncture Outcomes	107
Figure 81. Force vs. Time – Punctured Tank Cars Only	108
Figure 82. Force vs. Displacement – Punctured Tank Cars Only.....	109
Figure 83. Force vs. Speed – Punctured Tank Cars Only.....	110
Figure 84. Speed Normalized Force vs. Normalized Speed – Punctured Tests Only	111
Figure 85. Photographs of Impact Zone in All Tests with Non-puncture Outcomes	112
Figure 86. Force vs. Time – Non-Puncture Tests Only	113
Figure 87. Force vs. Displacement – Non-puncture Tests Only.....	114
Figure 88. Force vs. Impactor Speed – Non-puncture Tests Only.....	114
Figure 89. Normalized Force vs. Normalized Speed – Non-Puncture Tests Only.....	115
Figure 90. Summary of Peak Forces Across Tests	116
Figure 91. Summary of Displacements at Peak Forces Across Tests.....	117
Figure 92. Summary of Reduction of Diameter Percentages at Peak Forces Across Tests.....	117

Figure 93. Summary of Absorbed Energies at Peak Forces Across Tests.....	118
Figure 94. Absorbed Energy at Peak Force vs. Total Tank Thickness.....	118
Figure 95. Absorbed Energy vs. Outage.....	119
Figure 96. Normalized Force to Puncture Using Kirkpatrick’s Methodology	120
Figure 97. Normalized Force to Puncture Using Jeong’s Methodology	120
Figure 98. Impactor and Wall Forces vs. Time, Test 8 FEA	121
Figure 99. Impactor and Wall Forces vs. Time, Test 9 FEA	122
Figure 100. Energy vs. Time from Test 5 FE Model.....	125

Tables

Table 1. Summary of Shell Impact Tests.....	10
Table 2. Summary of Tested Tank Car Properties.....	13
Table 3. Thickness Differences Between Nominal and Measured Values.....	14
Table 4. Summary of Lading Conditions.....	15
Table 5. Summary of Impact Conditions.....	16
Table 6. Summary of Outcomes for Impactor Car and Tank Car in Each Test.....	18
Table 7. Summary of FEA.....	20
Table 8. Test 0 – DOT105J500W Tank Car Specifications.....	22
Table 9. Test 0 – Test Conditions and Results Summary.....	23
Table 10. Test 1 – DOT105A500W Tank Car Specifications.....	30
Table 11. Test 1 – Test Conditions and Results Summary.....	31
Table 12. Test 2 – DOT105A500W Tank Car Specifications.....	40
Table 13. Test 2 – Test Conditions and Results Summary.....	42
Table 14. Test 3 – DOT105J500W Tank Car Specifications.....	48
Table 15. Test 3 – Test Conditions and Results Summary.....	49
Table 16. Test 4 – DOT111A100W Tank Car Specifications.....	53
Table 17. Test 4 – Test Conditions and Results Summary.....	55
Table 18. Fluid Lading Material Properties.....	64
Table 19. Test 5 – DOT112A340W Tank Car Specifications.....	68
Table 20. Test 5 – Test Conditions and Results Summary.....	69
Table 21. Test 6 – DOT105J500W Tank Car Specifications.....	73
Table 22. Test 6 – Test Conditions and Results Summary.....	74
Table 23. Test 7 – DOT117J100W Tank Car Specifications.....	78
Table 24. Test 7 – Test Conditions and Results Summary.....	79
Table 25. Test 8 – DOT105J500W Tank Car Specifications.....	82
Table 26. Test 8 – Test Conditions and Results Summary.....	83
Table 27. Test 9 – DOT111A100W Tank Car Specifications.....	86
Table 28. Test 9 – Test Conditions and Results Summary.....	87
Table 29. Test 10 – DOT113C120W Tank Car Specifications.....	92
Table 30. Test 10 – Test Conditions and Results Summary.....	93
Table 31. Description of Energy Totals from FE Models.....	124

Executive Summary

Federal Railroad Administration (FRA) has a long-standing research program to examine the puncture resistance of railroad tank cars used in the transportation of hazardous materials within the United States. From 2007 to 2019, FRA has performed 11 tank car shell impact tests within this program at the Transportation Technology Center (TTC) in Pueblo, CO, with the Volpe National Transportation Systems Center (Volpe) and Applied Research Associates (ARA) performing modeling and aided with preparations for these tests. The objectives of the test program were to characterize the impact and puncture responses of tank cars and to support the development of finite element analysis (FEA) procedures to simulate tank car impacts and to evaluate the range of impact conditions under which various specification tank cars would puncture. This program included tests of several rail tank car specifications: DOT105, DOT111, DOT112, DOT117, and DOT113. Of these tests, DOT105 tank cars have been tested six times, DOT111 tank cars have been tested twice, and the remaining specification cars have been tested once. These tests were performed with: (1) different outage conditions (i.e., lading, fill level and initial pressure) based on typical service conditions and (2) different speeds based on pre-test analyses that predicted the possibility of puncture or impending puncture condition. In addition to these variations, impactors of different sizes (i.e., 23-inch by 12-inch, 12-inch by 12-inch, and 6-inch by 6-inch) were used in different tests.

The results of these tests and the corresponding FEA have been documented in a great detail in individual FRA technical reports over the course of this research program. This report contains a high-level summary of the 11 tests and corresponding analyses and presents discussion of numerous lessons learned over the course of the testing and analysis program. This report also includes comparisons of key results from the full-scale impact tests, e.g., force versus displacement behavior. The comparisons are made by using different groupings of tank cars, e.g., all DOT105 cars, all tests to result in a puncture, all cars initially at atmospheric pressure, etc. Out of the 11 tests summarized in this report, identified as Test 0 to Test 10, 6 tests resulted in puncture of the tank cars and 5 tests resulted in tank cars dented but not punctured by the impact.

Several variables, such as the percent outage, initial tank pressure, quality of the steel used in construction of the tank, thickness of the shell, speed of the impactor, and the size of the impactor affected shell punctures.

The following most significant findings were determined from this impact program:

- The testing and modeling approaches were improved and refined with each successive test. By standardizing the test approach, it became possible to capture the critical responses of a tank car during impact. This facilitated the accurate modeling of the impact event.
- The likelihood of puncture was strongly related to the impactor car speed, the outage (i.e., pressure and volume), the tank car construction (e.g., shell thickness, specification, and quality of shell material, etc.), and the size of the impactor that was used.
- Comparisons across the different tests showed that no matter what the outcome of the test, the initial responses of tank cars of the same specification were similar.
- The Lagrangian meshing of fluid with an equation-of-state (EOS) material model, were found to be generally applicable over a wide range of outage volumes and pressures.

- The detailed aerodynamic modeling of the air phase was not required. The pneumatic cavity approach was a reasonable representation of the air cavity in initially pressurized and initially unpressurized test conditions.
- The insulation and thermal protection used in the construction of the tank cars were found to affect the structural response of the tank car in some of the impact tests and thus may be important to consider in new or unproven models.

The ability to model tank car impact responses and puncture have improved through knowledge gained in each test, however, a substantially different test condition (e.g., new tank car material, design type, insulation type, lading condition, etc.) can still present a challenge to a predictive model. While the capabilities of predictive modeling have significantly improved over the duration of this research program, the role of testing is still important to verify the model results. Modeling supports the testing and can extrapolate beyond the tested conditions within limits, but modeling has not yet eliminated the need for full-scale testing for sufficiently different impact conditions.

1. Introduction

The Federal Railroad Administration (FRA) conducts research intended to improve the safety of hazardous materials transported on the general railroad system of the United States. In support of this goal, FRA sponsored a series of impact tests to the shells (sides) of tank cars built to various specifications. Between 2007 and 2019, FRA conducted 11 tests at the Transportation Technology Center (TTC) in Pueblo, CO. The Volpe National Transportation Systems Center (Volpe) performed modeling and aided with preparations for these tests. A companion finite element (FE) analysis, a type of engineering simulation, was performed alongside each full-scale test. Each test and its companion analyses were documented in its own detailed FRA technical report.

This report contains a summary of each test and its companion analyses. Test measurements from different tests are compared against one another. Patterns and trends from tests of similar conditions (e.g., tank cars of the same specification, or tank cars tested at elevated internal pressure) are identified and discussed.

1.1 Background

Three incidents that occurred between 2002 and 2005 resulted in the release of hazardous materials classified as toxic inhalation hazard (TIH) from tank cars and was documented by the National Transportation Safety Board (NTSB) (National Transportation Safety Board, 2005) (National Transportation Safety Board, 2006) (National Transportation Safety Board, 2004). The government and industry response to these incidents led to a research program, the Next Generation Rail Tank Car Program (NGRTC). The NGRTC focused on improving the crashworthiness of tank cars to maintain their integrity in potential future derailments, which would reduce the likelihood of a release of hazardous materials. Its three main objectives were:

1. Selecting and evaluating the most suitable materials, components, subsystems, and systems that would provide a significant improvement in structural performance
2. Selecting the most appropriate conceptual designs to gain potential structural improvements
3. Developing and using appropriate analytical approaches to model tank car responses and testing protocols to evaluate potential improvements.

The work of the NGRTC was specifically focused on improving the crashworthiness performance of tank cars that carry TIH materials. The NGRTC program included three full-scale shell impact tests of retired tank cars, with companion engineering analyses and simulations. This series of impact tests, conducted at the TTC in Pueblo, CO, was used to establish a testing protocol to quantify the performance of existing tank car designs in a shell impact, i.e., an impact to the side of the tank car. Such a scenario can and has occurred in many accidents when a derailment led to an alternating pileup, which exposed the sides of cars to impacts from trailing cars continuing in the direction of pre-derailment motion.

Following the conclusion of the NGRTC program in 2010, FRA built upon the knowledge gained through the testing and modeling performed under this program to expand the shell impact testing and analysis to additional tank car specifications. Tank cars constructed to different specifications will have different design pressures, different shell thicknesses, and

different safety features (e.g., a jacket and/or head shields). A tank car of a given specification has dimensions and capacity that is optimized to carry a given commodity. Different commodities may be transported at different service pressures and with different outage volumes. Clearly, it is not practical to test every conceivable combination of tank material, shell thickness, absence or presence of jacket, insulation, dimension, outage volume, pressure and impact speed that could be encountered by tank cars in the U.S. fleet. FRA's research program continued with tank cars transporting TIH material and has subsequently expanded to testing and analyzing tank cars intended for flammable liquid service (e.g., DOT111 and the recently developed DOT117 specification). The most recently performed tests and planned future tests will evaluate tank cars for cryogenic liquid service (i.e., DOT113 specification). By conducting full-scale shell impact tests on a variety of cars, constructed for a variety of service conditions, this program seeks to better understand the similarities and differences exhibited by the impact responses of tank cars under different conditions.

Figure 1 contains a timeline showing the 11 impact tests conducted between 2007 and 2019, including the tests conducted under the NGRTC program. As seen in this figure, three different sizes of impactors have been used in this research program. In Figure 1, one red star indicates tests where puncture occurred, and two red stars indicate puncture of the outer and inner shells (i.e., for the DOT113 tank car). The influence of impactor size on puncture response will be discussed.

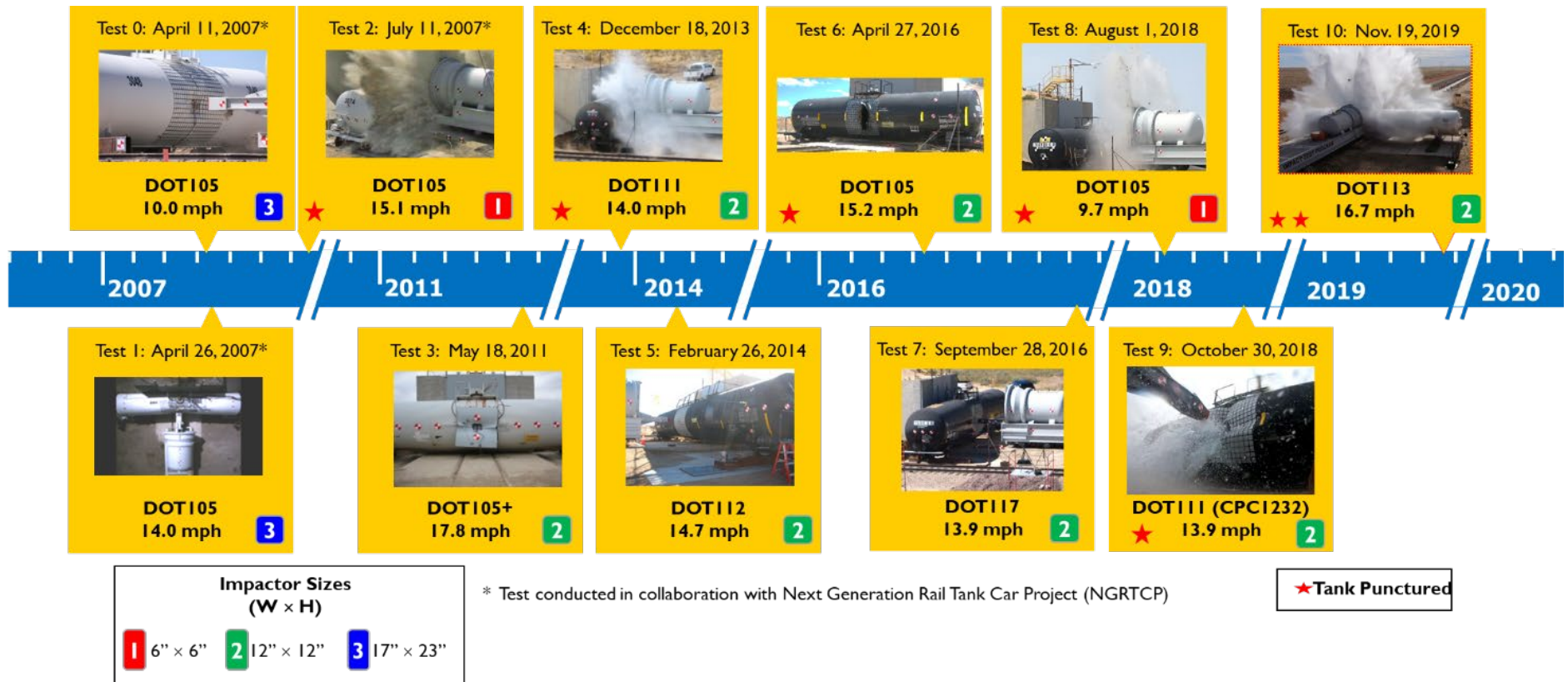


Figure 1. Timeline of Shell Impact Tests (2007–2019)

Figure 2 contains a description of the tank car specification marking system for tank cars used in the U.S. This figure provides a breakdown of the information contained in the stencil. Note that throughout this report, an abbreviated version of the tank car specification will typically be used to describe a particular car that was tested. For example, while the tank car used in Test 10 was a DOT113C120W tank car, it will generally be referred to as a DOT113 during discussion in this report.

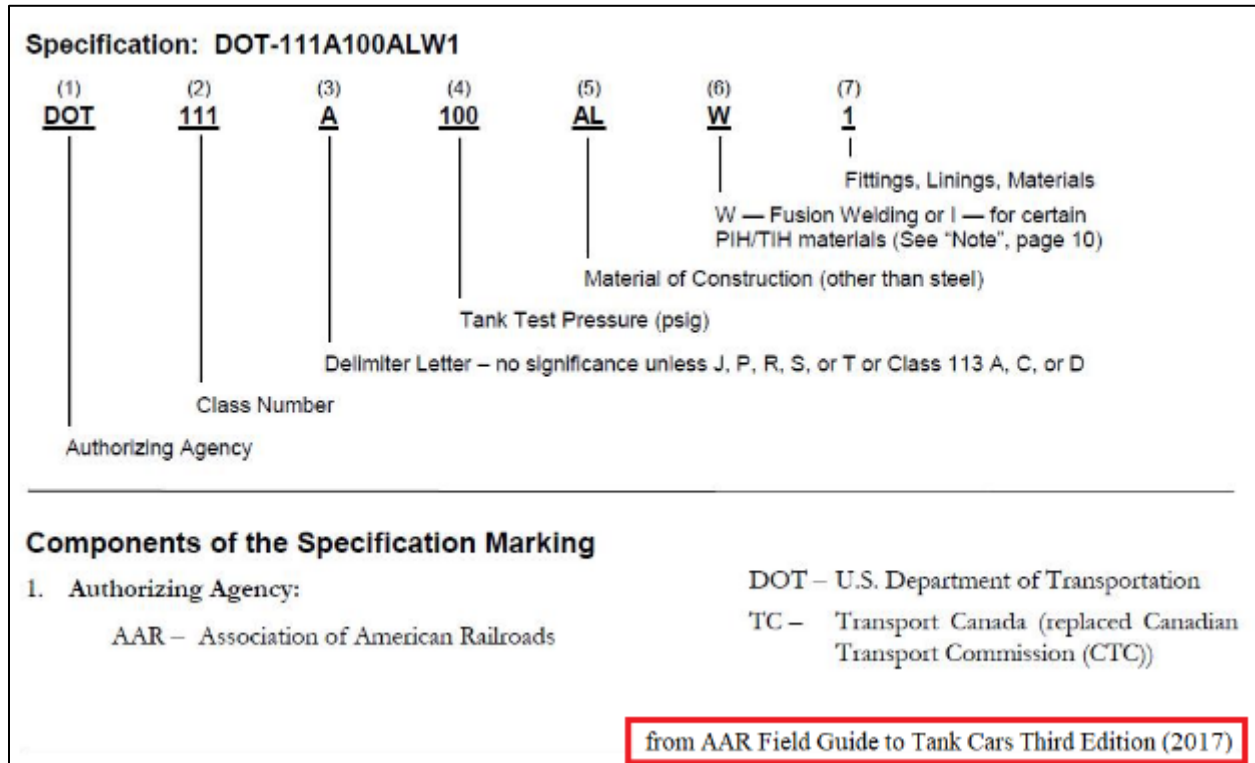


Figure 2. Railroad Tank Car Marking System

1.2 Objectives

The objectives of these tests were to identify the deformation mode, impact load-time history, and puncture resistance of tank cars in side impact. These tests were also intended to provide test data used for model development and validation efforts. Moreover, the impact conditions were developed so that the side impact test is: (a) safe, (b) repeatable, and (c) analyzable.

The objective of the analyses was to provide estimates of the tank car impact response for pre-test planning and validation of tank car impact and puncture modeling capabilities.

The objective of this report is to present the lessons learned in conducting the tests and analyses throughout this FRA research program and to identify, present, and discuss comparisons or trends that are observable across the variety of tank cars that have been tested within this program.

1.3 Scope

This report summarizes the findings of the various tank car impact reports and focuses on the lessons that were learned during the testing and modeling of shell impact behavior. This report does not discuss each test or model in detail, as that information is already included in the individual test reports.

1.4 Overall Approach

Various tests described in this report approached impact tests similarly. Figure 3 and Figure 4 contain flowcharts that summarize the typical finite element analysis (FEA) shell impact modeling approach and the typical testing approach. While these figures are specific to the process for one test, they represent the process with some minor differences (e.g., TC128 and A1011 materials were not always used in tank cars).

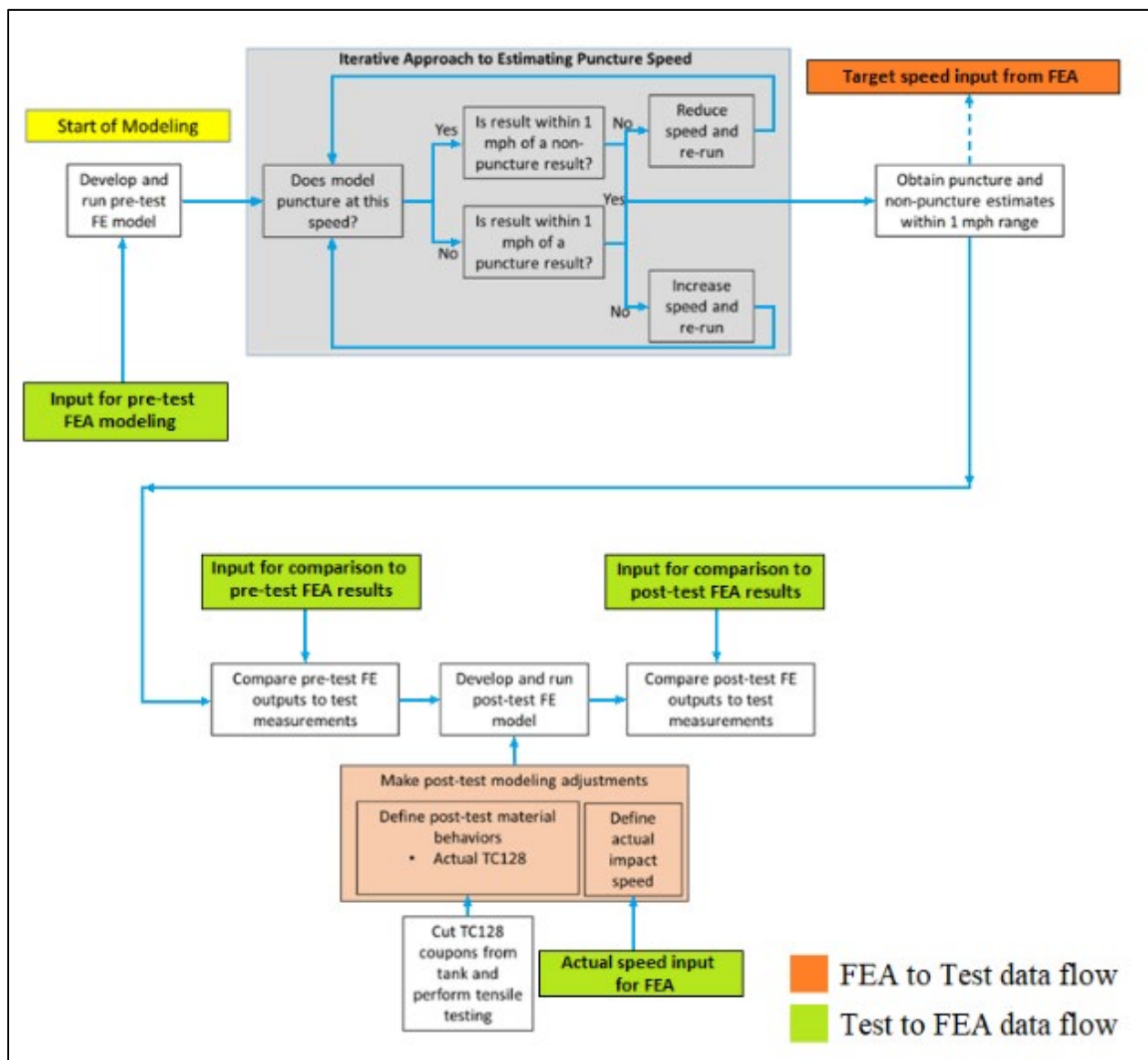


Figure 3. Flowchart Showing Typical FEA Modeling Approach

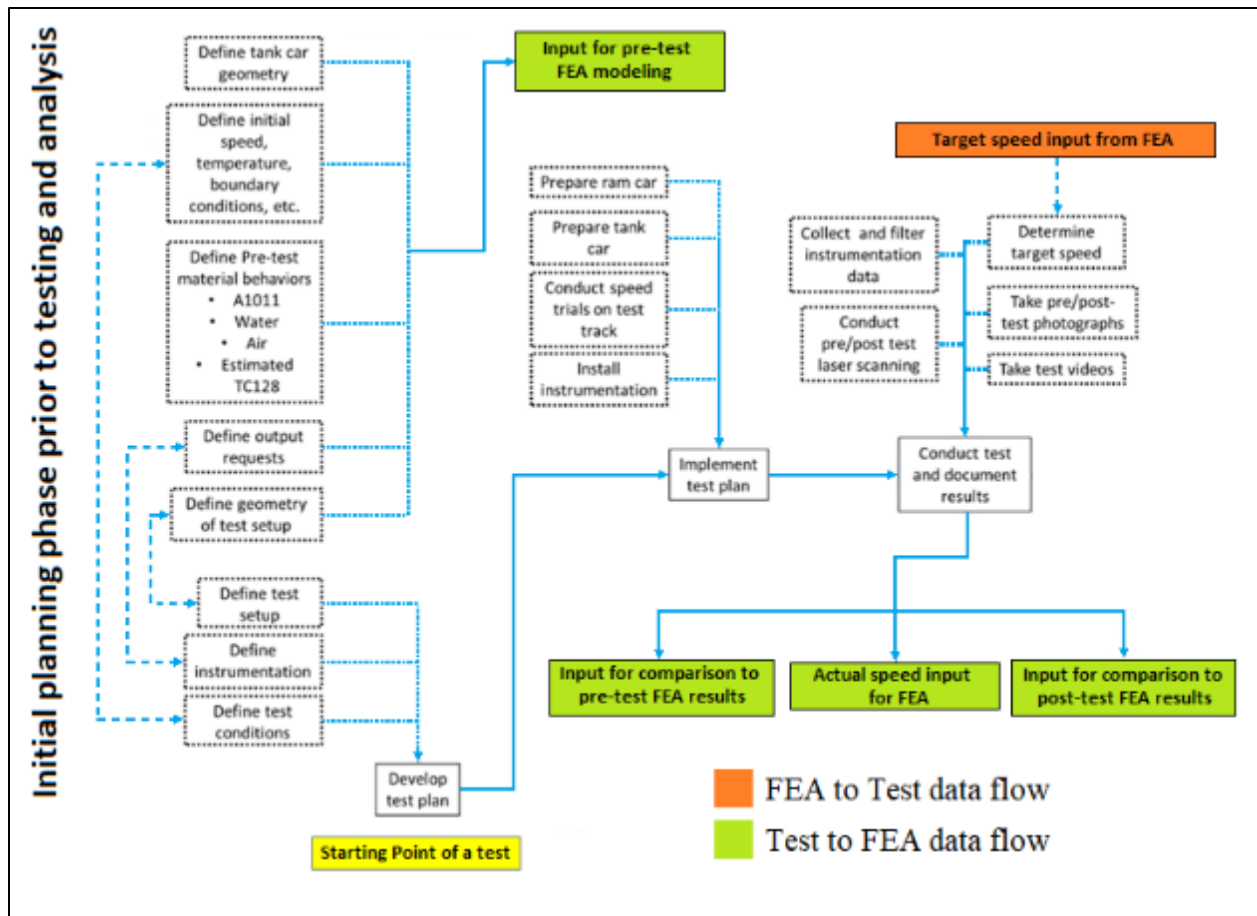


Figure 4. Flowchart Showing Typical Testing Approach

In general, the impact tests started with a pre-test FE model to estimate the threshold puncture speed of the tank car. The process involved creating FE models to identify a speed range in which to impact the tank car so that the desired result of either a puncture or an impending puncture is obtained. Since each tank car's specific material properties (e.g., yield strength, ultimate tensile strength, ductility, etc.) may not be known until after the impact testing is performed, typical material data were typically used in pre-test FE models. A detailed description of the process of developing material models for use in tank car impact simulations can be obtained from reviewing one of the detailed reports of the tests discussed in this report. To identify the puncture threshold speed, analyses were performed at various impact speeds to identify the speeds at which puncture and impending puncture conditions were observed. A narrow speed range (i.e., typically 1 to 2 mph) where the behavior changed from impending puncture to puncture was specified for testing.

The side impact tests were all performed at the TTC in Pueblo, CO. Each test was then planned and executed at a targeted impact speed in the identified speed range. As each test was also intended for comparison with corresponding FE models, measurements were made during each test to be used in such a comparison. In general, the key measurements made during each test included the impact speed, the acceleration-time history of the impactor car, the pressure-time history of the lading and outage, the displacements at the ends and support skirts and the indentation in the area around the point of impact. The acceleration-time history is typically used

to calculate the force-time history using the mass of the impactor car and the speed- and displacement-time histories.

In general, once the test was performed, samples from the tank shell were cut out and material characterization tests were performed on the tank's steel. The material properties from the characterization tests were used to develop material input parameters for the FE models. The same FE model of the tank car assembly that was used in the pre-test analysis was typically analyzed again with the material properties from the material characterization to compare the results with that of the test. This process was not a single pass process, but a multiple looped one involving several iterations to arrive at the best possible representation of the hardware and correlation of FE results to test results.

As the testing program developed and evolved over the course of 11 tests, modeling procedures improved as additional information from each test was captured. Specific model outputs particular to one or more tests are discussed in the corresponding sections in this report. The results from these impact tests have been used to develop FE procedures for modeling the various physical behaviors that occur during a tank car impact, to validate FE models of the impact scenario, and to improve the modeling procedures to obtain more reliable and accurate results from the original FE models. In the future, validated FE models could potentially be used to certify new tank designs with limited testing requirements.

1.5 Organization of the Report

[Section 1](#) contains an introduction to this report and to the previously conducted tests and analyses.

[Section 2](#) contains a summary of the general test setup and FE model considerations used for the 11 impact tests.

[Sections 3](#) through [13](#) are each dedicated to a single shell impact test and its corresponding analyses. These sections are all organized in a similar manner, where a summary of the specific details of that test and its companion FEA are described, key results from the test and the FEA are compared to one another, and any lessons learned that may be incorporated in future tests or FEA are described.

[Section 14](#) contains an assortment of plots and figures comparing results across multiple tank car tests. These results have been categorized in several different ways (e.g., all pressurized tank car results or all tests that resulted in a puncture outcome). Additionally, this section presents several approaches to normalizing data across the different tests.

[Section 15](#) offers a discussion to conclude this report on the history and potential future of the tank car testing and modeling program.

2. Summary of Shell Impact Tests and Analyses

This section contains several tables summarizing the tank car designs, lading conditions, and impact conditions from each of the 11 tests conducted to-date. While it would be useful to have a single table summarizing all the details of each test, such a table would be large and burdensome to navigate. This section contains similar summaries for the FEA performed alongside each test where details of the FE solver software, lading representations, and other modeling techniques are described.

FRA documented and published the results of the tests and corresponding FEA in a high-level of detail in individual technical reports. These reports contain much more detail about each test than will be found in this report, but each individual test report provides limited or no discussion of how that test compares or contrasts with the other tests conducted in this program. [Table 1](#) summarizes the 11 shell impact tests documented in this report and the corresponding individual test reports.

Table 1. Summary of Shell Impact Tests

Test	Test Date	Specifications	Citation	Comments
0	April 11, 2007	DOT105J500W	No standalone report	First shell impact test of a tank car
1	April 26, 2007	DOT105J500W		
2	July 11, 2007	DOT105J500W	(Kirkpatrick, S. W., 2010)	First test to puncture a tank car
3	May 18, 2011	DOT105J500W with protective panel	(Carolan, M. E., Jeong, D. Y., Perlman, B., murty, Y. V., Namboodri, S., Kurtz, B., Elzey, R. K., Anankitpaiboon, S., Tunna, L., & Fries, R., 2013)	Test using a protective sandwich panel
4	December 18, 2013	DOT111A100W	(Kirkpatrick, S. W., Rakoczy, P., MacNeill, R. A., & Anderson, A., 2015)	First test of an unpressurized tank car
5	February 26, 2014	DOT112J340W	(Rakoczy, P., & Carolan, M., 2016)	
6	April 27, 2016	DOT105J500W	(Carolan, M., & Rakoczy, P., 2019)	
7	September 28, 2016	DOT117A100W	(Rakoczy, P., Carolan, M., Eshraghi, S., & Gorhum, T., 2019)	First test to scan the tank surface near the impactor
8	August 1, 2018	DOT105J500W	(Wilson, N., Eshraghi, S., Trevithick, S., Carolan, M., & Rakoczy, P., 2020)	

Test	Test Date	Specifications	Citation	Comments
9	October 30, 2018	DOT111A100W (CPC-1232)	(Eshraghi, S., Trevithick, S., Carolan, M., Rakoczy, P., & Wilson, N., 2020)	First test of a non-jacketed tank car
10	November 19, 2019	DOT113C120W	(Wilson, N., Carolan, M., Trevithick, S., & Eshragi, S., 2021)	First test of a cryogenic tank car and a stainless-steel tank

2.1 Typical Test and Instrumentation Layout

Figure 5 shows the typical test setup used in the shell impact testing program. This test configuration was refined over the initial three tests (i.e., Tests 0, 1, 2). The tank car is removed from its trucks, placed on skids, and positioned against a rigid backing wall, perpendicular to the tracks leading up to the wall. The impactor car, equipped with the desired impactor head on its leading end, is initially positioned some distance from the standing tank car. The tracks leading to the wall are on a downgrade toward the wall. TTCI typically performs multiple speed trials on an adjacent track to the impact wall and has developed a procedure for estimating the distance for the initial release position of the impactor car based on the desired impact speed and ambient conditions (e.g., wind speed, temperature on test day).

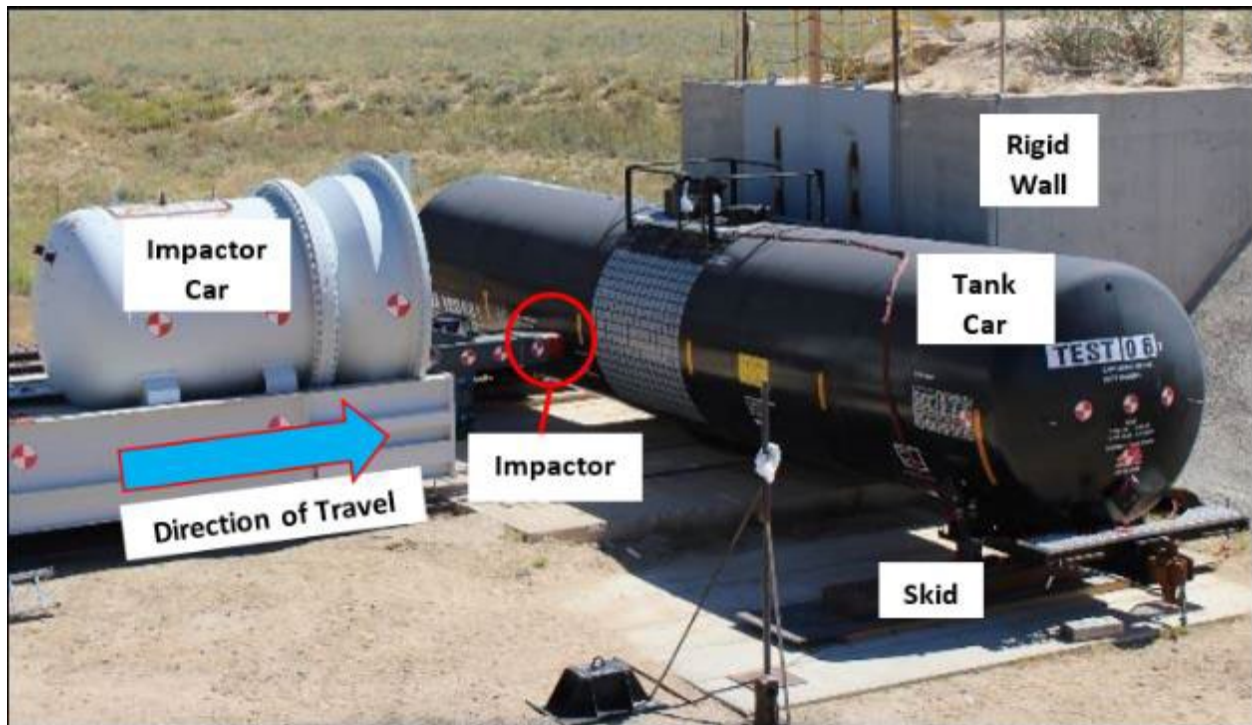


Figure 5. Typical Test Setup

Typically, instrumentation installed on the impactor car included tri-axial accelerometers at the front, center, and rear of the car. Redundant laser-based speed sensors are installed on the left and right sides of the impactor car that make use of ground-based reflectors installed just before the point of impact. Earlier tests used strain gauges on the impactor itself and more recent tests have included laser-based distance transducers measuring the distance between the impactor car

and wall, or the impactor car and the tank car. The impactor car is weighed before each test so that any changes in weight associated with different impactors, data acquisition systems (DAQ), cabling, or any structural modifications are considered for that test.

Typical instrumentation on the standing tank car includes an array of pressure transducers within the tank at various cross-sections along the length of the tank, longitudinally and vertically oriented string potentiometers (string pots) in the vicinity of the impact zone and string potentiometers between the skids or heads and the ground. In certain tests, instrumentation has also been installed in the vicinity of the pressure relief valve (PRV) to measure whether the PRV activated during the test. Earlier tests in this series included strain gauges installed on the tank in the vicinity of the impact zone, but this instrumentation has been discontinued in more recent tests. More recent tests have also included laser-based displacement transducers installed between the rigid wall and the back of the tank car to measure the rebound of the tank car after the impact.

In several of the more recent tests, pre- and/or post-test light detection and ranging (LiDAR) scanning has been performed on either the impact zone, or the entire standing tank car. The LiDAR scan results are assembled into a three-dimensional digital model of the deformed tank car. This geometry can then be readily compared with the deformed shape of the tank car in the FE model.

2.2 Test Properties and Parameters

Based on the observations made from the 11 tests in this series, the overall impact response of the tank car is influenced by numerous parameters. Some of these parameters, such as the impact speed of the impactor car, are within the control of the test team. Other parameters, such as the initial outage pressure and volume, can be controlled by the test team but must be chosen carefully to reflect the anticipated in-service conditions. Finally, parameters, such as the strength and ductility of the steel making up the shell of the tested car, cannot be controlled by the test team, but they can have a significant effect on the outcome of the test. The list below includes several parameters that can vary from test-to-test or car-to-car, but it should not be considered all-inclusive. The list is in alphabetical order and should not be inferred to reflect any relative significance of various parameters.

- Ductility of tank material
- Impact speed
- Insulation presence and type
- Jacketed versus non-jacketed
- Lading weight, density, and viscosity
- Outage pressure
- Outage volume
- PRV start-to-discharge (STD) pressure
- Sharpness of impactor (e.g., edge radius of impactor face)
- Shell diameter
- Shell length
- Size of impactor

- Strength of tank material
- Temperature of lading, outage, and tank
- Thickness of tank shell
- Weight of impactor

2.2.1 Tank Car Design Parameters

Table 2 contains the specifications, thicknesses, and materials used to construct the tank cars used in each test. It can be noted that in Table 2, the nominal thickness of the jacket and of the tank shell are reported.

Table 2. Summary of Tested Tank Car Properties

Test	Tank Car Specification	Tank Shell Material	Tank Shell Thickness (nominal, inch)	Jacket Thickness	Insulation
0	DOT105J500W	TC128 ¹	0.78	11-gauge ²	4-in. (ceramic fiber + fiberglass)
1	DOT105J500W	TC128	0.78	11-gauge	4-in. (ceramic fiber + fiberglass)
2	DOT105J500W	TC128	0.78	11-gauge	4-in. (ceramic fiber + fiberglass)
3	DOT105J500W With protective panel	TC128	0.78	11-gauge + 3-in. tube core panel	4-in. (ceramic fiber + fiberglass)
4	DOT111A100W	A515-70	0.44	11-gauge	4-in. glass wool blanket
5	DOT112A340W	TC128	0.62	11-gauge	1/2-in. ceramic thermal protection
6	DOT105J500W	TC128	0.78	11-gauge	4-inch urethane foam
7	DOT117A100W	TC128	0.56	11-gauge	1/2-in. ceramic thermal protection
8	DOT105J500W	TC128	0.78	11-gauge	4-in. urethane foam
9	DOT111A100W (CPC-1232)	TC128	0.5	N/A	N/A
10	DOT113C120W	A516-70 Carbon Steel (outer) 304 Stainless Steel (inner)	0.44 (outer) 0.25 (inner)	N/A	6-in. evacuated perlite

¹ TC128 refers to Association of American Railroads (AAR) TC128 Grade B steel (Association of American Railroads, 2000).

² An 11-gauge carbon steel jacket is approximately 0.12 inches thick.

Throughout this report and in the respective test reports, the nominal thickness of each tank car’s shell is typically presented. The nominal thickness of the tank car’s shell is also the thickness value defined in the FE models for each tank car.³ However, following many of the tests, material coupons were excised from the tank or, in the case of the DOT113 tanks where samples from plates used to manufacture the tank, were sent for mechanical testing. For some of these material coupons, the material testing report (MTR) included a value for the thickness of rectangular coupons excised from the tank car. Note that for some tank cars, the coupons excised from the shell were machined into cylindrical specimens for tensile testing and no thickness measurements of the original plate were retained. [Table 3](#) summarizes the nominal and actual shell thicknesses for those tests where actual thickness measurements were made. It can be observed that the actual thicknesses are higher by 0.02 to 0.03 inches compared to nominal thicknesses except for Test 4. It is possible that the plate suppliers of tank car manufacturers are erring on the cautious side by providing thicker plates compared to nominal thicknesses ordered, ensuring plates are not rejected by tank car builders for being too thin.

Table 3. Thickness Differences Between Nominal and Measured Values

Test ID	Car Specification	Nominal ⁴ (in.)	Actual Thickness from Post-test MTR (in.)	Difference (in.)	Percentage Difference
4	DOT111A100W	0.44	0.40	-0.038	-8.8
7	DOT117A100W	0.56	0.59	0.031	5.5
8	DOT105J500W	0.77	0.80	0.028	3.7
9	DOT111A100W	0.50	0.52	0.023	4.7
10	DOT113C120W	0.44 (outer)	0.46	0.026	5.8
10	DOT113C120W	0.25 (inner)	0.28	0.031	12.4

The results shown in [Table 3](#) underscore the need to measure the actual thickness of the tank car being tested, especially if the results of the test are to be used to either develop or validate an FE model. Test 4 was the only test where the thickness value reported on the MTR was below the nominal thickness of the tank car that was tested. Caution should be exercised in interpreting this result, since it is possible that the thickness of the tank’s shell was reduced during fabrication of the specimens for material testing that the MTR’s thickness values are based on. However, for all other tests, the MTR reported a coupon thickness that was greater than the nominal thickness of the tank. Since the shell would not have its thickness increased by the process of fabricating tensile test specimens, it can be concluded that the actual tank thickness in all these tests exceeded the nominal thickness by at least the value reported on the MTR. This additional material resulted in a tank shell that was anywhere between 3.7 and 12.4 percent thicker than expected based on the nominal thickness.

³ The DOT113 tank car (Test 10) used actual material thicknesses after these values were known.

⁴ Nominal thicknesses were obtained from the Certificate of Construction (CoC) or drawings

2.2.2 Lading Conditions

Table 4 summarizes the lading conditions for the tests conducted. The first three tests in this series used clay slurry to represent the lading that had a higher specific gravity. Subsequent tests used water as a stand-in for any lading, as the properties of water needed to perform FE modeling are more readily available and more consistent than a slurry. Additionally, for tests of tank cars intended for flammable liquid service, the commodities carried in the tank cars typically have a specific gravity of less than 1.

Table 4. Summary of Lading Conditions

Test	Tank Car Capacity (gallons)	Temperature of Water (unless noted otherwise) (°F)	Liquid Used in Test	Target Outage in Test (Percent)	Initial Outage Pressure (psig)	Comments on Lading Condition
0	17,300	45	Clay slurry	10.4	100	
1	17,300	55	Clay slurry	10.4	100	
2	17,300	83	Clay slurry	10.4	100	
3	17,300	50	Water	10.0	100	
4	24,000	53	Water	~3.0	Atmospheric	Outage level estimated post-test as ~2.25%
5	33,800	43	Water	4.0	Atmospheric	First test to use the fill-empty outage approach
6	17,360	50 (air) 55 (water)	Water	10.6	100	
7	30,100	70 (air)	Water	5.0	Atmospheric	
8	17,360	76 (air) 75 (water)	Water	10.5	100	
9	31,800	46 (air)	Water	5.0	Atmospheric	Leakage through manway observed before puncture
10	32,900 (water) ⁵	50	Water	17.6	50	Lading at ambient condition, tank intended for cryogenic service

⁵ Capacity listed as water gallons for DOT113 tank car. When loaded with cryogenic liquid, the volume will be reduced due to thermal contraction.

2.2.3 Test Speeds, Energies and Outcomes

The outcomes of the tests that have been performed in this program can be categorized by the post-test state of the tank car and by the post-test position of the impactor car. Table 5 summarizes the impact conditions for each test, the geometry of the impactor, target speed, measured impact speed, impactor car weight, and impact kinetic energy and the test outcome. In the event of a puncture outcome, this table also includes an approximate value for the speed that the impactor was traveling at the time of the puncture. This value will be referred to as the “residual speed” throughout the rest of this report. A lower value of residual speed at puncture indicates that the tank car came closer to stopping the impactor without a puncture compared to a test with a higher value of speed at puncture.

Table 5. Summary of Impact Conditions

Test	Impactor Geometry ⁶ (inch by inch), and corner radius	Target Impact Speed (mph)	Measured Impact Speed (mph)	Impactor Car Wt. (lbf)	Impact KE (10 ⁶ ft-lbf)	Test Outcome	Residual Speed at Puncture (mph)
0	17"×23" 1 in. radius	10	9.6	285,600	0.816	Non-puncture	N/A
1	17"×23" 1 in. radius	14	13.9	285,600	1.86	Non-puncture	N/A
2	6"×6" 1/2- in. radius	15	15.2	285,400	2.14	Puncture	11.5
3	12"×12" 1 in. radius	18	17.8	295,725	3.13	Non-puncture	N/A
4	12"×12" 1 in. radius	14	14.04	297,125	1.96	Puncture	6.0
5	12"×12" 1 in. radius	15	14.7	297,125	2.15	Non-puncture	N/A
6	12"×12" 1 in. radius	15	15.16	297,125	2.27	Puncture	0.5
7	12"×12" 1 in. radius	13.5	13.9	297,125	1.91	Non-puncture	N/A
8	6"×6" 1/2- in. radius	9.9	9.7	296,775	0.93	Puncture	0.5
9	12"×12" 1 in. radius	13.5	13.9	297,150	1.91	Puncture	0.5
10	12"×12" 1 in. radius	16.5	16.7	297,000	2.76	Puncture of Both Tanks	8.0

The kinetic energies of each test are shown as a function of the impactor speeds in Figure 6. The figure shows most of the tests were performed at an impactor speed between 13.5 and 15.5 mph. The measured weight of the impactor car was used to calculate the impactor energy for each test.

⁶ Impactor geometry is reported as the dimensions to the outer limits of the impact face. Each impactor featured rounded edges of a defined radius.

An average weight of 293,475 pounds was used to calculate the theoretical energy line in Figure 6. The weight of the impactor car was increased by approximately 10,000 lbf after Test 3, when some additional reinforcing structures were added to the end underframe to support testing at higher impact energies. Additionally, the 12-inch by 12-inch impactor is a cap installed over the 6-inch by 6-inch impactor, so tests using the larger impactor generally use a slightly heavier ram car. Not all the impactor car energies calculated for the various tests lie exactly on this line due to the slight variations in impactor car weights to the average weight used for the theoretical line. In Figure 6, a solid symbol indicates a test with a puncture outcome while a hollow symbol indicates a non-puncture outcome. Tests performed using the 17-inch by 23-inch impactor are denoted with a rectangular symbol. Tests performed using the 6-inch by 6-inch impactor are denoted with a diamond symbol. Tests performed using the 12-inch by 12-inch impactor are denoted with a circular symbol.

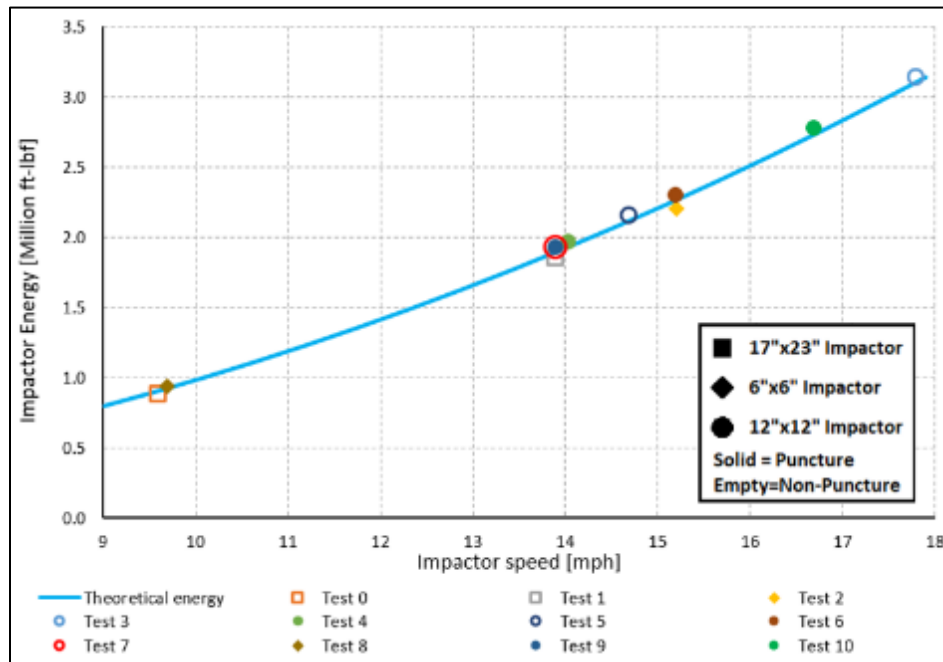


Figure 6. Impactor Energy as a Function of Speed for all Tests

Figure 7 plots the peak of the energy that was transferred to the tank car during each test on the vertical axis versus the initial kinetic energy of the impactor car for that test on the horizontal axis. The diagonal “1:1 line” indicates a test outcome in which the peak of the energy transferred to the tank car was exactly equal to the initial kinetic energy of the impactor car. Data points above this line are not possible, as that would be a situation in which the energy transferred to the tank car was more than the kinetic energy initially present in the impactor car. Data points below this line indicate a test where the kinetic energy of the impactor car exceeded the maximum amount of energy that the tank car and surroundings could absorb at the peak of the impact even. Data points that are far below the 1:1 line had a large amount of excess kinetic energy in the impactor car at the peak of the impact event.

Figure 7 shows most of the tests were conducted with a kinetic energy of the impactor car that was either at or just below the capacity of the tested tank car and environment to receive all the kinetic energy. Three tests stand out for their low amount of energy transferred to the tank car

and surroundings relative to the initial kinetic energy. For Tests 2, 4, and 10, puncture of the tank car occurred with a significant residual speed of the impactor car. Each of these three tests will be discussed subsequently in this report, but it is of note that each of these tests represented a significant change from previous tests. Test 2 was the first test designed to puncture the tank car, and it was the first test to use a 6-inch by 6-inch impactor. Test 4 was the first test to use an unpressurized tank car that was initially at atmospheric pressure, and it featured a much lower outage than used in previous tests. Test 10 was the first test of a tank-within-a-tank design using stainless steel for the inner tank.

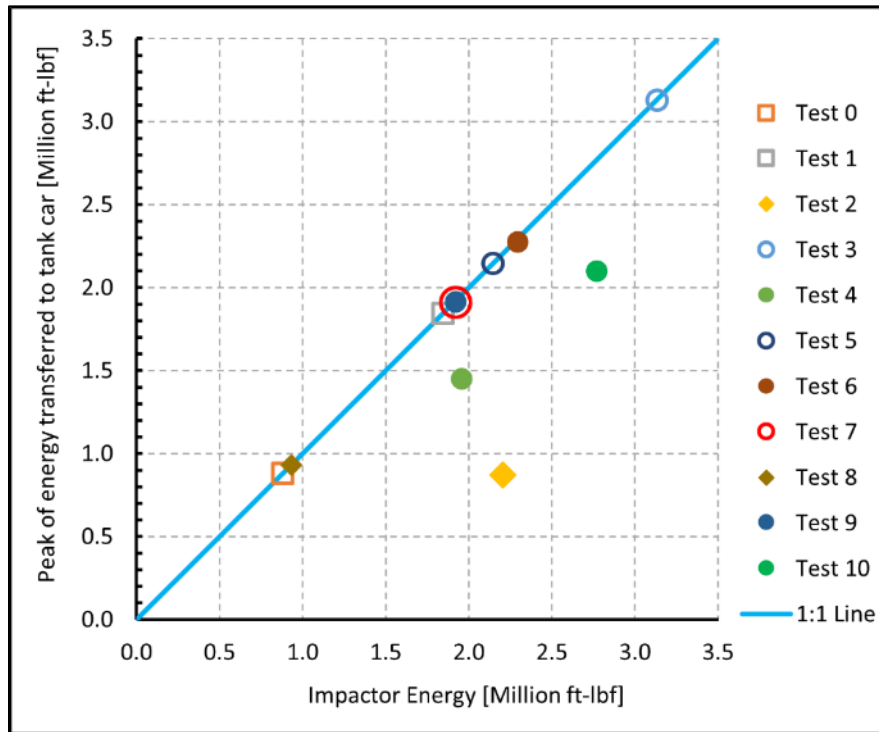


Figure 7. Peak of Energy Transferred to Tank Car vs. Impactor Energy

Each impact resulted in either a puncture of the tank car, or a non-puncture outcome. With a puncture of the tank car, the impactor either rebounded after puncturing or continued through the tank shell and came to rest embedded within the tank car. For a non-puncture impact response, the impactor car came to a stop and rebounded from the tank car.

Table 6 summarizes where each impact test conducted to-date falls based upon these three outcome criteria. The combination of a non-puncture outcome for the tank car and an impactor car that continues to travel forward is not a possible outcome for this test setup, owing to the rigid impact wall behind the tank car.

Table 6. Summary of Outcomes for Impactor Car and Tank Car in Each Test

	Puncture of Tank Car	Non-puncture of Tank Car
Impactor Car Rebounded	Tests 6, 8, 9	Tests 0, 1, 3, 5, 7
Impactor Car Continued	Tests 2, 4, 10	-

2.3 Summary of Analyses

For each of the 11 shell impact tests described in this report, a companion FEA accompanied the test. The FEA was performed using different modeling techniques, different software packages, and by different analysts for different tests. As more tests occurred and more modeling was performed, modeling techniques were improved using experience and knowledge gained from previous tests and FEA could be incorporated into subsequent models. [Table 7](#) summarizes the FEAs.

Table 7. Summary of FEA

Test	FE Software	Plastic Stress-Strain Response	Damage Initiation and Progression	Liquid Lading Modeling	Gas Lading Modeling	Comment
0	LS-DYNA	Piecewise linear elastic-plastic response	Damage evaluated from plastic strain levels	Lagrangian elements with low strength viscoelastic behavior	Constant internal pressure	Material properties based on data from other tank steel testing programs
1	LS-DYNA	Piecewise linear elastic-plastic response	Damage evaluated from plastic strain levels	Lagrangian elements with low strength viscoelastic behavior	Control volume and ideal gas pressure-volume (P-V) relationship	Material properties based on data from other tank steel testing programs
2	LS-DYNA	Piecewise linear elastic-plastic response	Damage evaluated from plastic strain levels	Lagrangian elements with low strength viscoelastic behavior	Control volume and ideal gas P-V relationship	Material properties for tank car shell based on data from previously tested tank cars
3	Abaqus 6.10	Piecewise linear elastic-plastic response	Bao-Wierzbicki (B-W) ductile failure criterion	Lagrangian elements, Equation-of-state (EOS) material	Lagrangian elements, ideal gas EOS material	Material properties for tank car shell based on data from previously tested tank cars. Material properties for sandwich panel assumed from minimum properties
4	LS-DYNA	Piecewise linear elastic-plastic response	B-W failure surface with element erosion	Lumped mass approach (pre-test) and arbitrary Lagrangian-Eulerian (ALE) fluid-structure interaction model (post-test)	Control volume and ideal gas P-V relationship	The fluid-structure interaction modeling had a significant effect on the internal pressure predictions of the model.

Test	FE Software	Plastic Stress-Strain Response	Damage Initiation and Progression	Liquid Lading Modeling	Gas Lading Modeling	Comment
5	Abaqus 6.13 (Abaqus/CAE preprocessor, Abaqus/Explicit)	Bilinear stress-strain response with a straight line from zero to yield and from yield to ultimate tensile strength	B-W ductile failure criterion	Lagrangian elements, EOS material	Smoothed particle hydrodynamics (SPH), ideal gas EOS material	Used half-symmetry in model. The material behavior of the steel used in the model is extremely important. Predictions were made with assumed material properties. Better agreement is obtained once actual test values were used
6	Abaqus 6.14 (Abaqus/CAE preprocessor, Abaqus/Explicit)	Piecewise linear elastic-plastic response	B-W ductile failure criterion	Hydraulic cavity	A pneumatic cavity defined for the pressurized air phase	Modeling the urethane foam insulation material between the jacket and tank was deemed important as opposed to air gap only
7	Abaqus 6.14 (Abaqus/CAE preprocessor, Abaqus/Explicit)	Piecewise linear elastic-plastic response	B-W ductile failure criterion	Lagrangian elements, EOS material	Ideal gas using the pneumatic cavity approach	The interaction between the tank car valve protector and concrete became important to match test data
8	Abaqus 6.14 (Abaqus/CAE preprocessor, Abaqus/Explicit)	Piecewise linear elastic-plastic response	B-W ductile failure criterion	Hydraulic cavity	Pneumatic cavity defined for the pressurized air phase	Companion car to Test 6, pre-test material data was estimated from Test 6 properties
9	Abaqus 6.14 (Abaqus/CAE preprocessor, Abaqus/Explicit)	Piecewise linear elastic-plastic response	B-W ductile failure criterion	Lagrangian elements, EOS material	Pneumatic cavity defined for the pressurized air phase	Undesired leakage from manway during test influenced pressure response, challenged model validation
10	Abaqus 2017 (Abaqus/CAE preprocessor, Abaqus/Explicit)	Piecewise linear elastic-plastic response	B-W ductile failure criterion	Hydraulic Cavity	Pneumatic Cavity	Several modeling challenges including stainless steel inner tank, vacuum between tanks, off-center impact and expanded perlite insulation

3. Test 0 – DOT105A500W (April 11, 2007) Limited Instrumentation Test

3.1 Summary of Test 0

Test 0 was performed as part of the NGRTC project on April 11, 2007, at the TTC in Pueblo. Test 0 featured a 17,391-gallon DOT105 tank car struck by a 17-inch by 23-inch impactor centered on the tank. [Table 8](#) summarizes the specification for the tested DOT105J500W tank car. [Figure 8](#) shows the test setup with the position of the tank car and impactor. The tank car was sitting on stub rails transverse to the impactor car's track and backed by an impact wall to resist post-impact motion. The test was designated as Test 0 since it was performed as a limited instrumentation assurance test before the first official planned test in the NGRTC program.

Table 8. Test 0 – DOT105J500W Tank Car Specifications

DOT105	Pressurized tank car
J	Jacketed for thermal protection, tank headshields, top and bottom shelf couplers
500	500 psig test pressure
W	Fusion welded tank



Figure 8. Test 0 – Test Setup Showing DOT105 Tank Car and Impactor

The objectives of Test 0 were to understand and validate the test environment and evaluate gross impact behaviors of the impactor and of the target tank cars at an impact energy that would be below the puncture threshold. The test protocol was untried before Test 0, and the intent was to create a repeatable controlled impact environment suitable to measure the energy required to puncture a tank car. A summary of the test was reported in the report for Test 1 (Witte, M., & Anankitpaiboon, S., 2007).

The test article was an unmodified DOT105 tank car in a loading condition considered typical for chlorine service. The tank car was filled with clay-slurry to the planned outage level. Witt et al. (2007) summarizes the test conditions and results. The actual impact speed was 9.6 mph. During the impact (Figure 9), the outer jacket and the inner tank of the chlorine car were dented as planned. The inner tank did not puncture, as Figure 10 shows. The dent in the outer jacket was approximately 7 5/8 inches deep. The dent in the inner tank was approximately 4 1/2 inches deep. These depths were measured relative to an 8-foot straight edge placed lengthwise over the dent. The dent in the outer jacket was slightly wider than the 8-foot straight edge.

The car stayed upright throughout the test. The rebound of the car was successfully reacted by the outriggers installed in the draft pockets of the car. Structural inspection after the impact showed no visible damage to the stub sills or their weld joints to the inner tank.

Instrumentation in the test consisted of multiple accelerometers on the tank car and on the impactor car, as well as strain gauges on the impactor. In addition, several real-time video cameras documented the impact event as well as one semi-high speed (250 frames per second) digital video camera. All the instrumentation data were successfully recorded. Table 9 summarizes the impact conditions and outcomes of Test 0.

Table 9. Test 0 – Test Conditions and Results Summary

Outage	10.4%
Target Speed	10 mph
Actual Speed	9.6 mph
Pressure	100 psig
Product	Slurry ($\rho=11.6$ lbs./gallon)
Impactor Dimensions	17"x23"
Impactor Weight	285,600 lbs.
Tank Car Weight (Estimated)	265,000 lbs.
Nominal Tank Thickness	0.77 in.
Nominal Jacket Thickness	11 gauge
Insulation and Thermal Protection	Ceramic fiber and fiberglass
Nominal Insulation Thickness	4.0 in.
Test Outcomes	Tank indented (no puncture), impactor car rebounded



**Figure 9. Test 0 – Impact Response
(Near maximum impactor displacement)**



Figure 10. Test 0 – Impact Damage to the Inner Tank Shell

3.2 Summary of Analyses

The development of tank car impact modeling methodologies was in the early stages of development before the execution of Test 0. A series of preliminary pre-test simulations were performed with the primary objective of supporting the development of the test procedure and selection of an impact speed below the puncture threshold of the tank. During the NGRTC program, Applied Research Associates, Inc. (ARA) and Volpe performed the analyses.

The ARA model for the Test 0 analyses was developed using the TrueGrid preprocessor code, and the LS-DYNA FE code was used for the analyses. LS-DYNA is an explicit nonlinear three-dimensional FE code for analyzing the large deformation dynamic response of solids and structures. The tank car model used in these analyses was based on a previous FE model of a DOT112A340W pressure tank car generated to analyze the loads and stresses in the tank car because of service and salvage operating conditions. This model was modified by changing the tank wall thickness, the stub sill was modeled in more detail, and the mesh resolution in the vicinity of the impactor was increased. [Figure 11](#) shows the resulting model for the DOT105 tank car, and [Figure 12](#) shows the analysis configuration for Test 0.

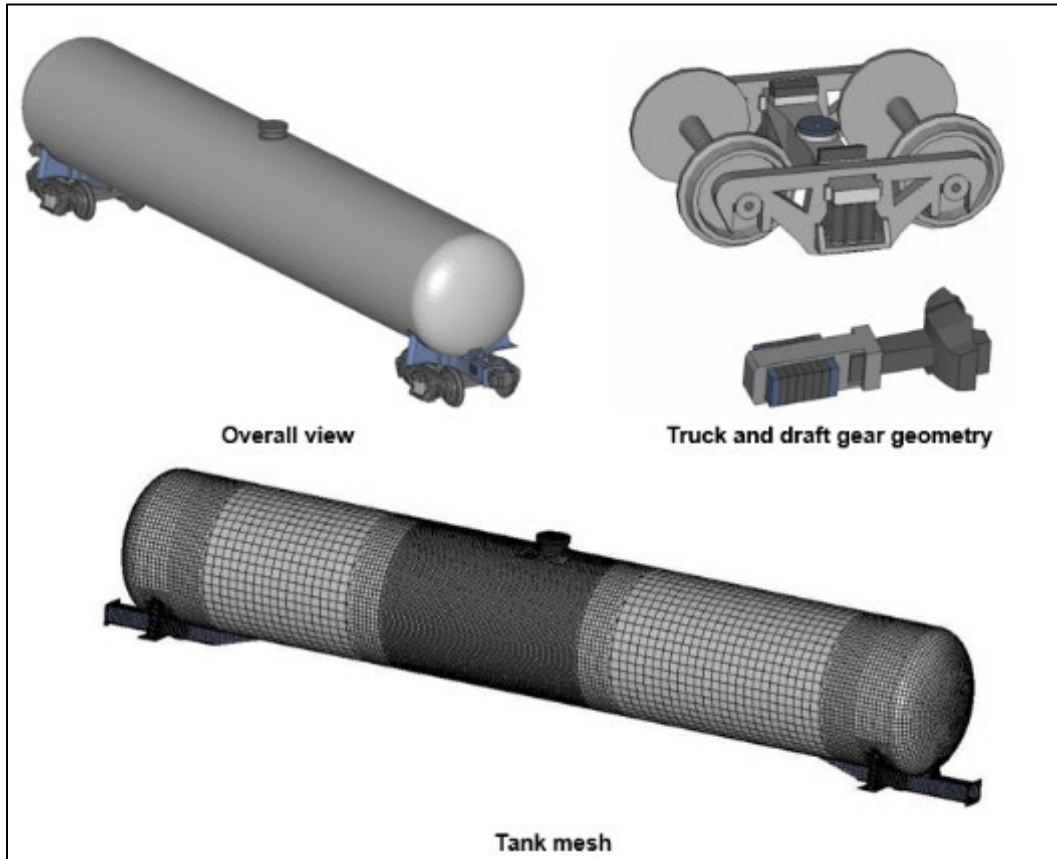


Figure 11. Test 0 – Updated Model Generated for a DOT105J500W Pressure Tank Car

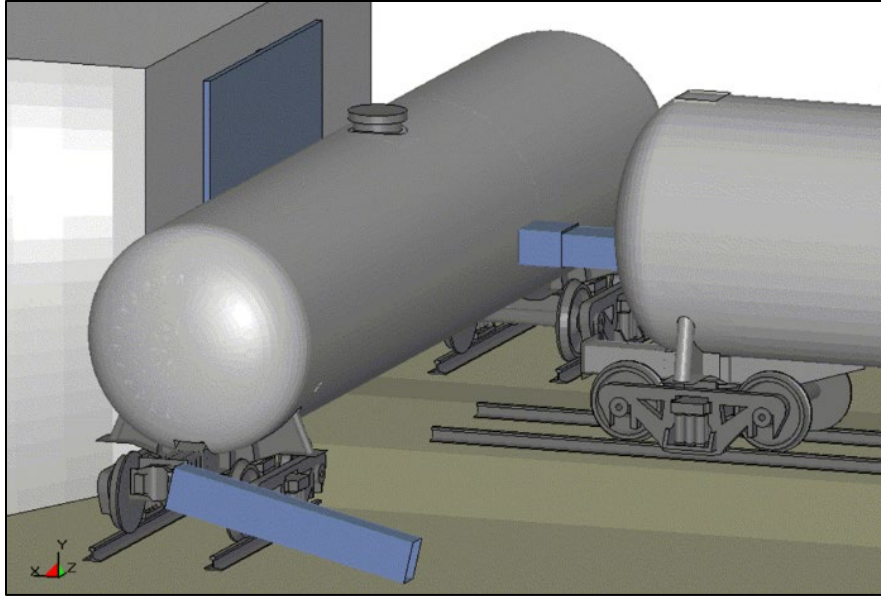


Figure 12. Test 0 – ARA Test 0 Impact Model

In addition to the pre-test analyses, the model was applied in post-test analyses to support the model development efforts. The post-test model was further updated to include the jacket, the jacket standoffs, correction of the commodity tank length, diameter and thickness, and the addition of the outrigger used to prevent vehicle rollover.

A lading model was included in the post-test model. A low strength viscoelastic material that filled the same volume as the lading in the test tank was used to represent the lading. This allowed the model to predict the momentum transfer of the lading, though no sloshing was supported by such a model. This model was not capable of modeling puncture. It was only used to study the structural response for a speed below puncture.

The models applied to Test 0 had several simplifications and assumptions applied. A model of the TTCI impactor car had not yet been developed, and a simplified rigid tank car model was used as the impactor surrogate in the ARA analyses. The correct mass of the impactor was applied, but the inertial characteristics were not accurately reproduced. Material test data was limited and approximate material behaviors for the tank, jacket, and insulation material were applied. No failure model was included in the analyses, and plastic strain levels were used to evaluate puncture risk.

The Volpe used Abaqus and LS-DYNA to create and solve the models with a top-down view, as [Figure 13](#) shows. The models used a surrogate rigid block (indicated in green) impacting a tank (i.e., manway, body bolster, draft sill, jacket, and thermal insulation were not modeled). However, the Volpe analyses considered a wider range of modeling approaches for the lading including Eulerian modeling (i.e., comparable to traditional computational fluid dynamics modeling).

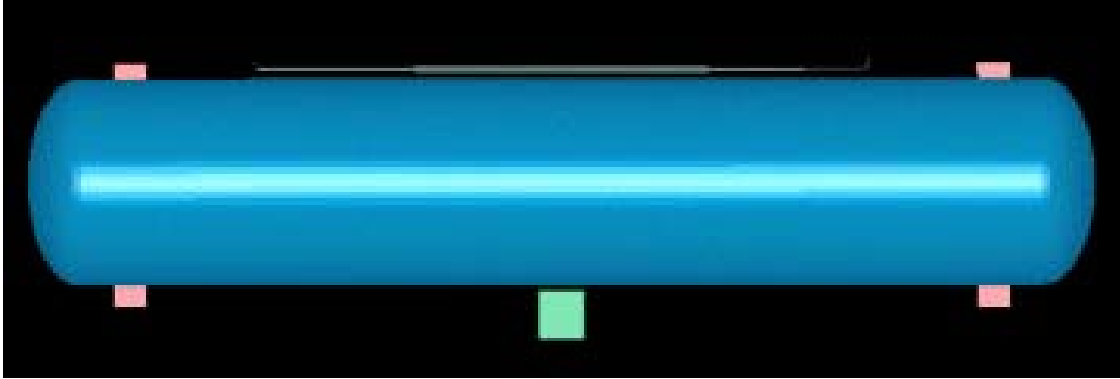


Figure 13. Test 0 – Volpe Test 0 Impact Model

3.3 Comparison of Test and Analysis Results

Due to the preliminary nature of the modeling at the time Test 0 was performed, only a single post-test simulation is presented in this report. The comparison of the Test 0 response with analyses identified features that needed to be accounted for in the modeling. One of these features was the modeling of the gap between the test tank car and the impact wall behind the tank. The test behavior results in a double impact response (i.e., two peaks in the force history). The first peak is the impact of the impactor car against the test tank car. The second impact is the test tank against the impact wall. Related to this impact, it was determined that the insulation properties of very low-density fiber insulation are more accurately (and easily) modeled by an air gap rather than using a crushable low-density foam material model. Thus, the combined gap between the tank and wall and the standoff distance between the jacket and tank shell produces a gap between the tank shell and wall for the secondary impact.

A second feature investigated was different modeling approaches for including the lading in the impact response. It was known that including the mass of the lading was important to include the inertial resistance of the impacted tank. The simplest and most computationally efficient approach is to smear the weight of the lading directly in the tank wall. In this approach, the lading weight is rigidly coupled to the tank motion. The alternate approaches involve explicitly modeling the lading inside the tank that allows a loosely coupled response that can include effects such as sloshing. An initial model was developed that included the lading using solid elements (i.e., Lagrangian model) for the lading, representing it as a soft elastomeric material.

Figure 14 shows a comparison of the measured and calculated force-displacement behavior for Test 0. The analysis shown is a post-test analysis with the preliminary explicit fluid model. The analysis shown was performed post-test, so it includes the measured impact speed. The overall agreement was good for the level of modeling fidelity and uncertainty at the time.

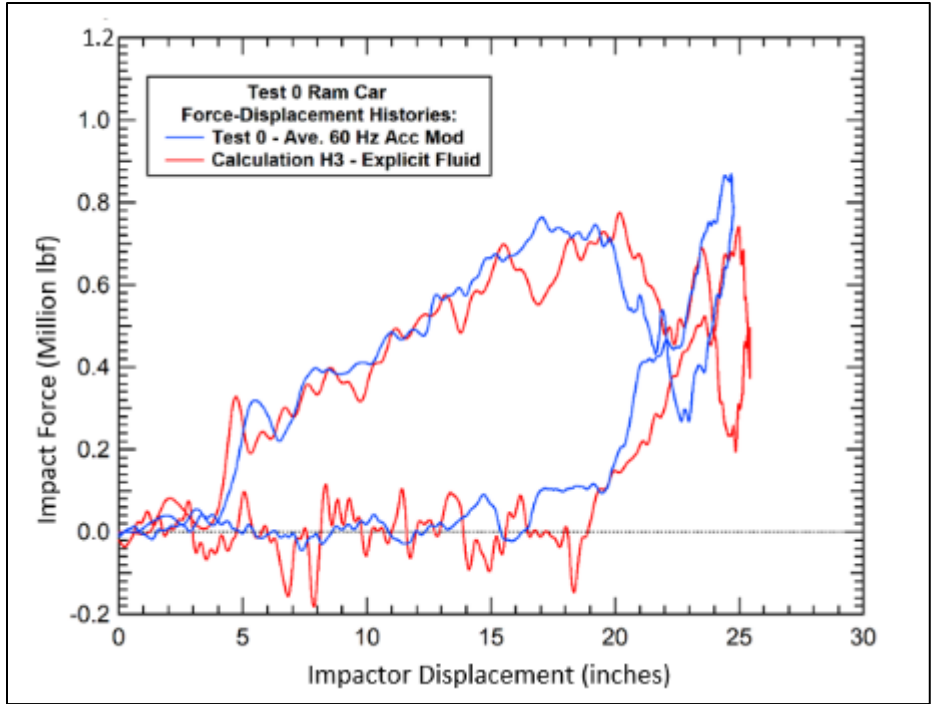


Figure 14. Test 0 – Comparison of Test 0 and ARA Post-Test Analyses

Figure 15 shows a corresponding comparison of the measured force-time history compared to the Volpe analysis. The comparison clearly shows the double peak force history caused by the collision dynamics of the tank impacting against the impactor and the collision wall. Again, the overall agreement was good for the level of modeling fidelity and uncertainty at the time.

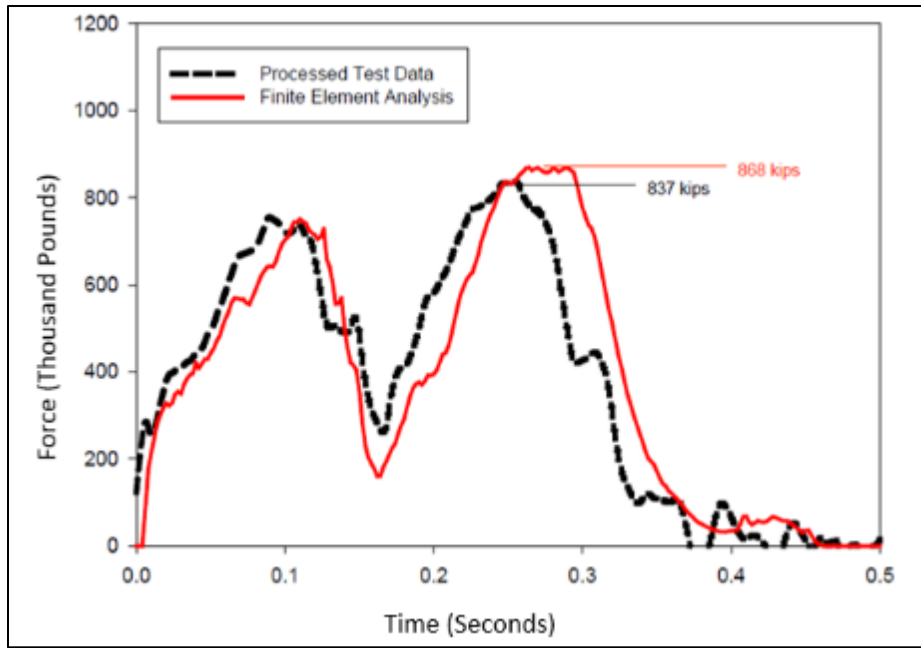


Figure 15. Test 0 – Comparison of Test 0 and Volpe Post-Test Analyses

3.4 Summary of Lessons Learned

Test 0 was a limited instrumentation assurance test performed before the first official planned test in the NGRTC program. No significant deficiencies were identified in this test that would postpone or significantly modify the planned Test 1. All channels successfully recorded data within their measurement limits. The actual impact speed was 0.4 mph below the targeted impact speed.

- The data provided by this test supported model development and verification to improve the physical predictions before the first fully instrumented test.
- Modeling the insulation as an air gap rather than crushable foam is appropriate for this type of fiberglass insulation.
- Modeling the lading effects is important and adding an explicit model for the lading that allows for a sloshing behavior provides enhanced fidelity.
- A sacrificial pipe in the brake supply line was installed on the impactor car. This pipe was fractured just before the impact of the tank car, and it was used to bring the impactor car to a halt after the impact. Having the brakes apply and stop the impactor car is important to avoid a second collision between the impactor and the tank car. There is a delay between the reduction in pressure and the application of the brakes. This delay is approximately 2 seconds and thus the brakes applied after the end of the impact event.
- The impactor was instrumented with strain gauges to measure longitudinal strains developed during the impact. It was stated that force could be inferred from the strain measurements.

4. Test 1 – DOT105A500W (April 26, 2007)

4.1 Summary of Test 1

Test 1 was performed as part of the NGRTC project on April 26, 2007, at the TTC. Test 1 was essentially a repeat of the Test 0 conditions but at a higher impact speed and with additional instrumentation in the test. Test 1 featured a 17,391-gallon DOT105 tank car struck by a 17-inch by 23-inch impactor centered on the tank. [Table 10](#) summarizes the specifications for the tested DOT105A500W tested tank car. The objective of the test was to quantify the deformation mode, impact load-time history and puncture resistance of a DOT105 tank car in a side impact. The test was performed by impacting an impactor car into the side of a ballasted chlorine tank car that was backed by a rigid impact barrier. The tank car was filled with clay-slurry to appropriate pressure and outage. The tank car was sitting on stub rails transverse to the test track and backed by an impact wall to resist the motion. Full instrumentation was installed to measure accelerations, strains, and displacements on the impactor and on the tank cars. [Figure 16](#) shows the tank car positioned against the impact wall with the impactor car's intended point of impact. Like Test 0, the tank car remained on its trucks and wheels for this test. [Table 11](#) lists the test conditions and outcomes for Test 1.

Table 10. Test 1 – DOT105A500W Tank Car Specifications

DOT105	Insulated, pressurized tank car
A	Top and bottom shelf couplers
500	500 psig test pressure
W	Fusion welded tank



Figure 16. Test 1 – Test Setup Showing Tank Car

Table 11. Test 1 – Test Conditions and Results Summary

Outage	10.4%
Target Speed	14.0 mph
Actual Speed	13.9 mph
Pressure	100 psi
Product	Slurry ($\rho=11.6$ lbs./gallon)
Impactor Dimensions	17'×23'
Impactor Weight	285,600 lbs.
Tank Car Weight (Estimated)	265,000 lbs.
Nominal Tank Thickness	0.77 in.
Nominal Jacket Thickness	11 gauge
Insulation and Thermal Protection	Ceramic fiber and fiberglass
Nominal Insulation Thickness	4.0 in.
Test Outcomes	Tank indented; impactor car rebounded

The objectives of this test and the subsequent Test 2 ([Section 5](#)) were to bound the impact conditions resulting in a puncture of the tank. The instrumentation in the impact tests were designed to measure the necessary accelerations, strains, displacements, and pressures to validate the tank car models. In many areas, sensors were placed to ensure redundancy in the critical information. A summary of the test was reported in the report for Test 2 (Witte, M., & Anankitpaiboon, S., 2007).

The desired impact speed of Test 1 was 14 mph, and the impactor car speed was measured optically at 13.9 mph using speed trap reflectors placed within 6 feet of the impact point. [Figure 17](#) shows the impact response in Test 1. The impact resulted in significant rotation of the target tank car during the test, which produced lifting forces on the front of the impactor car. Following the primary impact, there was a significant rebound of the impactor car from the tank car with a rebound speed of 7.6 mph. The tank car stayed upright throughout the test, but it did derail. The stub rail sections rolled over on the A-end, and the truck derailed on the B-end. The rebound of the impactor car was reacted by outriggers installed in the draft pockets of the car. Structural inspection after the impact showed no visible damage to the stub sills or their weld joints to the inner tank.



Figure 17. Test 1 – Shell Side Impact Behavior in Test 1 for Tank Car 3069

As predicted, the rigid impactor caused large dents in the outer jacket and the inner shell of the chlorine tank car without puncturing the inner tank. [Figure 18](#) shows the post-test dents in the jacket and in the commodity tank. The impact did result in the failure of one of the weld joints of the outer jacket near the impact area. The back of the tank car was also deformed by the reaction against the rigid impact barrier. The residual dent in the outer jacket was approximately 14 inches deep. The residual dent in the inner shell was approximately 10 inches deep.



Figure 18. Test 1 – Post-Test Dents in the Jacket and Shell of Tank Car 3069

4.2 Summary of Analyses

ARA's efforts to perform FE analyses for Test 1 are as follows. Due to the relatively short time interval between Tests 0 and 1, there was not a large model development effort. The ARA tank car model, as described in Test 0 above, was modified to include improved models of the jacket and jacket standoffs, improved outriggers, and refined mesh in the impact zone to better assess impact damage. Figure 19 shows the updated model of the DOT105 tank car. Another modification was the addition of an explicit model of the lading. The lading model consists of a low strength viscoelastic material that fills the same volume as the slurry added to the test tank.

The pre-test analyses supported the decision to select the target impact speed of 14 mph for Test 1. The calculated effective plastic strains for this impact speed were assessed to be below a level that would rupture the tank.

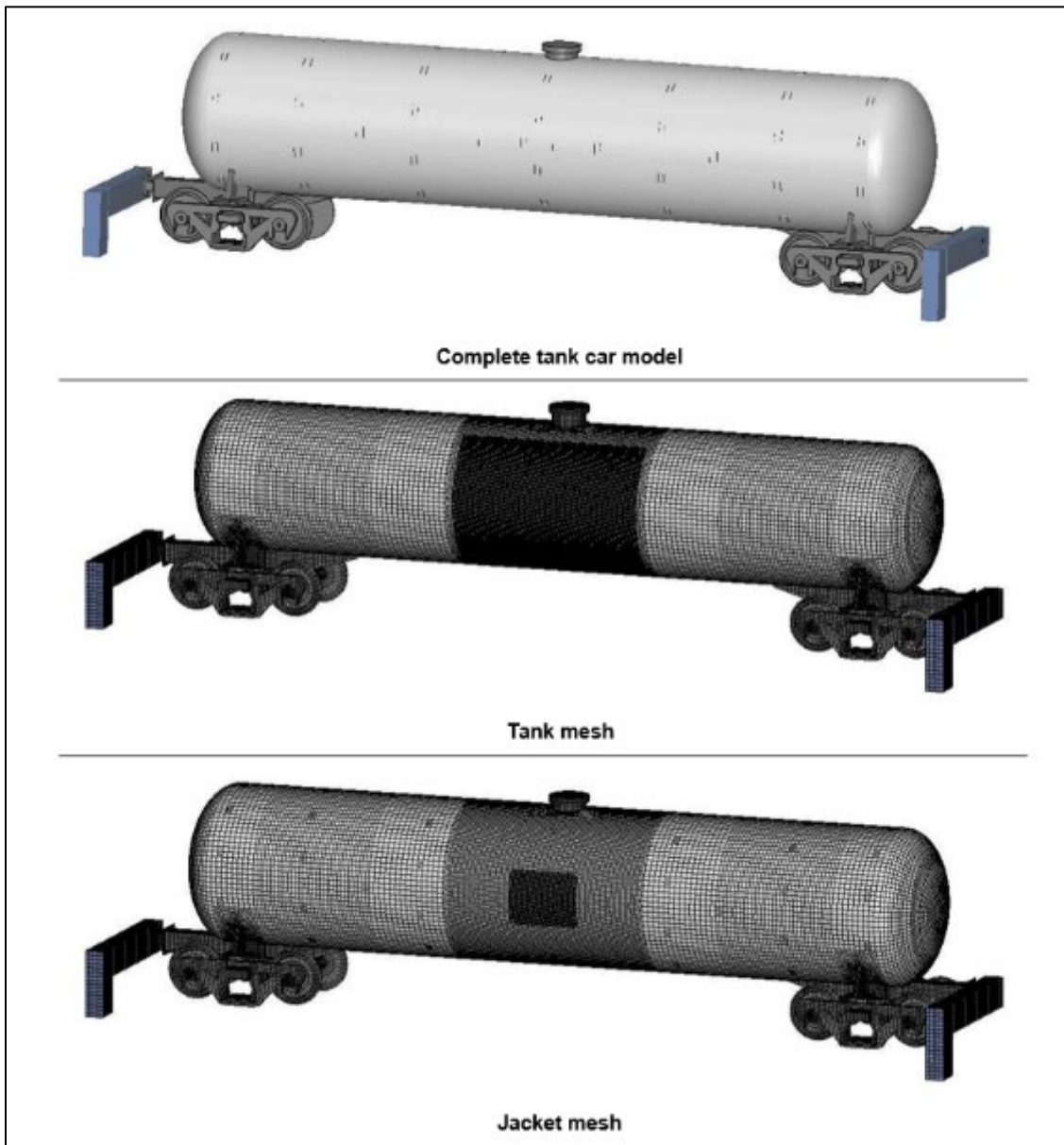


Figure 19. Test 1 – Updated Model Generated for a DOT105J500W Pressurized Tank Car

4.3 Comparison of Test and Analysis Results

Figure 20 shows the pre-test predicted impact response with the ARA model, including the sloshing of the lading model as seen in the cutaway view. This lading modeling approach was established to capture the momentum transfer of the coupled fluid-structure response but minimize effects such as breaking wave or splashing at the fluid free surface that can cause numerical stability problems.

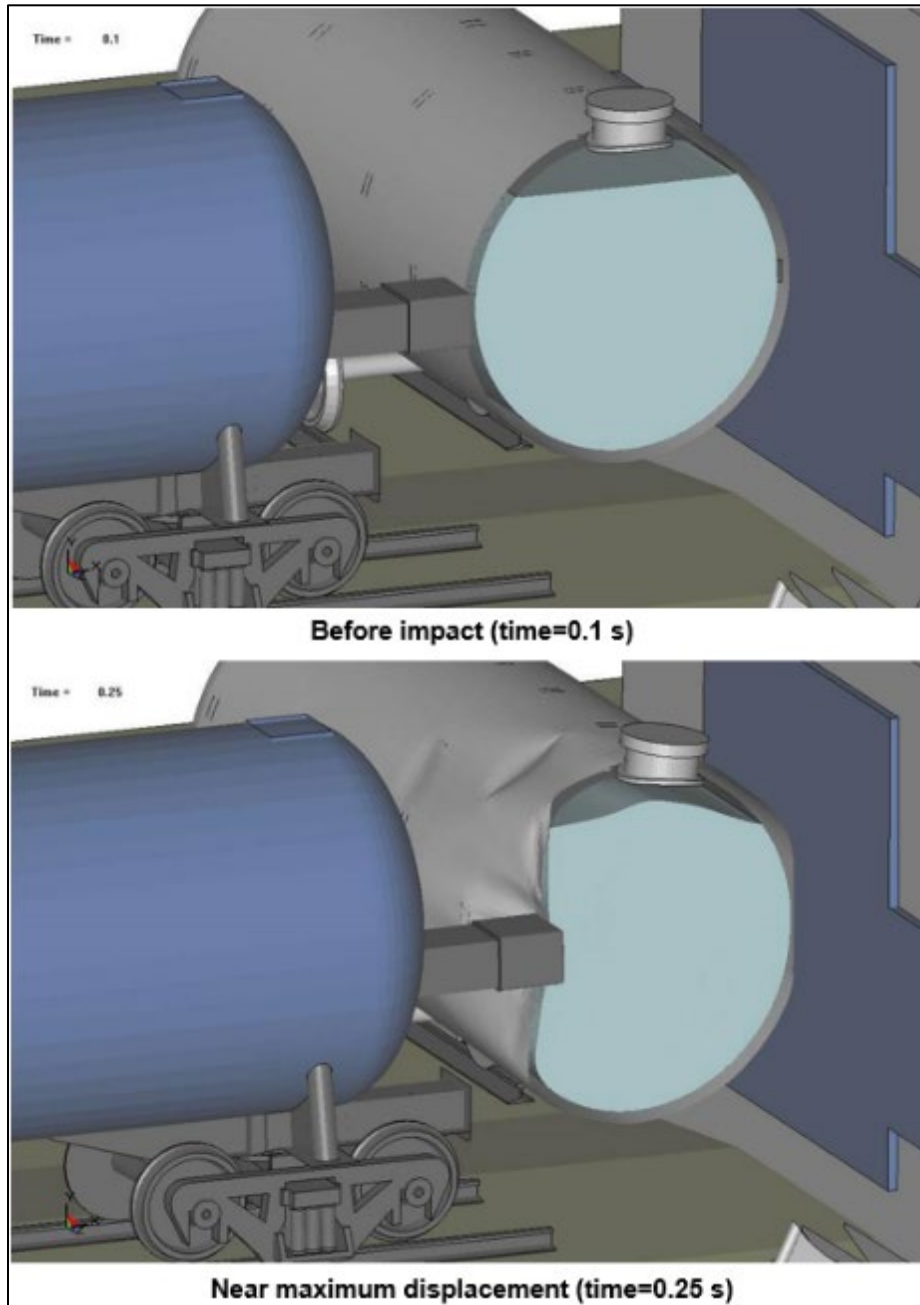


Figure 20. Test 1 – Calculated Test 1 Impact Response with Cutaway Showing Lading

Figure 21 shows a comparison of the pre-test predicted and measured impactor car acceleration history. The comparison shows that the characteristics of the double peak acceleration response and the quantitative comparisons of maximum accelerations agree reasonably well between the calculation and the test

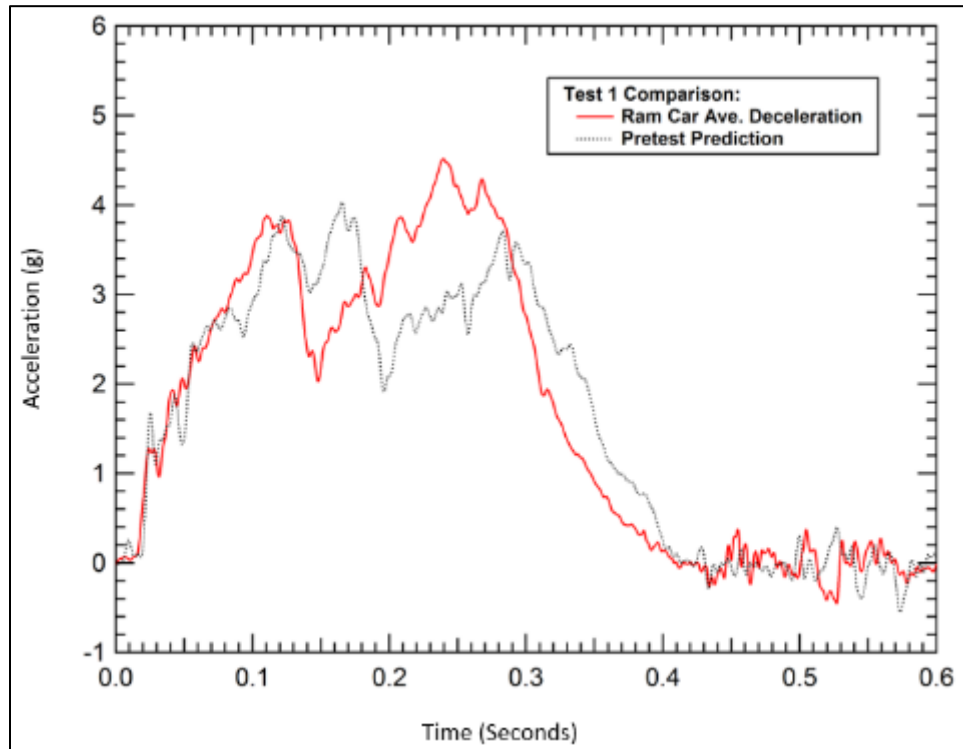


Figure 21. Test 1 – Comparison of the Measured and ARA’s Predicted Impactor Car Accelerations

A series of string potentiometers were included inside the tank to measure the tank deformations during the test. These measurements included a series of five string potentiometers spaced 18 inches apart longitudinally, centered on the impact location. In addition, a vertical string potentiometer was placed on the center line of the tank. All the string potentiometers successfully collected measurements of the tank distortions, with the exception of the vertical gauge that failed early in the impact response.

Figure 22 shows a comparison of the predicted and measured tank deformations. The solid lines are the predictions, and the dashed lines are the measurements. Overall, good agreement was obtained between the prediction and test. The 35-inch maximum impactor displacement, which was measured and plotted in Figure 24, corresponds to a 26-inch peak displacement in the belt line center position of the tank. The difference between these two values is primarily a result of the compaction of the space between the tank and jacket on the impact face and on the far side of the tank car between the tank and the impact wall.

The above comparison of the pre-test prediction and impact test serves as a validation of the model for the tank collision dynamics and impact deformation behavior. The responses include the initial impact, the reaction of the impact loads against the wall, and the post-impact rebound from the wall. Additional details of the impact behavior captured in the model included the target tank roll motion and lifting forces on the impactor car caused by the lateral support of the target tank truck on the stub rail sections and the action of the outriggers resisting a post-test rollover behavior.

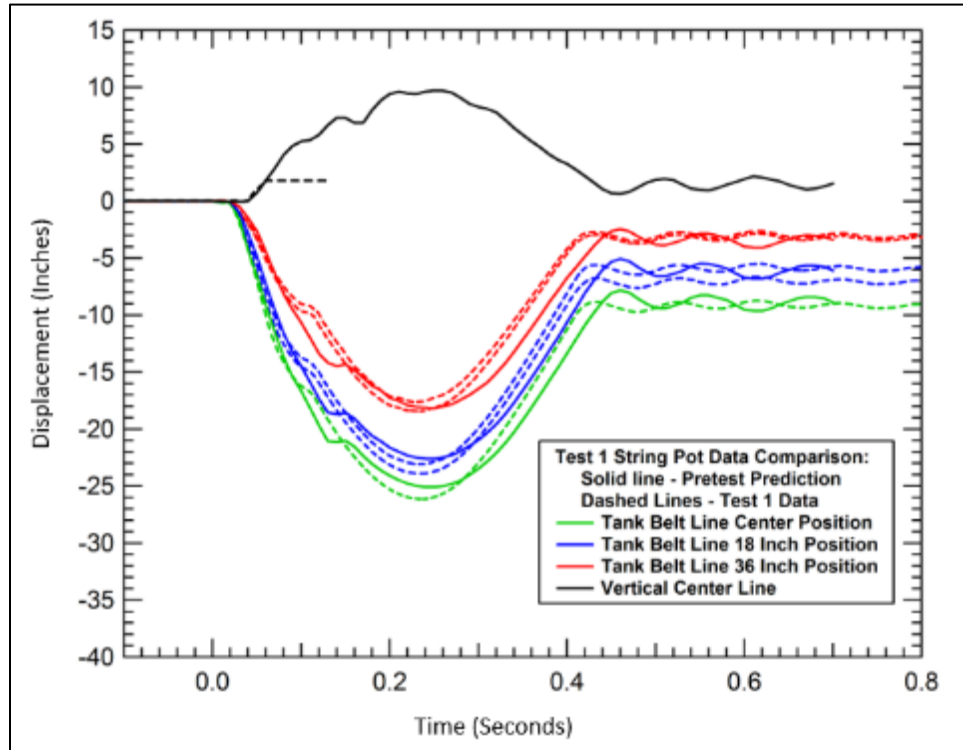


Figure 22. Test 1 – Comparison of the Measured and ARA’s Predicted Test 1 Tank Displacements

Figure 23 shows a corresponding comparison of the measured force-time history compared to the Volpe post-test analyses. The comparison clearly shows the double peak force history caused by the collision dynamics of the tank impacting against the impactor and against the collision wall. Figure 24 shows force-displacement results of the impactor. Again, the overall agreement was good for the level of modeling fidelity and uncertainty at the time.

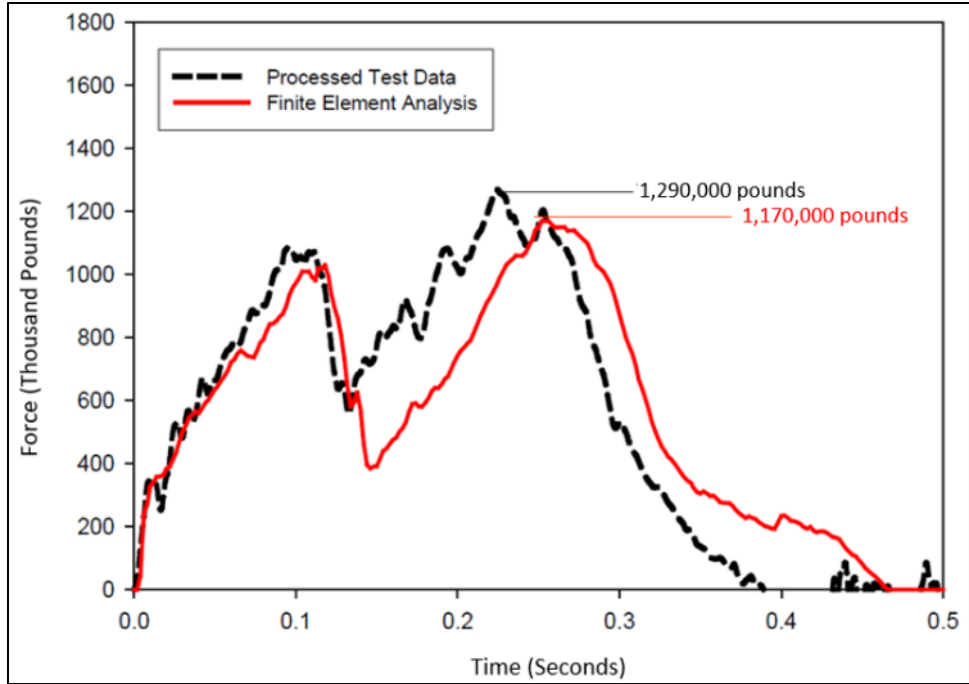


Figure 23. Test 1 – Comparison of Test 1 and Volpe Post-test Analyses

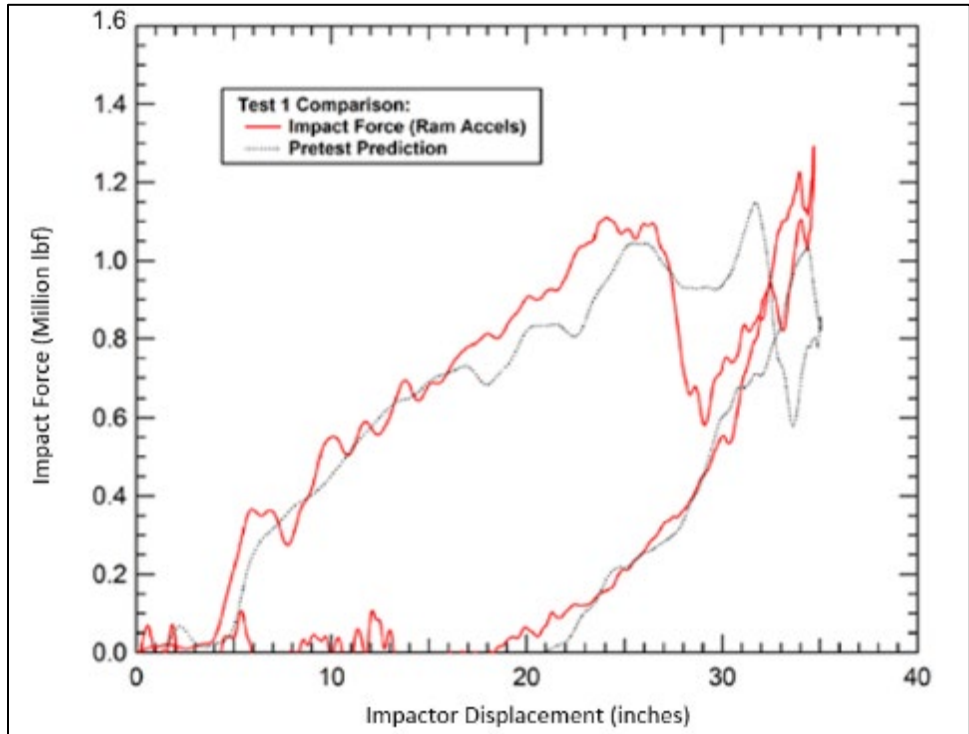


Figure 24. Test 1 – Test vs. Analysis Comparison of Force-Displacement Plot

4.4 Summary of Lessons Learned

Test 1 was successfully performed with a high percentage of data channels successfully collected. The actual impact speed was 0.1 mph below the targeted impact speed. The test provided a significant amount of data to support the analysis methodology development and validation.

Tape switches were installed on the leading face of the impactor and were backed only by the face of the impactor itself. It was believed that the jacket of the tank car dented in such a fashion that the tape switch never closed while contacting the tank car and never produced a trigger signal for some of the DAQ systems. The result of not receiving a trigger signal was loss of data within the DAQ system by new data overwriting old data. To prevent future data loss, a small wooden block was placed between the tape switches and the tank car to assure triggering.

Two of the high-speed cameras malfunctioned and did not produce data. One malfunction was due to a trigger wire fault and the other was due to inadvertent loss of power before the video data was permanently stored from its volatile memory. Because of redundancy in the views, no critical data was lost, but the loss of video data showed that precautions needed to be taken to prevent such failures in future tests. These precautions included enclosing signal wires routed on the ground in conduit to prevent damage and using a locking power connector on the cameras. Also, the seismic activity of the impact caused movement in some of the cameras, causing the image to sway. It was suggested a camera with stiffer mounting brackets be used for future tests. By adding redundant triggers to the camera network, reliability would be increased. Artificial lighting was considered to reduce shadowing on the overhead view.

There was a significant rebound of the impactor car from the tank car. The impactor car rebounded backward at a speed of 7.6 mph and stopped approximately 81 feet away from the tank car. The impactor car brakes triggered and set as anticipated, which kept the impactor car from rolling forward (downhill) for a second impact.

The tank car also experienced a large elastic rebound away from the wall after impact. The outriggers functioned as intended to keep the tank car upright. The impact caused both trucks to derail from the stub tracks. The stub track sustained damage because of the impact and the derailment. The ties were damaged and split on both ends of the tank car, and the rail had rolled over and spikes were loosened at the A-end of the tank car.

The vertical string potentiometer inside the tank failed during the test. This appeared to have been caused by the test preparation during which most of the string travel was taken out before the string was tied off. This resulted in the string potentiometer reaching the end of its travel before the tank completed its deformation. A transducer with 40 inches of travel is expected to be sufficient for such a measurement in future tests.

Another concern raised by this test is the potential high speeds (and impact energies) that would be required to exceed the puncture threshold of the DOT105 tank car or future tank cars with enhanced puncture resistance. Test team determined that the 17-inch by 23-inch impactor used in Tests 0 and 1 was too blunt to puncture the tank car within a safe and reliable speed. As a result, a new impactor end was specified with the impact face reduced to 6-inch by 6-inch for the subsequent puncture test. This size was selected to keep the puncture test speed near 14 mph, which was the target speed for Test 1.

There were significant concerns related to the adequacy of the impact barrier and the anti-roll performance of the outriggers. The rigid support barrier, the stub rails, and the outrigger anti-roll bars proved to perform adequately for the 10 mph impact of Test 0 and the 13.9 mph impact of Test 1. However, large carbody roll motions occurred in Test 1; therefore, for future tests at higher impact speeds, the tank car would not be left on its trucks due to concerns about carbody roll, accounting for all the energy in the system and rebound of the impactor car.

Conducting the impact test while having the freight trucks under the tank car allows the tank car's body to roll during the impact event, causes the freight truck suspension to absorb and dissipate some of the impact energy, and may contribute to the rebound of the impactor car. The carbody roll also causes edge loading of the impactor and extreme vertical loading of the impactor car suspension upon rebound, which may result in the derailment of the impactor car. Additionally, potential rollover of the tank car after rebounding from the impact wall was a concern. Not only was the derailment risk, edge loading, and potential rollover a big concern, but having the tank car on its trucks added complexity to the overall collision dynamics in the test and negatively affected the repeatability and reproducibility of the impact behavior during the test. This was a significant lesson learned from this test related to the suitability of this test protocol for continued use in Advanced Tank Car Collaborative Research Program (ATCCRP) and tank car safety testing.

Following are some of the conclusions that were made after the completion of Test 1:

- The test protocol will be modified to simplify the tank support conditions and lower the tank to better align the tank height, impactor height and impactor car center of gravity.
- Modeling will be applied to design a new smaller impactor to be used in subsequent analyses.

5. Test 2 – DOT105A500W (July 11, 2007)

5.1 Summary of Test 2

The side impact Test 2 was performed on July 11, 2007, at the TTC. Test 2 featured a 17,401-gallon DOT105 tank car struck by a tapered 6-inch by 6-inch impactor centered on the tank (Witte, M., & Anankitpaiboon, S., 2007). [Table 12](#) contains the specifications for the tested DOT105A500W tank car. The test was performed by running an impactor car into the side of a ballasted chlorine tank car that was backed by a rigid impact barrier. The tank car was filled with a clay-slurry to the appropriate pressure and outage. The test procedure was modified for Test 2 by lowering the tank position and mounting rigid support skids to the body bolster as [Figure 25](#) shows. The primary objective of these modifications to the target tank car and impactor car was to create a test procedure that was controlled, repeatable, and eliminated the post-impact roll of the tank.

Table 12. Test 2 – DOT105A500W Tank Car Specifications

DOT105	Insulated, pressurized tank car
A	Top and bottom shelf couplers
500	500 psig test pressure
W	Fusion welded tank



Figure 25. Test 2 – Tank Car 3074 Mounted on Support Skids

The objective of this test (combined with Test 1 described in [Section 4](#)) was to bound the impact conditions resulting in a puncture of the tank. Since Test 1 was below the puncture threshold, the objective of Test 2 was an impact sufficient to puncture the tank. The results of the first three impact tests (Tests 0 to 2) were expected to generate sufficient data for a quantifiable description

of the shell impact performance of the DOT105 tank car. A summary of the test was reported in the report for Test 2 (Witte, M., & Anankitpaiboon, S., 2007).

The impactor car was also modified before Test 2 by lowering the position of the impactor arm and adding the modified impactor head with a much smaller contact area, as [Figure 26](#) shows. The impactor arm was lowered (as was the target tank car) to more closely align the height of the centers of gravity (CG) of the target tank, impactor car and the line of impact. The modified impactor face was 6-inch by 6-inch square and had 1/2-inch radius on all edges and corners compared with the 1-inch radius of the 17-inch by 23-inch impactor used in Tests 0 and 1. The modified impactor significantly lowers the required impact speed to puncture the target tank and helps to establish an upper bound on the puncture conditions within safe limits for the test facility.



Figure 26. Test 2 – Modified Impactor Car and Impactor Head Used in Test 2

The targeted impact speed for Test 2 was 15 mph, and the actual impact speed in the test was 15.2 mph, which was 0.2 mph above the targeted speed. [Figure 27](#) shows the post-test condition of the tank car. As expected, the impact at this speed punctured the tank car. [Table 13](#) summarizes the impact conditions and outcomes of Test 2.

The post puncture energy was sufficient to push the tapered impactor head fully through the tank shell, creating an opening approximately equal to the cross-section dimensions of the impactor arm, about 21 inches wide and 32.5 inches high. The modified tank car support skids produced an impact response where the car stayed upright throughout the test and exhibited very little body roll.

Full instrumentation was installed to measure accelerations, strains, displacements, and pressures on the impactor and on the tank cars. High-quality data was collected in the test for model validation. There were no strain gauges on the impactor of the impactor car for Test 2.



Figure 27. Test 2 – Puncture Response Observed in the Full-Scale Impact Test 2

Table 13. Test 2 – Test Conditions and Results Summary

Outage	10.4%
Target Speed	15 mph
Actual Speed	15.2 mph
Pressure	100 psi
Product	Slurry ($\rho=11.6$ lbs./gallon)
Impactor Dimensions	6 in. \times 6 in.
Impactor Weight	285,400 lbs.
Tank Car Weight (Estimated)	265,000 lbs.
Nominal Tank Thickness	0.77 in.
Nominal Jacket Thickness	11 gauge
Insulation and Thermal Protection	Ceramic fiber and fiberglass
Nominal Insulation Thickness	4.0 in.
Test Outcomes	Tank indented and punctured

5.2 Summary of Analyses

ARA’s efforts to perform analysis are described as follows. For Test 2, modifications were made to the tank car and impactor car models to match the test conditions. These modifications included the attachment of the skirts to the tank car and the creation of a more detailed impactor car model and new impactor head, as [Figure 28](#) shows. The new impactor car model was important to accurately simulate the collision dynamics that are influenced by the relative inertial properties of the

impactor car and of the tank car (e.g., the relative CG heights). These models were applied pre-test in support of the modified test procedure and to predict the outcome of the test.

At the time Test 2 was performed, a detailed fracture model was not yet incorporated for prediction of the puncture energies. At the time of the test, the predictions were performed where failure of the tank was suppressed, and the calculated damage levels were used to assess whether puncture initiation was likely.

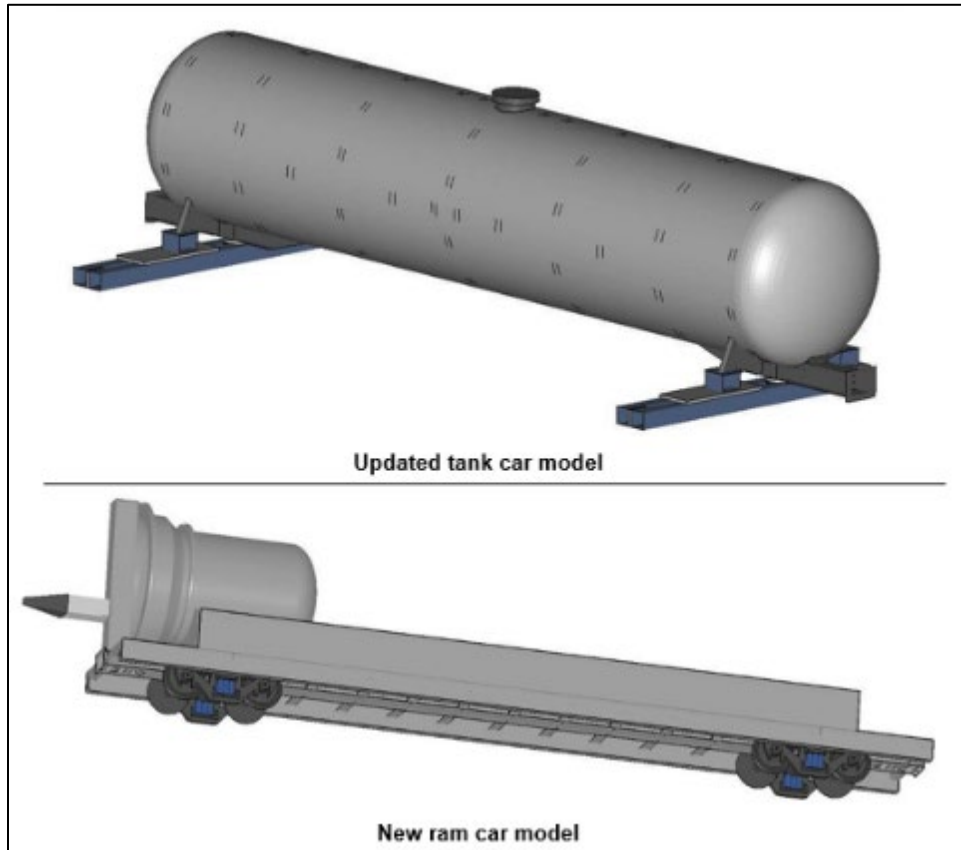


Figure 28. Test 2 – Updated Tank Car and Impactor Car Models for Test 2

In the post-test model, a piecewise linear elastic-plastic constitutive model was modified to include the B-W failure criterion. Such a model would be capable of predicting nonlinear stress-strain behavior of the material as it plastically deforms and fractures. Furthermore, it would be able to predict failure of the material, which depends on the state of stress and plastic strain history in the material. The potential material failure mechanism was assessed, and it was thought that shear fracture behavior would be important for tank car puncture, and thus, the B-W failure criterion was selected over other failure criteria.

5.3 Comparison of Test and Analysis Results

Figure 29 shows an example of the ARA pre-test prediction of the tank damage for Test 2. The maximum plastic strain in this test was predicted at approximately 50 percent under the 6-inch by 6-inch impactor at the inside surface of the tank for the 14-mph impact. From this strain level, it was determined that there was a high confidence that the impact speed selected for Test 2 would result in a puncture of the target tank.

Acceleration data of the impactor car was averaged, then filtered and finally multiplied by the impactor weight to calculate impactor force. Figure 30 compares the pre-test prediction of the force-deflection characteristics to the measured Test 2 force-deflection curve. Again, the agreement was very good up to a post-impactor displacement of approximately 23 inches, at which time the impactor punctured the tank wall and the measured force dropped dramatically. This comparison, along with the Test 1 comparison and the evaluation of many other quantitative measures from both tests, validated the ability of these models to accurately capture the impact response up to the point of fracture initiation. The development of accurate fracture modeling capabilities was identified as an important need for the program at this time.

Figure 31 compares the force-displacement results from the test and post-test analysis with the B-W failure criteria implemented.

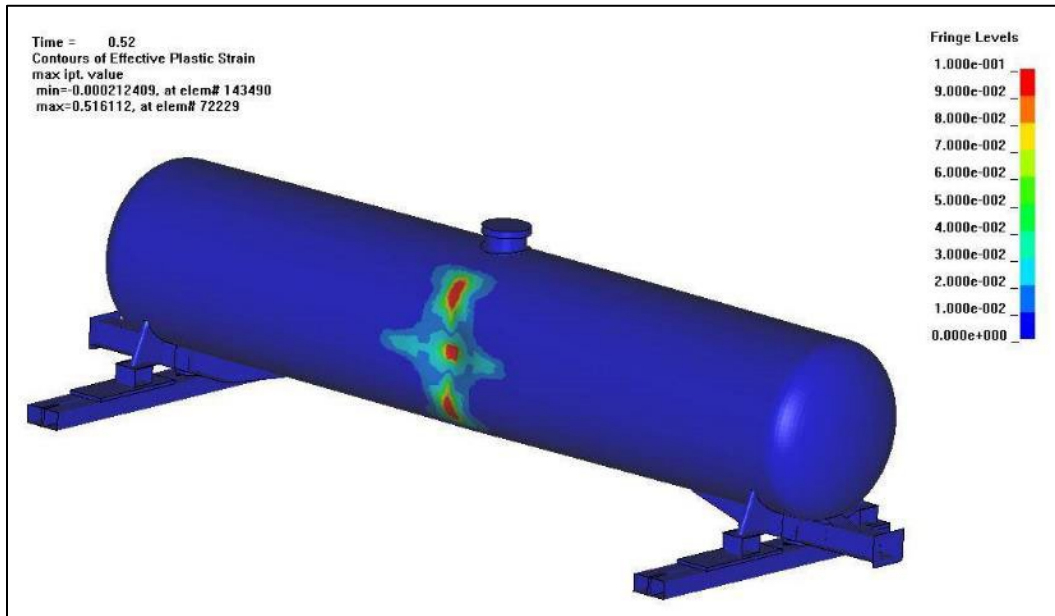


Figure 29. Test 2 – ARA’s Predicted Tank Damage for the Impact Conditions

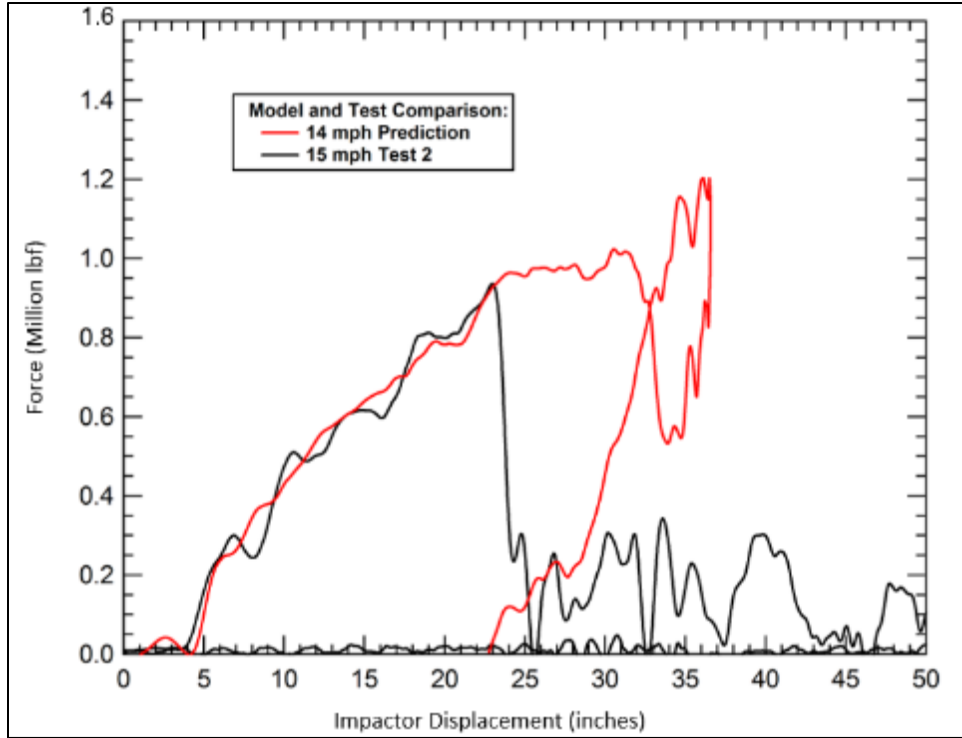


Figure 30. Test 2 – Comparison of Measured and ARA’s Predicted Force-Displacement Response

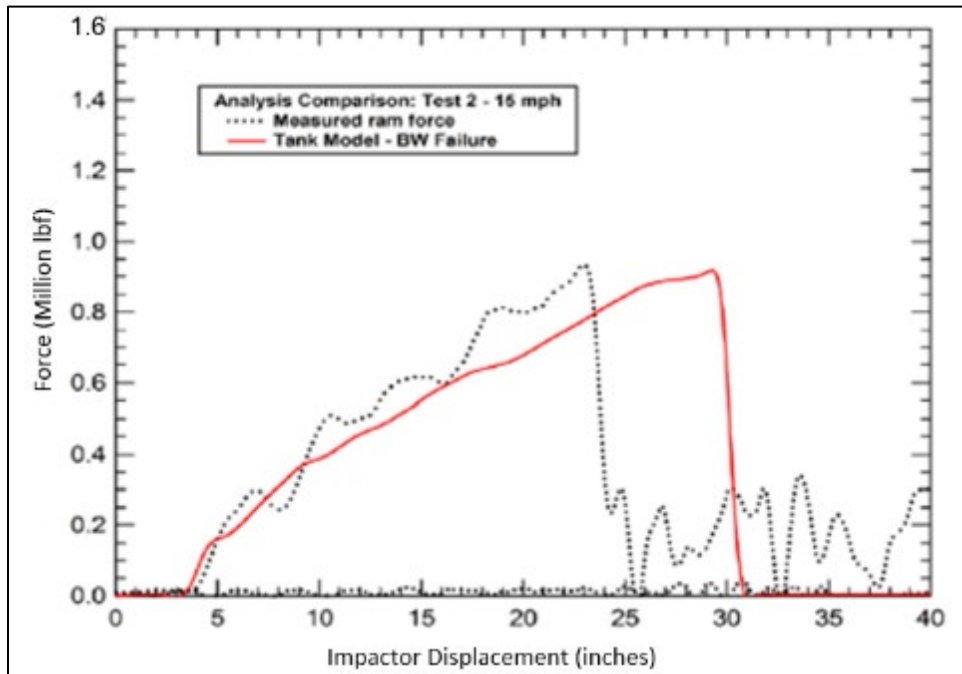


Figure 31. Test 2 – Test vs. ARA’s Post-Test Analysis Comparison of Force-Displacement Plot

5.4 Summary of Lessons Learned

Test 2 was successfully performed with a high percentage of data channels successfully collected. The actual impact speed was 0.2 mph below the targeted impact speed. The test provided a significant amount of data to support the analysis methodology development and validation.

Tests 0 and 1 were performed while the tank car remained on its trucks. There was an issue regarding the speed dependent edge loading of the impactor due to tank car roll and vertical loading of the impactor car due to impactor car rise, which accompanies the tank car roll. The method of remediation was to change the support system of the tank car and to improve the vertical alignment of both cars' CG with the line of action of the impactor. The Test 2 impact response (and associated analyses) showed little tendency to roll and did not result in significant lifting forces on the impactor car. The simplified support of the tank resulted in a more controlled repeatable impact response. The tank car came to rest while in contact with the barrier after the impact of Test 2. From Test 2 onward, the trucks were removed, and skids were mounted to the tank car. In addition, the tank car was lowered as far as practical, but still high enough to avoid the belly of the car to interact with the ground during impact.

All major components of the impactor car performed as intended. The impactor itself did exhibit a small amount of material flow on the high stress corners where it penetrated the tank car. Metal flow at the top eastern corner of the impactor was noted. This portion of the impactor was constructed from high-strength steel, but large forces concentrated on small corners were enough to deform its surface. The bulk of the impactor and impactor car appeared to have responded within the elastic region. The smaller impactor resulted in reduced speeds required to puncture the tank.

ARA's FE model had to be updated to match the test conditions, and thus, the trucks were replaced with skids. A new impactor car model with a new impactor head was also constructed. An update to the model of the impactor car was necessary to accurately simulate the collision dynamics, which are dependent on the relative inertial properties of the impactor car and tank car. For example, it was important to model the relative CG heights of the impactor car and tank car accurately.

The inclusion of a failure criterion to the FE model was another important addition to the FE model. The post-test model included the B-W ductile failure model, which was used to study the puncture of the tank car in more detail. One of the simplifications made to this model was to use planes of symmetry, and thus, only model a section of the tank car. The second simplification involved changing the model of the lading from an explicit definition of the lading to a model where the weight of the lading was uniformly distributed to the surrounding tank wall. The results were not significantly influenced by this simplification. The third simplification was made by only modeling the impactor head with the full weight of the impactor car.

This was the first test in which a trigger light was installed on the tank car for video recording. This feature visibly identified the instant of contact between the impactor and the tank car's jacket on the videos.

The following conclusions were made after the completion of Test 2:

- The selection of the impactor geometry is an area of ongoing interest. The impactor size distributions in real world derailments and impact resulting in tank releases are not known. The 6-inch by 6-inch impactor is representative of a smaller impactor seen in real world punctures, such as a broken rail or a coupler shank from a broken coupler.
- The selection of a 6-inch by 6-inch impactor size is important for future research since the design for different tank protection strategies will be different to protect against impacts of large blunt impact objects compared to small sharp impactors.
- The analysis capabilities for modeling tank car impact behaviors are reasonably accurate at the time. However, the ability of the models to determine the conditions that will result in a puncture of a tank are not as equally developed. Additional material damage and failure model development is identified as a need for the tank car safety research program.

6. Test 3 – DOT105J500W with Protective Panel (May 18, 2011)

Test 3 featured a DOT105J500W tank car equipped with a protective sandwich panel. [Table 14](#) summarizes the tank car specifications.

Table 14. Test 3 – DOT105J500W Tank Car Specifications

DOT105	Insulated, Pressurized Tank Car
J	Jacketed Thermal protection ⁷
500	500 psig Test Pressure
W	Fusion welded tank

This test was intended to evaluate the potential improvement in puncture resistance that could be offered by an engineered metal structure installed on a DOT105 tank car’s shell. The 6-foot by 6-foot sandwich panel was hung using cables from the manway in the center of the tank car, as [Figure 32](#) shows. The sandwich panel was attached in this manner to allow it to “flex” in response to the impact.



Figure 32. Test 3 – Test Setup Showing Tank Car and Impactor

⁷ In addition to thermal protection, the tank had tank headshields, top and bottom shelf couplers. These features did not contribute to the structural response during the shell impact test.

The panel was fabricated from 3-inch outer diameter, 0.083-inch-thick ASTM A1010 steel pipes stacked together and slot welded to 0.12-inch thick ASTM A1010 face sheets. The face sheet was continuous on the outer surface and used 3-inch-wide strips running circumferentially with 3-inch spacing on the inside surface. The protective panel weighed approximately 900 pounds, which is approximately equivalent in weight to a 0.6-inch-thick steel plate covering the same surface area.

6.1 Summary of Test 3

Table 15 summarizes the impact conditions and outcomes of Test 3.

Table 15. Test 3 – Test Conditions and Results Summary

Outage	10%
Target Speed	18.0 mph
Actual Speed	17.8 mph
Pressure	100 psig
Product	Water
Indenter Dimensions	12 in. × 12 in., 1 in. radius fillet
Impactor Weight	295,725 lbs.
Tank Car Weight (Estimated)	206,600 lbs. ⁸
Nominal Tank Thickness	0.78 in.
Nominal Jacket Thickness	11 gauge
Insulation and Thermal Protection	Ceramic fiber and fiberglass
Nominal Insulation Thickness	4.0 in.
Test Outcomes	Tank not punctured, impactor car rebounded

An objective of this test was to verify if a metal protective panel that was retrofitted over the existing jacket would be able to prevent the inner tank from getting punctured at speeds higher than in previous tests. The test speed of 17.8 mph was not expected to result in puncture of the inner tank if the sandwich panel performed as intended. Material information about the components and the fabrication process of the panel can be obtained from the detailed Test 3 report (Carolan, et al., 2013). The center point of the panel was positioned such that it aligned with the center point of the 12-inch by 12-inch impactor. Also, the dimensions of the panel were chosen to distribute the energy coming from the impactor striking the panel rather than concentrating on the impact location.

⁸ The estimated tank car weight in Test 3 was lower than that of Test 2 as Test 3 (and all subsequent tests) used water as the lading in the tank, where Tests 0–2 used a clay slurry having a higher density than water.

The impact dented and tore the protective panel, dented the tank car jacket, and dented the commodity tank as shown in [Figure 33](#) and [Figure 34](#). The tank was not expected to puncture, and the tank did not puncture, although a crack initiated in a weld seam near the contact area. The contents of the tank were not released due to this impact.



Figure 33. Test 3 – Damage to Protective Panel



Figure 34. Test 3 – Deformation to Jacket and Tank

The number of transducers for this test was very limited compared to the number of transducers used in Test 1 and Test 2. Only 11 accelerometers and 2 pressure transducers were used for this test.

6.2 Summary of Analyses

Volpe performed the pre- and post-test FEA for this test. A series of FE models of sandwich panels evaluated at the component level were created leading up to Test 3 and are described in the detailed test report (Carolan, et al., 2013). The FE modeling performed in support of Test 3 used the Abaqus/Explicit software, version 6.10. The sandwich panel geometry was incorporated into an FE model of the DOT105 tank car. [Section 6.3](#) compares the post-test analysis results to

the test results. The results from this test were intended to develop a procedure for testing and modeling for future tests. With improved correlation between FEA models and test results, FEA models could be used to significantly reduce the number of impact tests in the future.

A detailed description of the FE model developed for Test 3 was not included in the Test 3 report (Carolan, et al., 2013), as that report included considerable discussion of the development of the sandwich panel designs.

6.3 Comparison of Test and Analysis Results

This report presents a limited set of results. Results from the FE model were compared to the measured results. Acceleration data of the impactor car was averaged, then filtered and multiplied by the impactor weight to calculate the impactor force. Figure 35 shows the force-displacement results of the impactor.

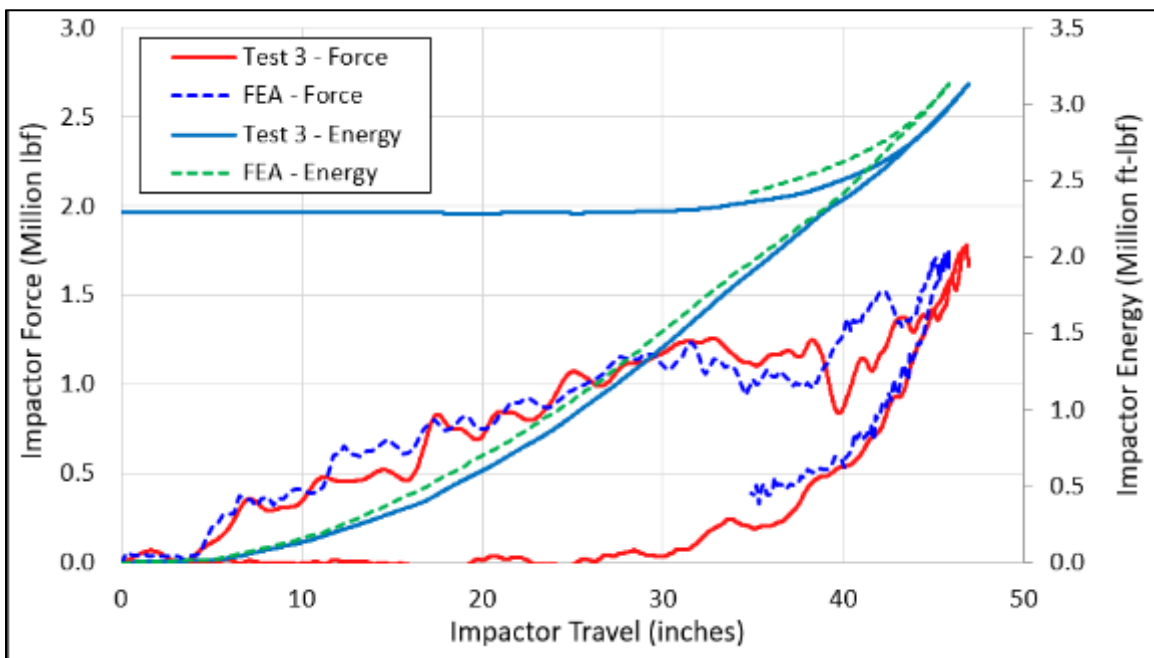


Figure 35. Test 3 – Test vs. Analysis Comparison for Force-Displacement Plot

6.4 Discussion and Lessons Learned

This test had the highest impact speed among the 11 tests discussed in this report. The impact speed was 17.8 mph. Since the weight of the impactor car remained fairly constant, this test also had the highest amount of kinetic energy (i.e., 3.13 million foot-pounds). From the tank car point of view, having a protective panel provided an additional layer of resistance to puncture in two ways. The protective panel enhanced the tank car shell's puncture resistance by blunting the impactor's pressure. A 12-inch by 12-inch impactor with 1-inch rounded corners was used during the test, and the protective panel distributed the impactor's pressure into a larger contact region on the tank's shell. This larger contact region prevented localized pressure from initiating and propagating into a puncture. Additionally, the panel itself absorbed some amount of the kinetic energy of the impact, thereby reducing the energy that needs to be absorbed by the tank. While the tank did not puncture, a post-test inspection of the circumferential weld in the impact

zone revealed cracking in the weld. This crack did not fully penetrate the thickness of the tank's shell, and the lading was not released.

Test 3 was the first test to use the 12-inch by 12-inch impactor. This impactor was designed as a "cap" that would fit over the existing 6-inch by 6-inch impactor. The 12-inch by 12-inch impactor was designed to be removable, so future tests could make use of either impactor. Since the 12-inch by 12-inch impactor fits over the existing 6-inch by 6-inch impactor, the total weight of the impactor car will be higher for any test using the larger impactor.

Shielding was provided for all external instrumentation near the point of impact. The intent was to provide protection from high-speed liquid ejecting from inside the tank. For sensors such as accelerometers, welded or bolted shields were used. For cameras near the impact zone, high strength clear plastic shells were used. Ultimately, this protection was not necessary for this test, as the tank did not puncture.

This was the first test to feature a ruggedized camera on board the impactor car, focusing on the tip of the impactor. This video was helpful for observing the behavior of the sandwich panel. The onboard video camera was added to the standard instrumentation plan for future tests.

7. Test 4 – DOT111A100W (December 18, 2013)

7.1 Summary of Test 4

On December 18, 2013, the research team performed Test 4 at the TTC. Test 4 featured a DOT111A100W tank car that was equipped with an insulating jacket, insulation materials between the tank and jacket, and external heating coils. The 24,081-gallon DOT111 tank car was struck by a 12-inch by 12-inch impactor centered on the tank side. The test was performed by running the impactor car into the side of a ballasted chlorine tank car filled with water that was backed by a rigid impact barrier. [Figure 36](#) shows the tank car configuration before the test. [Table 16](#) contains the tank car specification.



Figure 36. Test 4 – Target Tank Car Mounted on Support Skids

Table 16. Test 4 – DOT111A100W Tank Car Specifications

DOT111	Unpressurized Tank Car
A ⁹	Top and Bottom shelf couplers
100	100 psig Test Pressure
W	Fusion welded tank

This test was the first shell impact test performed on a tank car built to a specification other than DOT105. The DOT111 tank car is also referred to as a general-purpose tank car and is typically used to transport commodities that are liquids at atmospheric pressure. Thus, the DOT111 is

⁹Despite the separator character “A,” this tank was jacketed and had heating coils and sloped shell rings.

considered an unpressurized tank car, even though it is designed to withstand internal pressure. The purpose of this test was to evaluate the DOT111 tank car's performance in a side impact scenario and to perform validation of FEA models for tank car impact and puncture behaviors. Figure 37 shows the test setup. The tank was supported on skids attached to the tank at the bolsters and center plate. The skids allowed the tank to freely slide on the ground, but resist rolling motions, and contribute to the controlled impact dynamics of the tank car.

Figure 38 shows the impactor car and impactor head. This photograph was taken before the test. Additional reinforcement was added to the impactor car end underframe before Test 3, increasing the weight by approximately 10,000 pounds.

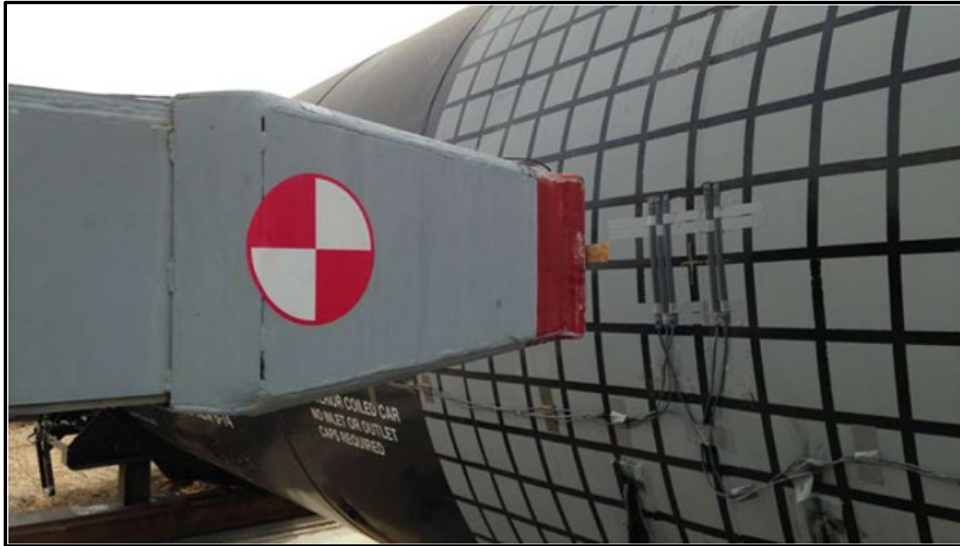


Figure 37. Test 4 – Test Setup Showing Tank Car and Impactor



Figure 38. Test 4 – Impactor Car Configuration Before Test

Table 17 summarizes the impact conditions and outcomes of Test 4.

Table 17. Test 4 – Test Conditions and Results Summary

Nominal Outage	3%
Actual Outage	2.0–2.3%
Target Speed	14 mph
Actual Speed	14.04 mph
Pressure	Atmospheric
Product	Water
Impactor Dimensions	12 in.×12 in.
Impactor Weight	297,125 lbs.
Tank Car Weight (Estimated)	270,200 lbs.
Nominal Tank Thickness	0.44 inch – A515-70 plate
Actual Tank Thickness	0.40 in.
Nominal Jacket Thickness	11 gauge
Insulation and Thermal Protection	Ceramic fiber and fiberglass
Nominal Insulation Thickness	4.0 in.
Test Outcomes	Tank indented and punctured, Impactor car continued into tank

As a result of the impact speed of 14 mph, the rigid impactor dented and punctured the jacket and the shell of the DOT111 tank car. The tank car stayed upright throughout the test, with controlled translational motions provided by the skid support. [Figure 39](#) shows the state of the tank car and impactor car after impact. The impact caused one of the weld joints on the jacket near the impact area to fail. The back of the tank car was deformed by the reaction against the rigid impact barrier. The impact site was at the heater coils, and local buckling was seen at the heater coil return bends. The impactor car remained lodged within the tank car following the test. This required that a 10-foot by 10-foot section to be cut around the center of the impact to allow for removal of the impactor head while still maintaining the deformation shape for inspection. [Figure 40](#) shows the final shape of the punctured interior panel section after removal from the tank.

The objective of this test was to evaluate the DOT111 tank car’s performance in a side impact scenario and to perform a validation of the computational models for tank car impact and puncture behaviors. The instrumentation in the impact tests were designed to measure the necessary accelerations, displacements, and pressures to validate the tank car models. In many areas, sensors were placed to assure redundancy in measuring the critical information.



Figure 39. Test 4 – Post-test Puncture Response of the Tank Car



Figure 40. Test 4 – Post-test Puncture Damage of the Tank Car

7.2 Summary of Analyses

ARA performed the pre- and post-test FEA for this test. ARA's modeling effort was done using LS-DYNA.

The models of the DOT111 tank car used to analyze the Test 1 side impact conditions were developed from drawings provided by FRA and by adapting models developed in past tank car research programs.

Given the complexity, size, and time required to perform the analyses, several models were developed to consider different aspects of the overall tank behavior. Two primary models were used. One was a global model that included a shell-based model of the full tank car, and a model for the impactor car and the test environment at the TTC. The purpose of the model was to predict the global motions and interactions of the test article, reaction wall, ground, and the impactor car. The other primary model included a tank model with a detailed solid element patch in the impact zone, using a user defined B-W material model validated for tank puncture analyses in previous research. This model was otherwise simplified with far-field shell elements and had simplified boundary conditions. The purpose of this model was for detailed assessment of puncture zone. The two models were considered separately to facilitate the assessment of global response and detailed puncture force calculation within the time available. Model size, required run time and numerical complexities prevented combining all the features into a single model, given the available computing resources and the schedule to perform the pre-test calculations.

The global response model represents the test setup at the TTC used for the side impact test. Figure 41 shows that the model includes a shell element DOT111 tank car model mounted on skids, the full impactor car, the reaction wall and ground, and rail. The impactor car, reaction wall and ground, and skid models were previously developed for other tests using the same equipment and facilities and were repurposed for this effort. Similarly, the previously developed models for these components were also adapted for these analyses.

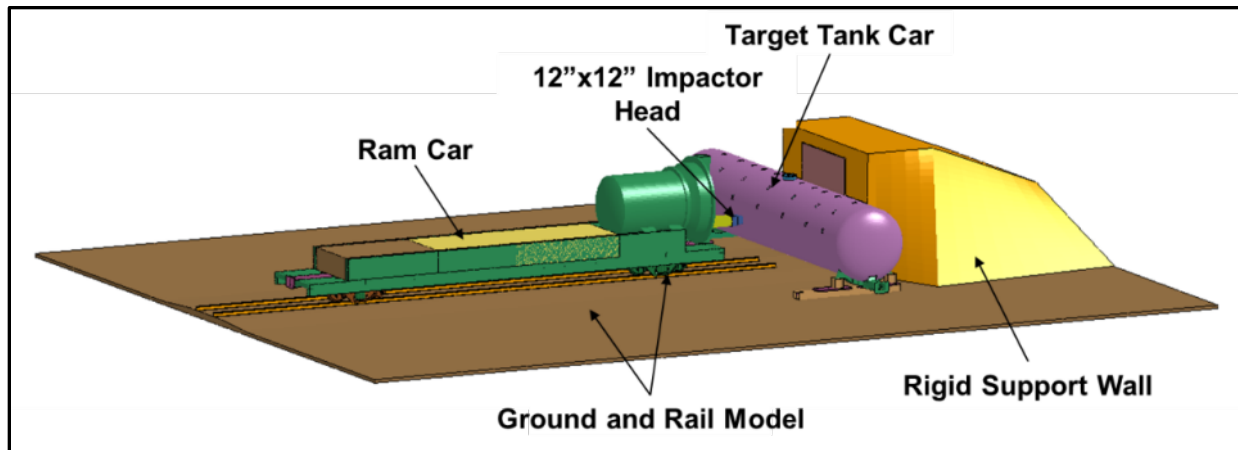


Figure 41. Test 4 – Global Response Model of DOT111 Tank Car Side Impact Test

Figure 42 shows the model of the DOT111 tank car used in the global response setup. The model was adapted from previously created skid mounted side impact tank car models, accounting for the length, diameter, and materials of the DOT111 car. The slight taper along the bottom of the DOT111 was not accounted for in this model. It was assumed that treating the tank and jacket with a cylindrical geometry was adequate. Separate analyses were performed with other simplified models to assess the effect of the taper, which was found to be negligible.

For this global response model, the manway/top fitting model was modified per the DOT111 specification. Also, heater coils were added to the inner tank. The coils were tied to the tank shell with a shell-edge-to-surface interface. A variation in material properties through the weld and heat affected zone (HAZ) were not explicitly treated in the model.

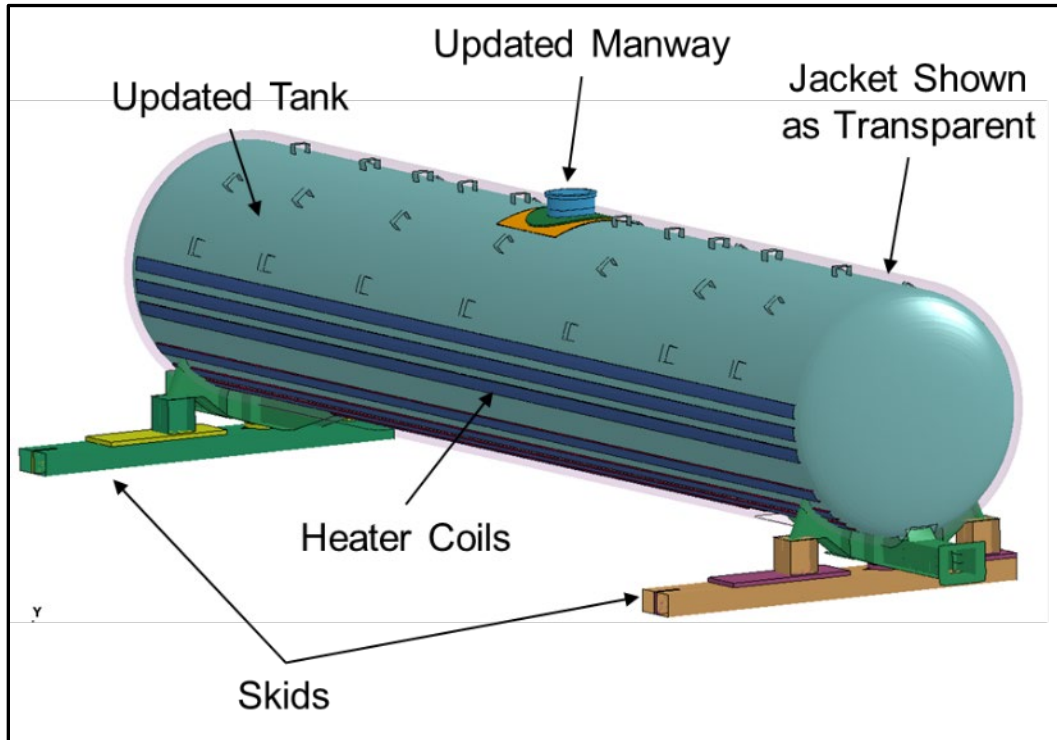


Figure 42. Test 4 – Skid Mounted DOT111 Tank Car Model Used in Global Response Model

To optimize run time, this tank car model was constructed entirely with shell elements, including the impact zone. ARA’s existing database of piecewise linear plasticity material models (LS-DYNA Material Type 24) were applied for the respective materials in the tank car. The model jacket, coil, and inner tank shell meshes were refined in the impact zone, with a typical element size of 0.5 inches. The elements transitioned to approximately 2 inches outside the impact zone. [Figure 43](#) shows a detail of the inner tank and coil mesh in the impact zone.

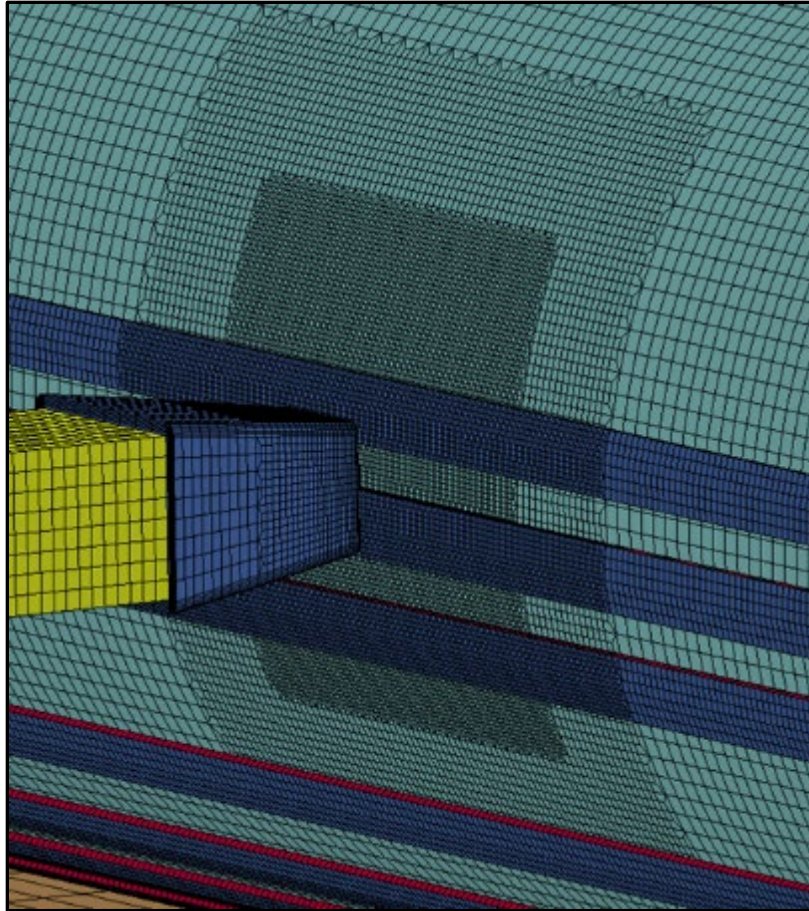


Figure 43. Test 4 – Impact Zone of Shell-Based Tank in Global Response Model

In pre-test predictions, lading was accounted for with a lumped mass approach by increasing the tank's material density. As discussed in subsequent sections, an explicit approach to modeling the lading was also investigated in post-test analyses using the global response model.

Regardless of the lading model approach, tank pressurization was modeled by defining a P-V relationship for a given outage volume. The relationship is developed based on the assumptions that the outage volume has an ideal gas behavior at an initial gauge pressure of 1 atmosphere and is compressed by the reduction in volume of the tank, with the lading having an incompressible fluid behavior. Figure 44 shows an example of the input pressure versus relative volume curve for the unpressurized tank with a 3 percent outage volume. In the calculations, as the tank volume changed, internal tank pressure was updated according to this defined relationship. The pressure was applied to all inner tank elements. At its initial volume, the tank pressure was set to 0 psig.

A similar but separate model for the DOT111 was developed, whose purpose was for accurate puncture behavior modeling and puncture force prediction. Figure 45 shows an overview of the puncture model. This model employs previously developed modeling methodologies, which have been demonstrated to predict tank puncture reasonably well. The method uses a highly refined solid element mesh in the impact zone. User defined B-W material models are used with the solid elements to predict the stress-strain development, damage accumulation, and material failure reasonably well. For this model, refined B-W solids were used through the inner tank,

heater coils and outer jacket impact zone. Figure 46 shows a detail view of the impact zone with the solid inner tank and heater coil B-W patch.

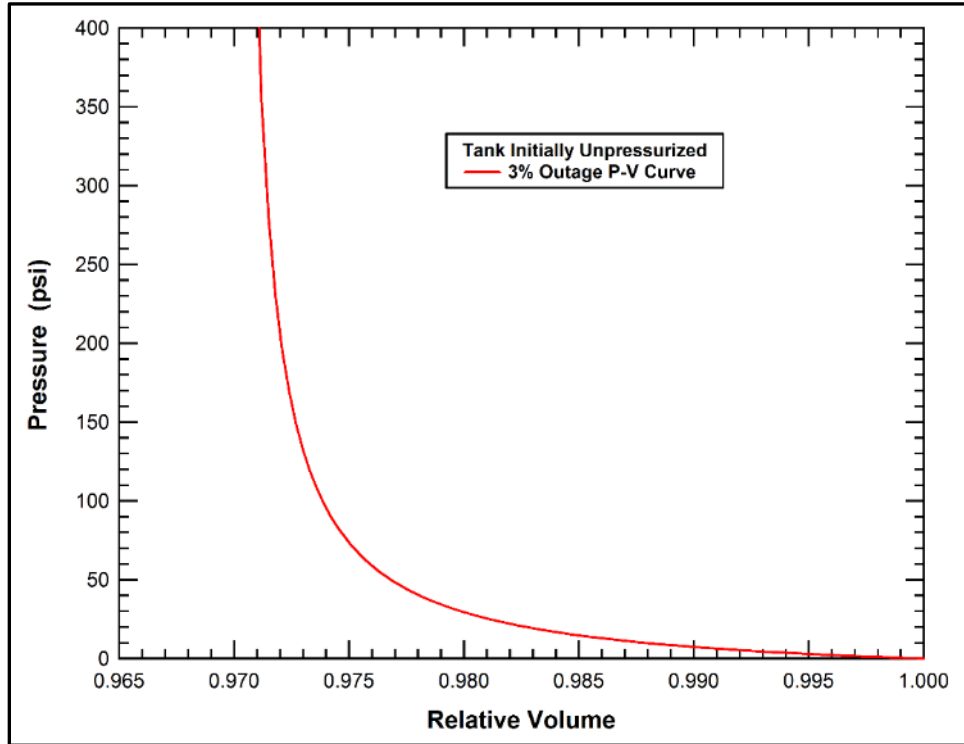


Figure 44. Test 4 – P-V Curve for an Unpressurized Tank with 3 Percent Outage

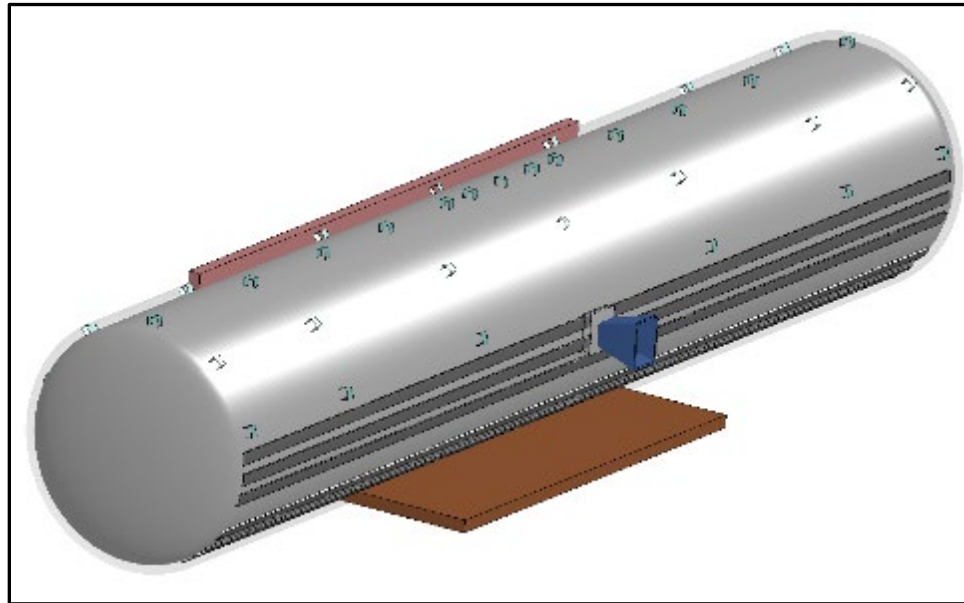


Figure 45. Test 4 – Puncture Model Overview

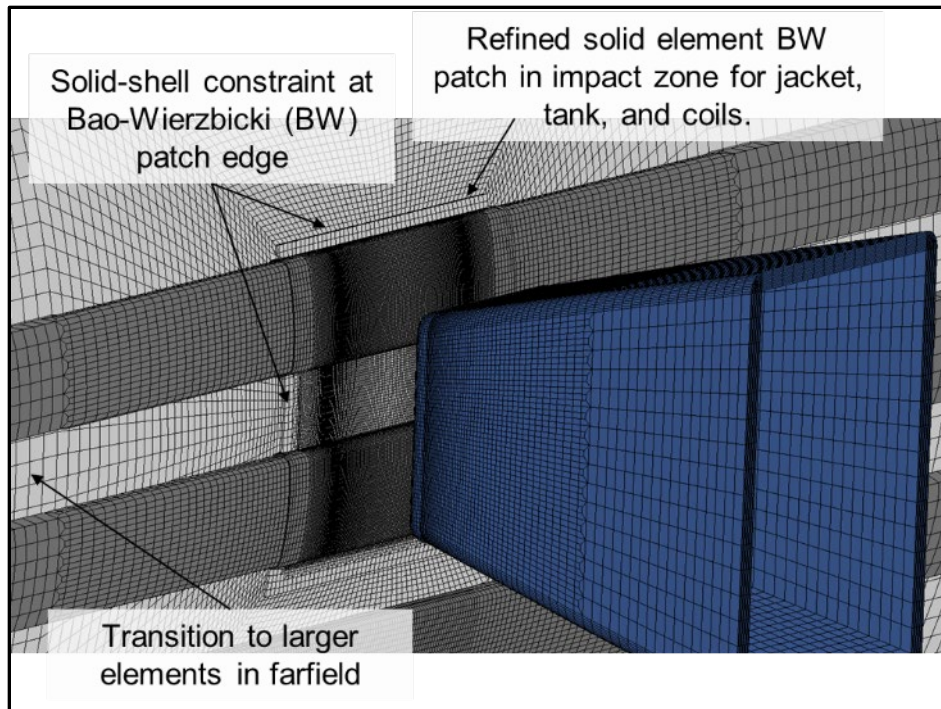


Figure 46. Test 4 – Close-up of Impact Patch in Detailed Puncture Model

The rest of the tank and jacket is like the shell element mesh approach developed for the global response model. Typical element sizes for the tank jacket and coils are as follows:

- Solid element B-W impact zone: 0.05 to 0.1 inch (weighted toward impactor edges)
- Near-field shell transition zone: 0.25 to 1.0 inch
- Far-field shell elements: 2 inches

Such refinement comes at a high computational cost, but it is necessary to accurately predict puncture force. To optimize the calculation efficiency, other aspects of the model were simplified compared to the global response model. For example, the impactor was simplified to include only the 12-inch by 12-inch impactor tip. The density of the impactor tip was increased to account for the entire impactor car mass. A simple rigid support wall was added behind the tank, representing the contact area with the reaction wall at the TTC.

It was noted that the tank was approximately 5 inches above the concrete pad at the bottom. This pad was not included in pre-test FEA model. Evidence of tank/pad interaction was not clear from the review of the test video, but post-test examination of the site indicated the tank likely contacted the ground pad. Furthermore, there was a fitting that encroached in this space that was not modeled. The pad below the tank shown in [Figure 45](#) was added post-test after noting the close proximity of a concrete pad below the tank jacket. Initial calculations did not have the vertical boundary. The stub sills, skids, and vertical support were not included, as they were far away from the impact zone. Likewise, gravity was neglected as well in the puncture model. The same volume dependent tank pressurization approach was used again for the puncture model.

A limited set of results are discussed in this report, while the complete set of model and test results can be found in the report for Test 4 (Kirkpatrick, S. W., Rakoczy, P., MacNeill, R. A., & Anderson, A., 2015).

7.3 Comparison of Test and Analysis Results

Figure 47 shows a comparison of the puncture model pre-test predictions and measured force-displacement behavior. The predictions were performed with an initial impactor car speed of 15 mph, while the measured speed from the test was 14.04 mph. The difference in speed would lead to slightly different traces but not enough to explain the overall discrepancy seen. The peak puncture force seen in the test was 962,000 pounds at 42 inches of displacement. The pre-test predictions with and without coils bounded the tested puncture force but at approximately 10 inches more displacement. As a result, the predicted energy absorption was higher than tested.

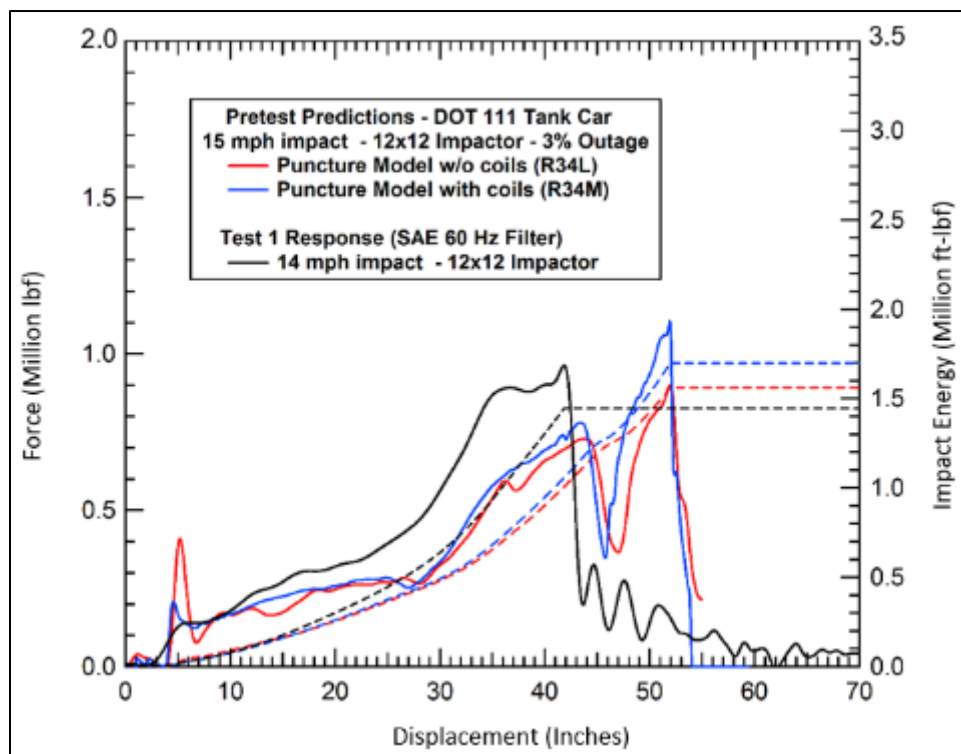


Figure 47. Test 4 – Comparison of ARA’s Predicted and Measured Force-Displacement and Impact Energy

The pre-test puncture model simulation with heater coils over-predicted the puncture force by approximately 14 percent. Note that the coil-tank welds were not included in the pre-test models. It is likely that much of the difference in puncture force resulted from the strength reduction caused by the heater coil welds extending through the puncture zone. Multiple fractures were observed near the coil welds, indicating effects of stress concentrations and reduced ductility compared to the base metal properties. In the absence of material data to model the welds and HAZ, the effect of the heater coil welds on failure initiation in the puncture zone was not considered directly. Characterizing weld materials in the vicinity of the impact zone on future test articles will help improve pre-test prediction accuracy.

The response of the tank shows that it is significantly stiffer than predicted. This was suspected to be a result of a lower-than-expected outage volume, which lead to more rapid tank pressure buildup and tank stiffness as the tank volume decreased under impact loading. At the low outage tested, the impact and puncture response is quite sensitive to variations in the outage volume. Several post-test calculations were performed to explore the sensitivity of the impact force response to variations in the outage volume.

The initial series of analyses used simple shell impact models of the tank at various outage volumes to investigate the influence on the force deflection behaviors. The calculated force deflection responses from the simplified analyses with outage volumes between 2 and 3 percent are compared in Figure 48. Based on the response of these variations compared to the test, it was estimated that 2.0 to 2.25 percent outage will best match the test. This agrees with the calculated outage for the test based on the measured height of the outage before the test (2.1 to 2.3 percent). As a result, an outage volume of 2.25 percent was used for the subsequent explicit lading model investigation.

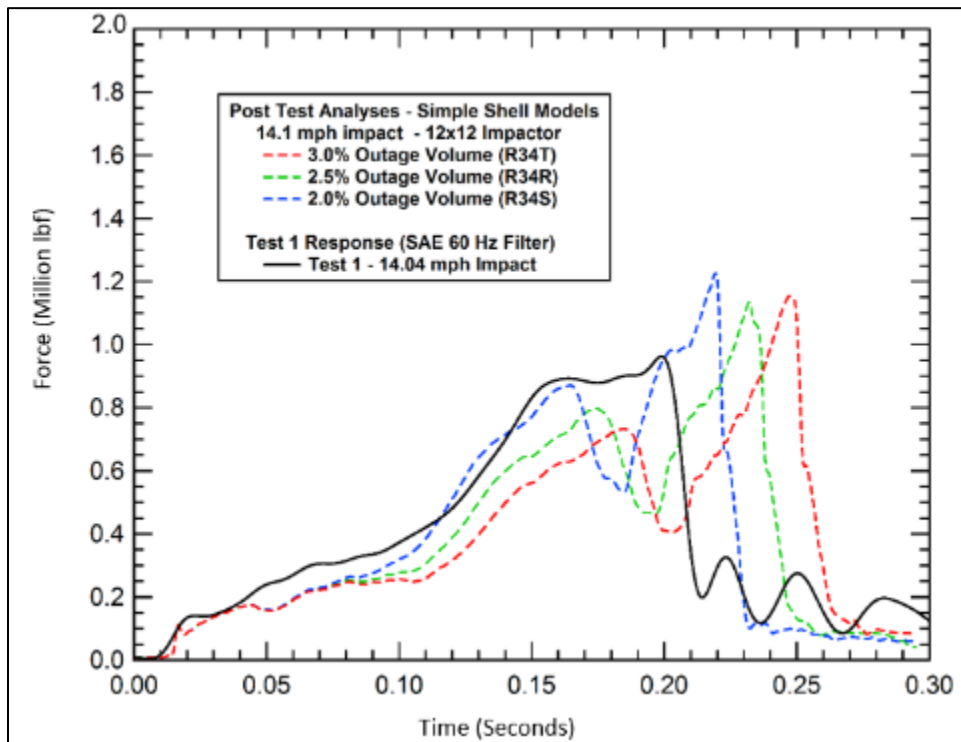


Figure 48. Test 4 – Effect of Outage Volume on Impact Force: 2 to 3 Percent Outage Range (ARA’s simple shell model without heater coils)

The pre-test analyses used a lumped mass approach for the lading by increasing the inner tank density to obtain a combined weight of the tank and lading. It was expected that if explicitly modeled, the effects of the tank lading dynamics would be accurately reproduced and smooth out the dip in predicted force response, which was not observed in the test.

To evaluate the effect of a coupled fluid-structure interaction (FSI) response, the global response model was adapted to include an ALE mesh to represent the fluid lading. The ALE mesh, shown in Figure 49, defines a fluid control volume that was set up to travel with the motion of the tank. In the analysis, the ALE fluid mesh interacts with the existing Lagrangian tank shell. The control

volume extends outside the initial tank surface to allow for the localized increase in radius as the tank dents and deforms under impact. Full enclosure of the tank shell throughout the calculation is important to capture the lading-tank interaction without leakage. The fluid lading is modeled with the material properties of water, which are summarized in [Table 18](#).

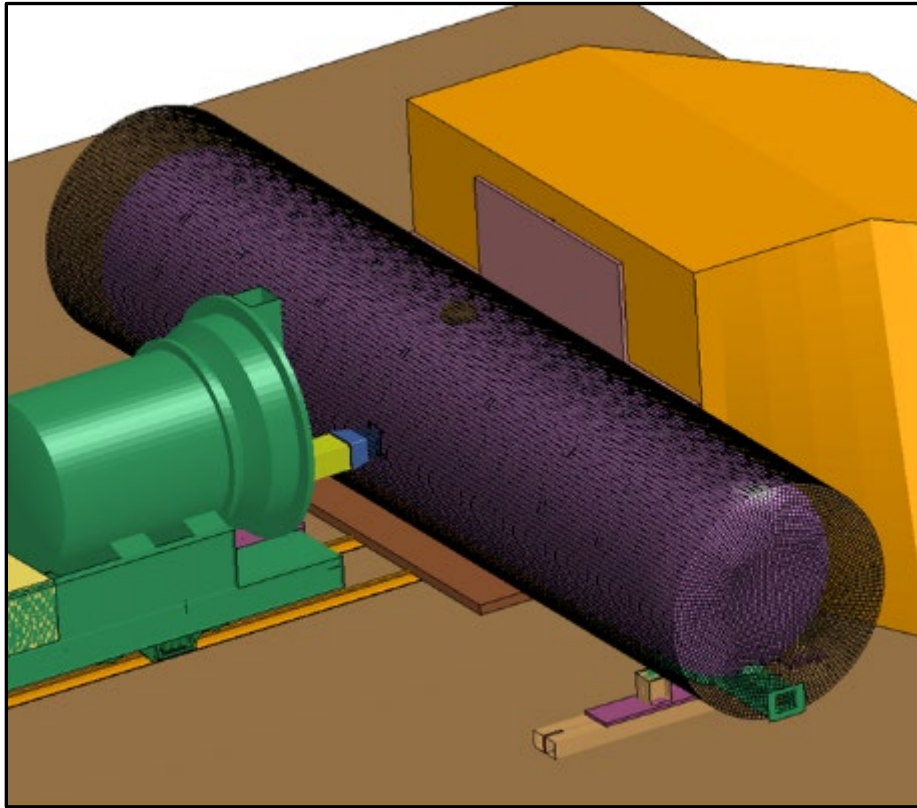


Figure 49. Test 4 – ALE Lading Mesh Added to the Global Response Model

Table 18. Fluid Lading Material Properties

Density, ρ	9.353×10^{-05}	lbf-s ² /in. ⁴
Density, ρ	1,000	kg/m ³
Dynamic Viscosity, μ	1.260×10^{-07}	lbf-s/in. ²
Dynamic Viscosity, μ	8.735×10^{-04}	Pa-s

[Figure 50](#) shows the comparison of the measured and calculated force-displacement behaviors using the ALE lading model. The correlation of force-displacement responses is better than previous analyses with a lumped mass lading approach. From the early displacement, through the tank stiffening that occurs at approximately 30 inches and to the elimination of the sharp unloading seen in previous simulations, the model tracks with the tested response reasonably well. As seen in previous comparisons, the rupture force and ductility are expected to be over predicted in this shell element global model. The higher ductility of this model results in higher energy absorption compared to the test, though most of the energy-displacement curve correlated very well. It is expected that the detailed puncture model with the solid B-W patch would be able to capture rupture behavior more accurately. Unfortunately, the added numerical complexity of

combining the puncture model with the ALE model would significantly increase runtime for models that are already computationally expensive. This combination was not undertaken for this post-test investigation, but is recommended to be considered for future efforts.

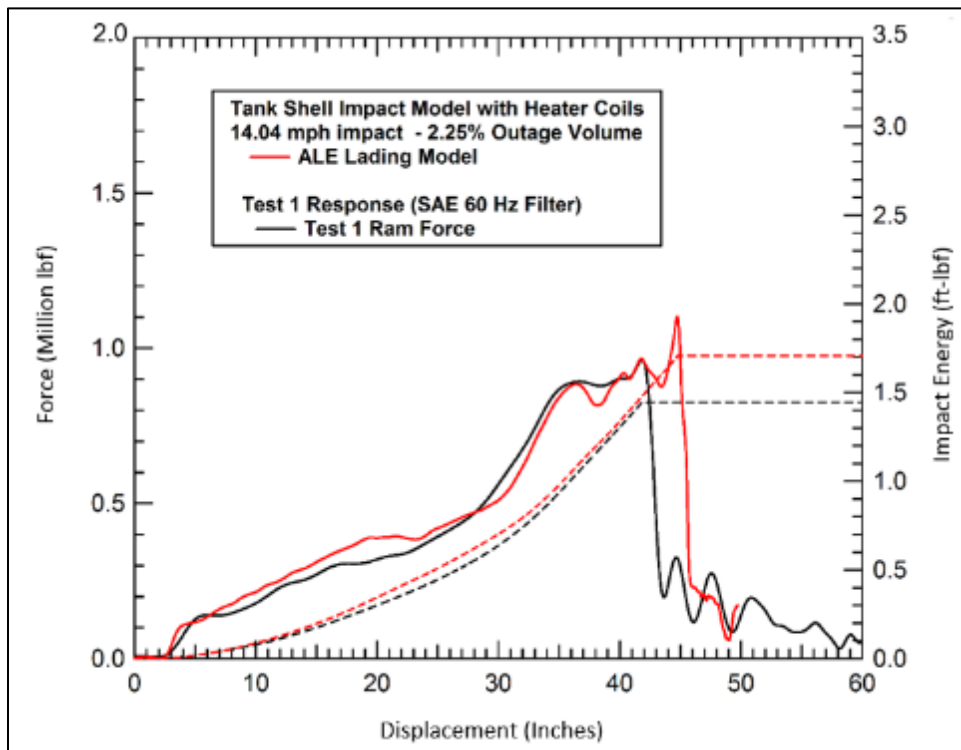


Figure 50. Test 4 – ARA’s Predicted Force and Energy Response With Explicit Lading Model

Figure 51 shows the internal tank pressure predicted with the ALE lading compared with the measured pressure as a function of the impactor displacement. The model correlates reasonably well with the average test pressure, except for the final pressure spike near puncture and post-puncture response. Note that some discrepancy is expected because the pressures compared in the figure were obtained somewhat differently: the test trace is an average of dynamic pressure measurements at discrete points, whereas the calculated trace is the hydrostatic pressure obtained from the P-V methodology used in the analysis. The peak pressure discrepancy seen in Figure 52 is due to elevated puncture strength in the analyses and slightly delayed rupture behavior. In this region of the tank response, the rapidly decreasing tank outage volume near peak compression causes a correspondingly rapid rise in tank pressure. The post-puncture release of pressure is also not accurately simulated with the control volume approach used in the analysis, leading to differences with the observed behavior. However, accurate post-puncture response modeling in this regard was not an objective of the analysis. The good overall comparison with the test confirms that the lading dynamics are important to accurately simulate the overall force development leading to puncture.

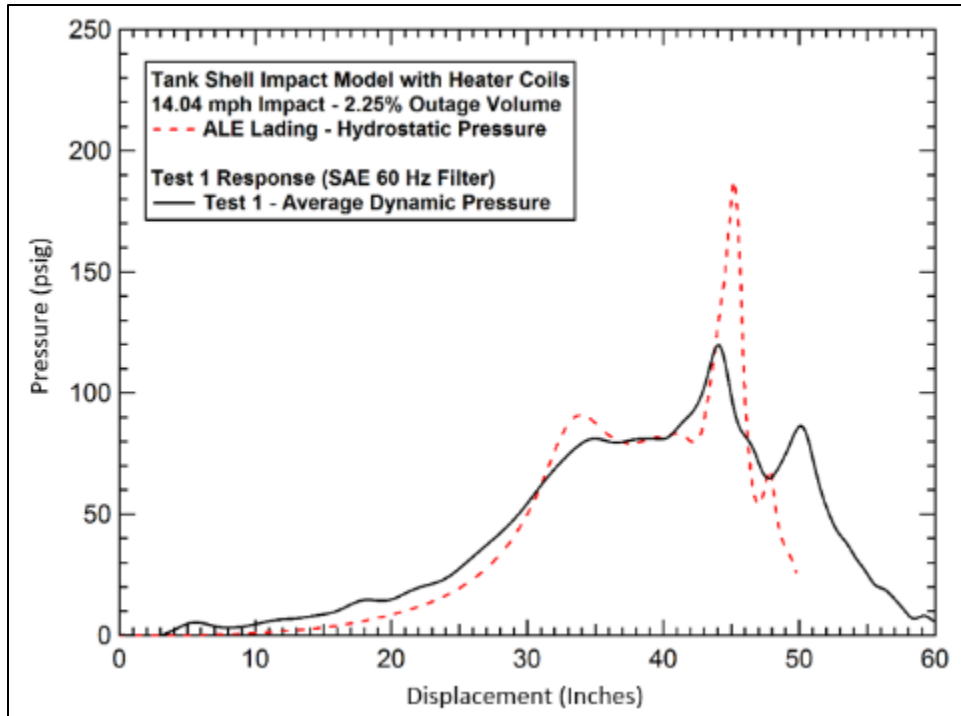


Figure 51. Test 4 – ARA’s Predicted Tank Pressure with Explicit Lading Model

7.4 Summary of Lessons Learned

The volume of water used to fill the tank car was based on flow meter readings and was not explicitly measured. The gas outage percentage was determined to be 3 percent during the test by using the specified tank volume and determining the volume of fluid added based on flow meter readings. Post-test analysis suggested that the outage volume was between 2.1 and 2.3 percent. The FE model was very sensitive to the outage volume percentage, and it was concluded that the outage needs to be determined or measured more accurately in the future to achieve better correlation between FE models and test results. This outage sensitivity was particularly notable for Test 4, where the tank car was intended to represent typical operating conditions for an unpressurized tank car. While the previously tested DOT105 pressurized tank cars had outages at 10 percent; the unpressurized tank cars typically feature outages of less than 5 percent. As the outage volume decreases, a small percentage error in measuring the outage can have a more significant effect on the test results. Further, as the unpressurized tank car was tested starting at atmospheric pressure, the outage is more easily compressed than with the previously tested DOT105 tank cars that were at an initial pressure of 100 psig.

The action of the PRV was not modeled. The PRV activated during the test and thus relieved some of the gas volume to the atmosphere. During the simulation, it was assumed that the gas volume was unchanged, and a fixed P-V relationship was applied throughout the simulation. It is expected that the P-V relationship will change as the gas volume changes due to pressure relief. The fluid-structure interaction modeling had a significant effect on the internal pressure predictions of the model and would seem to be the natural choice for future models, at least for unpressurized tank cars.

In this test, three of the five string potentiometers measuring the deformation of the tank along the direction of impact reached their limit at 24 inches. Future tests should consider using string potentiometers with longer displacement ranges to capture the entire range of deformation of the tank car. Enough range should be left on the potentiometers during installation, such that they can capture the entire deformation range of the tank cars.

This was the first test to feature a ruggedized camera on board the impactor car during which the tank car was punctured. This video was helpful for observing the puncture behavior of the tank, even though the tank car was jacketed and thus the tearing of the tank shell was not directly observable. This test demonstrated that the onboard camera would function in a test involving puncture and splashing of released water.

8. Test 5 – DOT112A340W (February 26, 2014)

Test 5 featured a DOT112A340W tank car loaded with lading under typical conditions for unpressurized liquids. [Table 19](#) describes the tank car specification.

Table 19. Test 5 – DOT112A340W Tank Car Specifications

DOT112	Pressurized Tank Car
A	Top and Bottom shelf couplers
340	340 psig Test Pressure
W	Fusion welded tank

This test was a follow-up to Test 4, examining the potential improvement in shell puncture resistance that could be realized for unpressurized tank cars if a thicker tank shell was used. As a stand-in for an unpressurized tank car with a thicker shell, a DOT112 tank car was used in Test 5. DOT112 tank cars are usually pressurized in operating conditions, but it was loaded as if it were an unpressurized tank car. [Figure 52](#) shows the test setup.



Figure 52. Test 5 – Test Setup Showing DOT112 Tank Car and Impactor

8.1 Summary of Test 5

[Table 20](#) summarizes the impact conditions and outcomes of Test 5. Test 5 was performed using water as the lading in the tank. As the tested tank car was designed to transport commodities having a lower density than water, the tank car was considerably heavier in the test condition than would be encountered in revenue service.

Table 20. Test 5 – Test Conditions and Results Summary

Outage	3.3%
Target Speed	15.0 mph
Actual Speed	14.7 mph
Pressure	Atmospheric
Product	Water
Indenter Dimensions	12"×12"
Impactor Weight	295,175 lbs.
Tank Car Weight (Estimated)	355,600 lbs.
Nominal Tank Thickness	0.62 in.
Nominal Jacket Thickness	11 gauge
Insulation and Thermal Protection	Ceramic thermal protection
Nominal Insulation Thickness	0.50 in.
Test Outcomes	Tank not punctured, impactor car rebounded

The objective of the test was to quantify the deformation mode, impact load-time history and puncture resistance of a DOT112 tank car loaded as if it was in revenue service as an unpressurized tank car in a shell impact without puncturing the tank. The objectives of the analyses were for pre-test planning and for validation of tank car impact and puncture modeling capabilities. The test was intended to dent the tank car, but not puncture the tank's shell. The impact deformed the tank car and punctured the external jacket, but it did not puncture the tank's shell.

The impact was on the weld seam of the external jacket and the impact caused a fracture along this weld seam. The inner tank dented, but it did not experience any puncture because of the impact. [Figure 53](#) shows the post-test conditions of the jacket and tank.

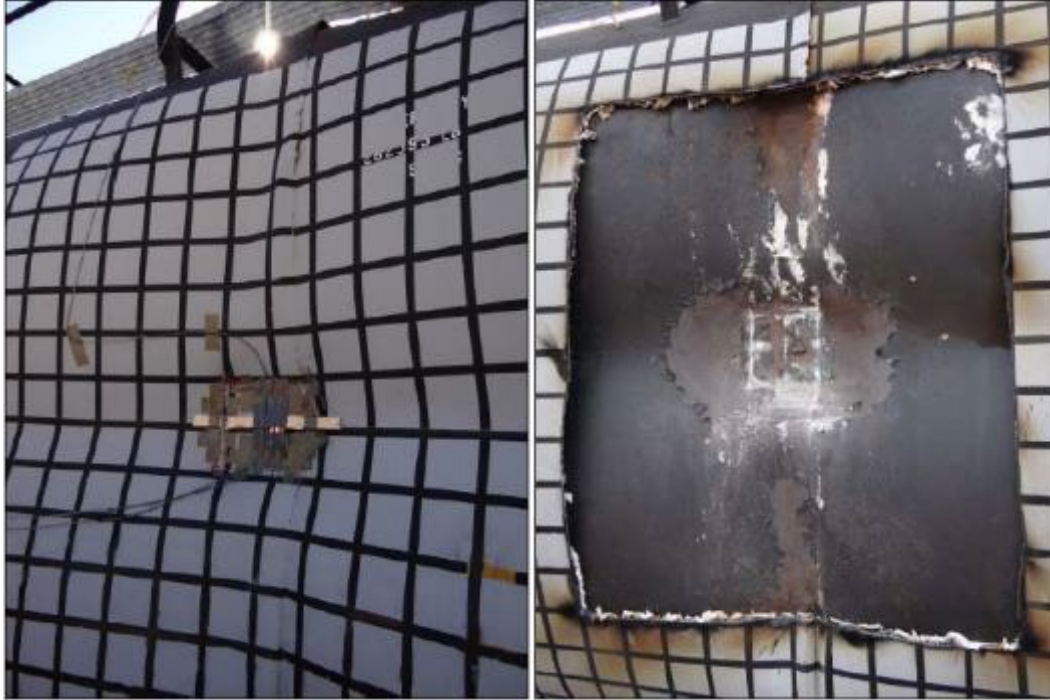


Figure 53. Test 5 – Deformation of the (left) Jacket and (right) Tank Shell Due to Impact

8.2 Summary of Analyses

Volpe performed the pre- and post-test FEA. The FE model was constructed using half-symmetry to reduce the model's runtime. The half-symmetry simplification was used in the FE models from this test onward, for tests having an impact at the centerline of the tank car. Test 5's FE model was built in Abaqus/CAE preprocessor and analysis was performed on the model with Abaqus/Explicit.

Material properties of the A-1011 steel jacket, water and air were the same for pre- and post-test FE models. Material coupons were not cut from this tank car after testing. Rather, a bilinear stress-strain curve with one line representing the elastic zone and a second straight line representing the plastic zone from yield to ultimate tensile strength for TC128 material was used in the FE model. This ensured that the modeled material will not have a fracture toughness higher than the actual material. The B-W ductile failure criterion was used to model material failure in the impact zone.

The water in the tank was modeled using an Us-Up EOS model and a temperature of approximately 40 °F. The water was meshed using conventional Lagrangian elements. The air in the tank was modeled using an ideal gas relationship, an initial temperature of approximately 40 °F and an initial pressure of 1 atmosphere (absolute). A new modeling technique, compared to previous simulations, was used to model the air within the tank. This modeling technique modeled the air particles as discrete particles, allowing the pressure within the tank to vary with time and along the length of the tank.

8.3 Comparison of Test and Analysis Results

A limited set of results are discussed in this report, while the complete set of model and test results can be found in the report for Test 5 (Rakoczy, P., & Carolan, M., 2016). These results include comparisons of test results to FEA results for force and energy versus impactor travel, as Figure 54 shows.

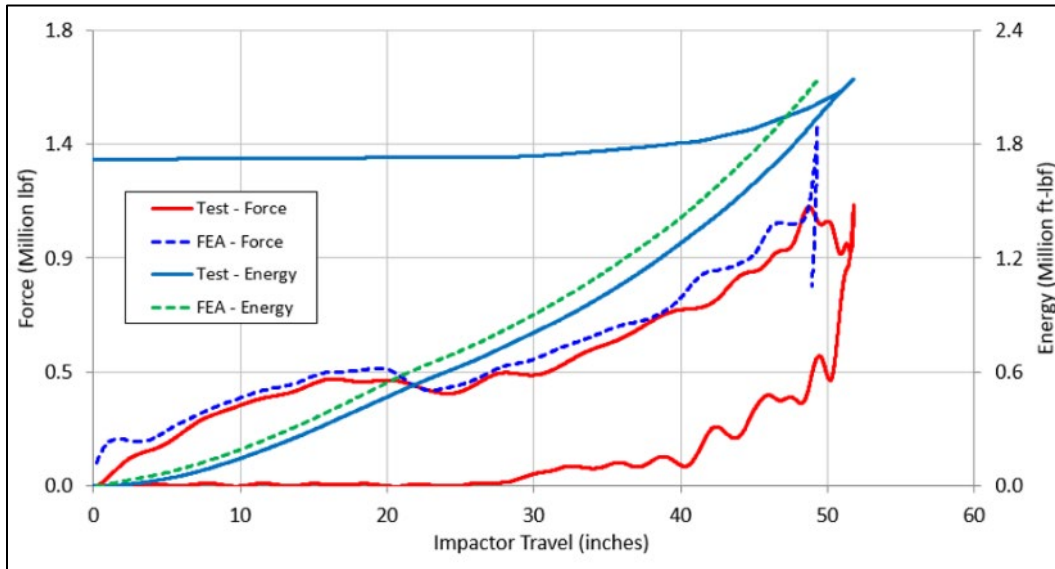


Figure 54. Test 5 – Test vs. Analysis Comparison of Force and Energy vs. Displacement Plot

8.4 Discussion and Lessons Learned

From the lessons learned in Test 4, the outage volume was measured more carefully for Test 5, and the filling procedure was changed in Test 5. The tank was filled to the brim (i.e., shell-full condition) and the volume was determined. Using this volume as the capacity of the tank, 4 percent of the fill volume was removed to have a more accurate outage volume. This approach was thought to remove any discrepancies between the volume stenciled on the tank car and the accuracy of the flow meter used to measure the volume that the tank car was filled with. The same flow meter was used to measure the filling volume and the removal of the desired volume to reach the required outage. After removing the desired volume of water, the height from the top of the water to the top of the tank was measured to be approximately 8.75 inches, which served as a second reference value to determine the outage volume.

Displacement transducers mounted at 48 inches on either side to measure deformation along the direction of motion of the impactor as it reached their limit during the test. If possible, a displacement transducer with larger travel could be used in future tests.

In the FE models, the material model of the TC128 Grade B normalized steel was created with the minimum mechanical properties that still complied with the specification. This simplification assumes that the tank car met the minimum requirements for TC128B steel. Using this approach would also not allow for an accurate estimation of puncture speed if it turned out that the tested car was made of a TC128B steel that greatly exceeded the minimum properties. It has become a

standard practice to extract material coupons from the tank car that was used during a test. This allows the most accurate modeling of the material properties and behavior.

In the pre-test model, friction behavior was modeled between the exterior of the water surface and the interior of the tank wall with a coefficient of friction equal to 0.3. In the post-test model, this was revised to a value of 0.02. The coefficient of friction of 0.3 was still active between the water exterior surface and the interior surface of the head of the tank. It was found that the higher coefficient of friction at the cylindrical region of the tank was making the model excessively stiff, and the higher value at the tank car head is unlikely to affect the results in the center of the tank car. This result emphasized the need to carefully control the model input parameters, especially when modeling the fluid response using an explicit mesh rather than a simplified modeling approach.

A Coulomb-type friction model was applied at the skids in the FE model. In the pre-test model, the friction transitioned linearly from stiction to slip and then applied a constant force once slip occurred. In the post-test model, the friction transitioned linearly, but once slip occurred the resisting force was linearly reduced back to zero. The post-test model provided better agreement between the model and the test results. In the pre-test model, the tank car was placed against the restraining wall. In the post-test model, a 0.5-inch gap was allowed between the tank and the retaining wall to better represent the test conditions.

The outage volume in the model was determined in a similar manner to the loading procedure. Rather than using the desired 4 percent outage volume, the geometry of the model was used and 8.75-inches of water was removed from the top level of the water once the geometry was filled to 100 percent. This corresponded to an outage volume of 3.25 percent. The outage in Test 5's model was adjusted to match the height of the air space above the free surface of the water, rather than the volume of the air. For tests using a small outage, the height between the free surface of the water and the 12 o'clock position on the tank can play a significant role in the measured or simulated force-displacement response. This is because once the fluid wave reaches this height, the water in that cross-section of the tank is incompressible and the impactor encounters a much higher resistance to additional indentation.

The vertical string potentiometer within the tank was mounted in reverse, i.e., to measure reduction in length rather than extension. This resulted in the vertical string potentiometer only having displacement of 5 inches and then snapping during the test. Care should be taken to ensure correct string potentiometers are chosen for the application, they have enough range to capture the peak response of the test, and they are properly mounted to perform the measurement. Pre-test FE model results can be used to estimate the anticipated magnitude and direction (i.e., extension or retraction) of string travel anticipated in the tests.

9. Test 6 – DOT105J500W (April 27, 2016)

Test 6 featured a DOT105 tank car struck by a 12-inch by 12-inch impactor. [Table 21](#) summarizes the specifications for the tested tank car.

Table 21. Test 6 – DOT105J500W Tank Car Specifications

DOT105	Pressurized Tank Car
J	Jacketed for thermal protection, tank headshields, top and bottom shelf couplers
500	500 psig Test Pressure
W	Fusion welded tank

Before this test, Tests 0, 1, and 2 featured a DOT105 tank car struck by either a 17-inch by 23-inch impactor or a 6-inch by 6-inch impactor. Test 3 featured a DOT105 tank car struck by a 12-inch by 12-inch impactor, but the tank car in Test 3 also included a protective panel that is not a typical feature of any tank car. Thus, Test 6 was the first test to evaluate the performance of an unmodified DOT105 tank car when struck by a 12-inch by 12-inch impactor. [Figure 55](#) shows the test setup.



Figure 55. Test 6 – Test Setup Showing DOT105 Tank Car and Impactor

9.1 Summary of Test 6

The objective of the test was to quantify the deformation mode, impact load-time history and puncture resistance of a DOT105 tank car in a shell impact. [Table 22](#) summarizes the test conditions and results.

Table 22. Test 6 – Test Conditions and Results Summary

Outage	10.6%
Target Speed	15.0 mph
Actual Speed	15.2 mph
Pressure	100 psig
Product	Water
Indenter Dimensions	12 in.×12 in.
Impactor Weight	295,725 lbs.
Tank Car Weight (Estimated)	205,800 lbs.
Nominal Tank Thickness	0.78 in.
Actual Thickness ¹⁰	0.80
Nominal Jacket Thickness	11 gauge
Insulation and Thermal Protection	Urethane foam
Nominal Insulation Thickness	4.0 in.
Test Outcomes	Tank punctured; impactor car rebounded

The objectives of the analyses were for pre-test planning and for validation of tank car impact and puncture modeling capabilities. Test 6 was intended to be performed at a speed that would approximate the threshold where the response of the tank car changes from non-puncture to puncture. The impact test resulted in puncture of the tank after the impactor car had slowed to less than 1 mph. This confirmed that pre-test modeling could be used to estimate the threshold speed, providing some confidence in the modeling process.

The test was intended to dent the tank car, but not puncture the tank’s shell. The impact deformed the tank car and punctured the external jacket and the tank’s shell. The impactor was brought to a stop because of energy absorbed by the tank car and rebounded from the tank car though it punctured. This outcome implied the impact speed only slightly exceeded the threshold puncture speed. The impactor car did not continue to penetrate the tank car after puncture. The internal pressure ejected a segment of the shell from the impacted area and created a large hole in the tank. This was the first test that featured a puncture and a rebound of the impactor car. This has also been, to-date, the only test where tank car material was separated and ejected from the tank. [Figure 56](#) shows the deformed tank car, with the left side figure showing the jacket in place and the right side showing the tank shell with the jacket removed.

¹⁰ Actual thickness not measured for Test 6, but it was assumed to be the same as Test 8 as “sibling” cars were used in these two tests.



Figure 56. Test 6 – Impact Zone Post-testing (left) With and (right) Without Jacket

Test 6 was instrumented the same way as Test 5. It was the first test where laser scanning of the impacted region was implemented. After the test, two different LiDAR scans were performed on the punctured tank car. One scan was used to generate a three-dimensional representation of the geometry of the tank car itself. A separate, more detailed scan was performed on the ejected portion of the tank car. These LiDAR scans proved useful for comparing the patterns of damage and deformation on the actual tank car to the final deformed shape of the FE model and would be added to subsequent test plans.

9.2 Summary of Analyses

Volpe performed the pre- and post-test FEA for this test. The FE models were built with the Abaqus/CAE preprocessor, and the model was executed with Abaqus/Explicit version 6.14.

Two models were developed for the pre-test investigation. The first model did not allow puncture and thus was constructed without ductile failure material behavior and without mesh refinements. The second model allowed puncture with the associated failure behavior and refined mesh in the puncture zone, including solid elements. The simulation techniques used in the DOT105 tank car models included modeling an elastic-plastic material response for the tank and jacket, ductile failure implementation of the B-W triaxiality-based damage initiation model, and modeling of the water and air phases within the tank.

The pre-test analyses with puncture capabilities used material models for the TC128 steel shell based upon previously published data. Two material models were developed to bound the range of expected speeds between puncture and non-puncture outcomes of the test where the exact material behaviors would not be known until after the test. After the test, the FE model was

updated to include material plasticity and damage behaviors based on the results of coupon tests from the actual DOT105 tank car shell used in Test 6.

For this DOT105 tank car test, a hydraulic cavity was defined for the water phase, with a pneumatic cavity defined for the pressurized air phase. The cavity approach is a simplified modeling technique that represents the fluid constituents (e.g., either gas or liquid) using an average pressure over the entire volume. This dual-cavity approach to fluid modeling gave satisfactory representation of the fluid response seen in this test, while offering considerable computational efficiency over an explicit representation of the liquid phase such as Lagrangian elements or smoothed particle hydrodynamics (SPH).

Where previously tested tank cars featured a fiberglass or ceramic blanket of insulation, the DOT105 used in Test 6 featured a urethane foam insulation. The review of the test data revealed that the foam insulation contributed more significantly to the stiffness of the tank car than the previous insulations encountered in the testing program. A simplified urethane foam material model was developed in the post-test FE models to investigate the effects of this insulation on the model's agreement with the test measurements. The post-test model demonstrated relatively better agreement with the test measurements with the inclusion of the foam insulation.

9.3 Comparison of Test and Analysis Results

A limited set of results are discussed in this report, while the complete set of model and test results can be found in the report for Test 6 (Carolan, M., & Rakoczy, P., 2019). All the FE results from Test 6 presented in this report are from the post-test model that included the updated material properties of the tank car shell material, the urethane foam insulation and with nominal tank thickness. Figure 57 shows the impact force and energy versus impactor displacement results for Test 6.

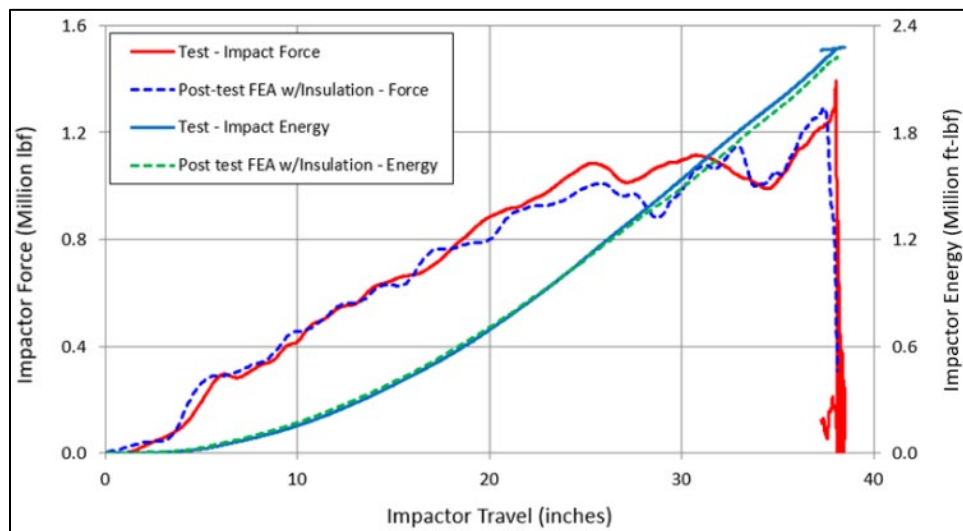


Figure 57. Test 6 – Test vs. Analysis Comparison of Force/Energy-Displacement Plot

9.4 Summary of Lessons Learned

During Test 6, instrumentation data was not lost, and transducers did not reach their measurement limits. The ejected portion of the shell caused some cables to be damaged, but data up to the point of puncture was usable. The actual impact speed was 0.2 mph higher than the targeted impact speed.

This was the first test to use LiDAR scanning to scan a section of the tank car, which added value to the analysis and interpretation of the results and was added to future test plans as a standard measurement.

Modeling the insulation material between the jacket and tank was identified as important for future analyses of tank cars equipped with foam insulation. Previously tested tank cars that used fiberglass or ceramic blanket insulation were modeled without including the insulation, with no apparent effect to the comparison between test and model. Test 6 revealed the potential for the insulation to contribute to the structural response of the tank car in the standardized test setup. Because the tank car is placed against or adjacent to the rigid impact wall in the standardized test setup, the jacket is initially the only portion of the tank car contacting the wall. When the impact causes the commodity tank to translate toward the wall, its motion is resisted by the insulation being compressed between the tank and jacket on the wall side of the test setup. If the insulation is excluded, or offers insignificant structural resistance, the commodity tank can develop some relative speed before quickly decelerating when it makes contact with the jacket and wall. However, if the insulation offers structural resistance to crushing, the tank is unable to develop much relative speed because a load path from the tank through the insulation into the jacket and wall exists from the start of the impact. While insulation materials are generally not intended to contribute to the structural response of the tank car, the results of this test have revealed that they may do so.

The characterization of the material properties of the shell of the tank car being tested and the use of these properties in the post-test FE model allows the attainment of a higher level of confidence in analysis results. Post-test material characterization should be considered for each tank car tested in the future, as considerable variations in the properties of a single steel alloy (i.e., TC128B) have been observed from various tank cars tested in this program up to this point.

10. Test 7 – DOT117J100W (September 28, 2016)

Test 7 featured a DOT117 tank car struck by a 12-inch by 12-inch impactor. [Table 23](#) summarizes the specifications for the tested tank car.

Table 23. Test 7 – DOT117J100W Tank Car Specifications

DOT117	Unpressurized tank car for carrying flammable liquids
J	Jacketed for thermal protection, tank headshields, top and bottom shelf couplers
100	100 psig test pressure
W	Fusion welded tank

While it is designed to withstand internal pressure, the DOT117 tank car is classified as an unpressurized tank car, like the DOT111. The DOT117 tank car tested was 1 year old and had never been used in revenue service. [Figure 58](#) shows the test setup.



Figure 58. Test 7 – Test Setup Showing DOT117 Tank Car and Impactor¹¹

10.1 Summary of Test 7

The objective of Test 7 was to quantify the deformation mode, impact load-time history, and puncture resistance of a DOT117 tank car in a shell impact. The objective of analyses was to provide estimates of the tank car impact response for pre-test planning and for validation of tank car impact and puncture modeling capabilities. The test was intended to be performed at a speed that would approximate the puncture threshold speed, with the test conditions being comparable to Tests 4 and 5. As in Tests 4 and 5, Test 7's tank car was partially filled with water. The flammable liquids the DOT117 tank car was designed to carry are less dense than water, so the tested car was heavier than a tank car in typical revenue service. The impact deformed and punctured the external jacket but did not puncture the tank's inner shell. [Table 24](#) summarizes the test conditions and results.

¹¹This photograph shows Test 6 on the head of the tank car used in Test 7 due to inconsistent ways of counting the tests up to this point by Volpe, TTCL, and FRA. Consistent numbering was used for all subsequent tests.

Table 24. Test 7 – Test Conditions and Results Summary

Outage	5%
Target Speed	13.5 mph
Actual Speed	13.9 mph
Pressure	Atmospheric
Product	Water
Indenter Dimensions	12"×12"
Impactor Weight	297,125 lbs.
Tank Car Weight (Estimated)	315,300 lbs.
Nominal Tank Thickness	0.56 in.
Actual Tank Thickness	0.59 in.
Actual Jacket Thickness	11 gauge
Insulation and Thermal Protection	Ceramic thermal protection
Nominal Insulation Thickness	0.50 in.
Test Outcomes	Jacket torn, tank not punctured, impactor car rebounded

There was no change from Test 6 regarding acceleration or displacement measurement transducers and their locations. There was one less pressure transducer used in Test 7 compared to the previous test. The PRV pressure was not measured. However, displacement of the PRV was measured with a string potentiometer to determine whether it activated during the test.

The impact zone was centered on a circumferential weld seam on the tank. The post-test inspection showed no cracking of the weld seam. The impact zone on the jacket occurred near an area with a weld seam and two overlapping steel sheets. [Figure 59](#) shows the post-test impact zone, with the left side figure showing the jacket and the right side showing the tank inner shell.



Figure 59. Test 7 – Post-test Images of (left) the Tank Car with Jacket and (right) Tank Inner Shell

10.2 Summary of Analyses

Volpe performed the pre- and post-test FEA. The simulation approaches used in the DOT117 model included modeling an elastic-plastic material response for the tank and jacket, modeling ductile material failure with the B-W triaxiality-based damage initiation model, and modeling the water and air phases within the tank. As a part of the pre-test and the post-test modeling studies, non-puncture models and puncture-capable models were developed. The FE models used half-symmetric conditions, with a vertical symmetry plane at the centerline of the tank car to reduce the size of the model.

The water phase was modeled using an Us-Up EOS material model with Lagrangian elements, while the air phase was modeled using the same pneumatic cavity approach from Test 6. The water was limited from experiencing any tensile stresses.

Since pre-test models were intended to estimate the speed ranges over which the tank was expected to puncture or not puncture, analyses were run at different speeds. Based on the pre-test models, 13 mph was recommended for non-puncture condition and 14 mph was recommended for puncture condition. The test was performed at a target speed of 13.5 mph with a range of ± 0.5 mph. Post-test models were analyzed at the measured test speed of 13.9 mph, using material properties determined from tested samples extracted from the tank.

10.3 Comparison of Test and Analysis Results

A limited set of results are discussed in this report, while the complete set of model and test results can be found in the report for Test 7 (Rakoczy, P., Carolan, M., Eshraghi, S., & Gorhum, T., 2019). These results include comparisons of test results to FEA results for force and energy versus impactor travel, as Figure 60 shows.

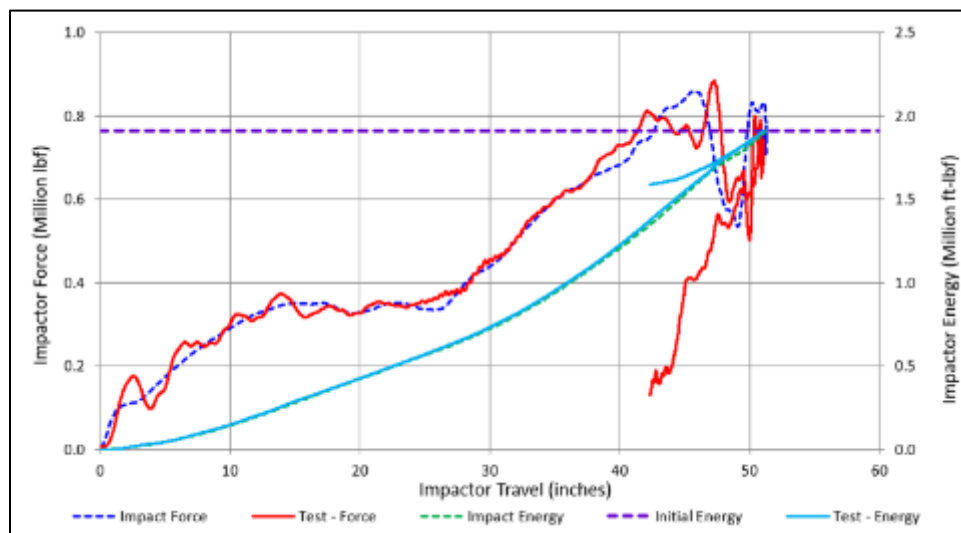


Figure 60. Test 7 – Test vs. Analysis Comparison of Impactor Force-Travel Plot

10.4 Discussion and Lessons Learned

Due to the DOT117 tank car shell sloping downward toward its center from either end, there was little clearance between the housing protecting the bottom outlet valves and the concrete slab

between the rails at the test site. As the tank car deformed, the bottom housing interacted with the concrete slab, breaking away a large chunk of concrete.

The post-test FE model was updated not only to include the actual TC128B material behavior and to represent the overlapping jacket sheets in the puncture zone, but also to reflect the geometry of a deformable concrete slab beneath the tank car that was struck during the test. The geometry of the rigid wall and ground were updated in the post-test FE model to accurately reflect the test setup based on pre-test measurements. The tank car-slab interaction added complexity to the model validation process, but it did not affect how the tank car itself was modeled. In future tests, steps should be taken to provide the highest practical clearance between the concrete slab and the tank car to avoid this unnecessary complication.

Care should be taken in the future to allow all pressure transducers enough cabling length, since it was believed that the deformation of the tank caused tension on some cables, which resulted in a sudden increase in their recorded values.

Pre-test material properties for the TC128 shell of the tank car were developed from data provided by the car's manufacturer from tensile tests conducted on plates used to manufacture the test car's shell. After the impact test, material coupons were cut from the tank car shell and subjected to tensile testing. Post-test material characterization indicated that the actual tank car material had higher ductility than the pre-test material properties, but it also had lower strength. Note that generic material properties of TC128 material or even the material properties obtained from previous TC128 material tests may not represent the material properties of the tank shell material being tested. The post-test material characterization outcome underscored the importance of characterizing the actual material of construction for each tank car tested to improve the accuracy and thus, the confidence in the FE models. While pre-test data may be available for the steel plates used in the tank car, this result indicates that if the tensile testing was performed before certain fabrication processes (e.g., rolling, welding, and heat treatment), the material properties may not represent the material properties found in the as-built tank car.

11. Test 8 – DOT105J500W (August 1, 2018)

Test 8 featured a DOT105 tank car struck by a 6-inch by 6-inch impactor. [Table 25](#) summarizes the specifications for the test tank car.

Table 25. Test 8 – DOT105J500W Tank Car Specifications

DOT105	Insulated, pressurized tank car
J	Jacketed thermal protection
500	500 psig test pressure
W	Fusion welded tank

Before this test, Test 6 featured a DOT105 tank car struck by a 12-inch by 12-inch impactor at 15.2 mph. Test 6 resulted in puncture of the tank with a very small residual energy. [Figure 61](#) shows the test setup for Test 8.



Figure 61. Test 8 – Test Setup Showing DOT105 Tank Car and Impactor

11.1 Summary of Test 8

The objective of Test 8 was to quantify the deformation mode, impact load-time history, and puncture resistance of an existing DOT105 tank car in a shell impact. Tests 6 and 8 used tank cars from the same production run, with a 12-inch by 12-inch impactor in Test 6 and a 6-inch by 6-inch impactor in Test 8. A secondary objective of Test 8 was to replicate the outcome of Test 6, where the impact speed caused simultaneous puncture of the tank car and rebound of the impactor car. This outcome would indicate that the impact energy only slightly exceeded the energy to cause puncture using a 6-inch by 6-inch impactor. The objectives of the analyses were to provide estimates of the tank car impact response for pre-test planning and for validation of tank car impact and puncture modeling capabilities. [Table 26](#) summarizes the Test 8 conditions and results.

Table 26. Test 8 – Test Conditions and Results Summary

Outage	10.6%
Target Speed	9.9 mph
Actual Speed	9.7 mph
Pressure	100 psig
Product	Water
Indenter Dimensions	6 in. × 6 in.
Impactor Weight	296,775 lbs.
Tank Car Weight (Estimated)	206,000 lbs.
Nominal Tank Thickness	0.78 in.
Actual Tank Thickness	0.80 in.
Nominal Jacket Thickness	11 gauge
Insulation and Thermal Protection	Urethane foam
Nominal Insulation Thickness	4.0 in.
Test Outcomes	Tank punctured, impactor car rebounded

Test 8 used similar instrumentation to that of Test 7. The test was intended to puncture the tank's shell without excessive kinetic energy left in the impactor car. The impact deformed the tank car and punctured the external jacket and the tank's shell. The impactor was brought to a stop because of energy transfer to the tank car and rebounded from the tank car although the tank car punctured. This outcome implied the impact speed only slightly exceeded the threshold puncture speed. [Figure 62](#) shows the deformed tank car, with the left side figure showing the jacket and the right side showing the tank shell with the jacket removed.



Figure 62. Test 8 – Post-test Images (left) Tank and Jacket and (right) Tank Shell

11.2 Summary of Analyses

Volpe performed the pre- and post-test FEA for this test. The numerical FE models were built with the Abaqus/CAE preprocessor and the model was solved with Abaqus/Explicit. Puncture capable and non-puncture capable models were developed to study parameters such as the insulation behavior. Half-symmetry was applied to the model. The FE model developed for Test 8 used the Test 6 post-test FE model as a starting point, as the tank cars used in both tests were constructed in the same production run. The most significant change was re-meshing the impact zone in the Test 8 model, as Test 8 used a 6-inch by 6-inch impactor.

Simulation techniques used in the DOT105 tank car FE models included modeling the tank and jacket with elastic-plastic material response, ductile failure implementation of the B-W triaxiality-based damage initiation model, and modeling of the water and air phases within the tank. The air and water phases of the lading were each modeled using a fluid cavity modeling approach. A hydraulic cavity was defined for the water phase and a pneumatic cavity was defined for the pressurized air phase. These techniques were the same techniques used in the Test 6 FE model.

11.3 Comparison of Test and Analysis Results

A limited set of results are discussed in this report, while the complete set of model and test results can be found in the report for Test 8 (Wilson, N., Eshraghi, S., Trevithick, S., Carolan, M., & Rakoczy, P., 2020). These results include a comparison of test results to FEA results for force and energy versus impactor travel. [Figure 63](#) shows these comparisons.

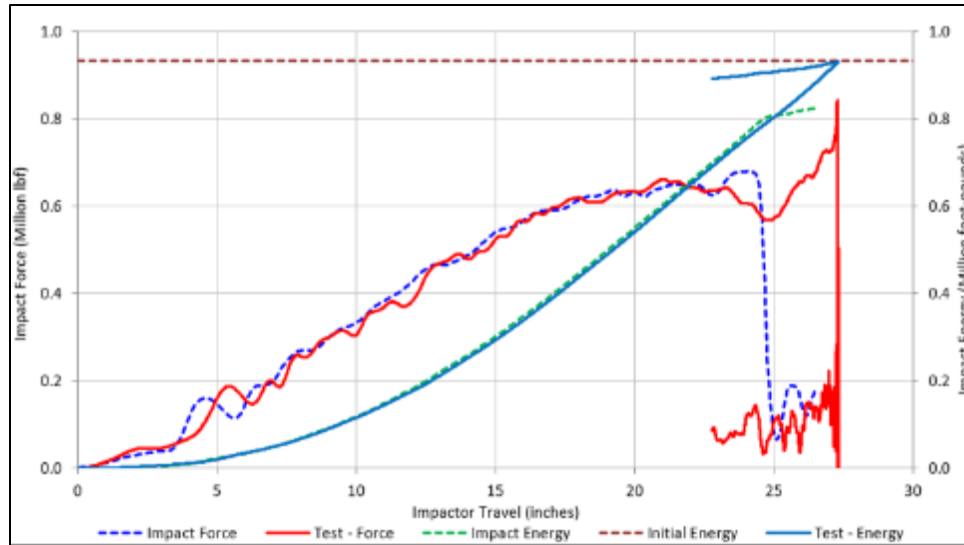


Figure 63. Test 8 - Test vs. Analysis Comparison of Force and Energy vs. Displacement Plot

11.4 Discussion and Lessons Learned

No significant changes were made to the FE model post-test. The pre-test FE model was based on the post-test model of Test 6, including the insulation between the tank and the jacket. The post-test FE model of Test 8 was updated to include material behaviors developed based on tensile testing performed on the actual material from Test 8’s tank car; however, the material properties were like the properties from Test 6’s tank car.

Post-test material characterization from Test 8’s tank car used 2-inch rectangular, 8-inch rectangular, and 2-inch cylindrical coupon geometries to investigate the effects of coupon geometry on the material model development process. It was concluded that while all geometries are suitable for determining the mechanical properties of the steel, cylindrical coupons are the best suited for calibrating a material model for use in puncture simulations. The coupon tests and material model development are documented in a separate report (Eshraghi, S., 2020).

12. Test 9 – DOT111A100W (CPC-1232) (October 30, 2018)

Test 9 featured a DOT111 tank car that met the voluntary industry standard Casualty Prevention Circular (CPC)-1232, struck by a 12-inch by 12-inch impactor. [Table 27](#) summarizes the specifications for the tested tank car.

Table 27. Test 9 – DOT111A100W Tank Car Specifications

DOT111	Unpressurized tank car
A	Top and bottom shelf couplers
100	100 psig test pressure
W	Fusion welded tank

CPC-1232 was a voluntary standard adopted by the AAR for tank cars used to transport certain flammable liquids before the creation of the DOT117 tank car standard. Because the U.S. Department of Transportation did not adopt the CPC-1232 standard within the Hazardous Materials Regulations (HMR), a tank car meeting CPC-1232 standard would also be required to meet specification DOT111. Before this test, Test 4 featured a DOT111 tank car and Test 7 featured a DOT117 tank car, each struck by the same 12-inch by 12-inch impactor. Test 4 resulted in puncture of the tank with an excess of kinetic energy from a 14.04 mph impact, while Test 7 resulted in a non-puncture outcome from a 13.9 mph impact.

The tank car used in Test 9 had been involved in a derailment which caused a dent to the tank head at the A-end of the tank car. This dent at the head of the tank car was not expected to affect the outcome of the shell impact test, because the point of impact was far away from the accident affected zone. However, to ensure integrity of the test, visual and magnetic particle inspections of the A-end tank head were performed on this tank car. The inspections found no indication of cracks in the metal. [Figure 64](#) shows the test setup used in Test 9.



Figure 64. Test 9 – Test Setup Showing DOT111 Tank Car

Additionally, a small rectangular opening was observed on the tank wall about halfway between the damaged A-end of the tank car and the manway. This opening was likely made during the cleanup following the derailment to ensure that this car was unloaded and depressurized. This damage was repaired on site, at the TTC. A replacement patch of TC128B was welded in, and then the area around the weld was heat treated.

12.1 Summary of Test 9

The objective of Test 9 was to quantify the deformation mode, impact load-time history, and puncture resistance of an existing DOT111 tank car in a shell impact. Tests 4, 5, 7, and 9 used tank cars that were not initially pressurized and struck by a 12-inch by 12-inch impactor. A secondary objective of this test was to understand how the puncture resistance of the DOT111 tank car constructed to meet CPC-1232 standard compared to the other unpressurized tank cars from previous tests. Comparisons across multiple tests are included in this report, in [Section 14](#). [Table 28](#) summarizes the Test 9 conditions and results.

Table 28. Test 9 – Test Conditions and Results Summary

Outage	5%
Target Speed	13.5 ± 0.5 mph
Actual Speed	13.9 mph
Pressure	Atmospheric
Product	Water
Indenter Dimensions	12"×12"
Impactor Weight	297,150 lbs.
Tank Car Weight (estimated)	319,100 lbs.
Nominal Tank Thickness	0.50 in.
Actual Tank Thickness	0.52 in.
Nominal Jacket Thickness (in.)	No Jacket
Insulation and Thermal Protection	No Insulation
Nominal Insulation Thickness (in.)	N/A
Test Outcomes	Tank punctured, impactor car rebounded

The objectives of these analyses were to provide estimates of the tank car impact response for pre-test planning and for the validation of tank impact and puncture modeling capabilities. The DOT111 tank car did not have a jacket or insulation.

The instrumentation used in Test 9 was like that of Test 8. The test was intended to puncture the tank's shell without excessive kinetic energy left in the impactor car. The impact deformed the tank car and punctured the tank's shell. The impactor was brought to a stop because of energy transfer to the tank car and rebounded from the tank car although the tank car punctured. Leakage through the top fittings and PRV was observed during this test. This outcome implied

the impact speed only slightly exceeded the threshold puncture speed. [Figure 65](#) shows the punctured tank car.



Figure 65. Test 9 – Post-test Image of the Tank

12.2 Summary of Analyses

Volpe performed the pre- and post-test FEA. Due to the similarities in tank car design and test setup, the modeling procedure for the analyses performed for Test 9 were like the modeling procedures used to model Test 7. The simulation techniques used in the DOT111 tank car models included modeling the tank with elastic-plastic material response, ductile failure implementation of the B-W triaxiality-based damage initiation model, and modeling of the water and air phases

within the tank. The water phase was modeled with Lagrangian elements with an EOS material. A pneumatic cavity was defined for the pressurized air phase. While modeling the water using the hydraulic cavity approach used in Tests 6 and 8 would further reduce simulation time, this modeling technique was found to provide poorer agreement for tests performed using a small outage initially at atmospheric pressure, such as Test 9.

As a part of the pre-test and the post-test modeling studies, non-puncture models and puncture-capable models were developed. These two models were mainly developed to reduce model solution time and to examine modeling techniques before their implementation in the puncture-capable model. All the models used half-symmetry, with a vertical-longitudinal symmetry plane at the centerline of the tank car. This simplification reduced the size of the model and hence the solution time.

Two post-test FE models were created to represent the upper and lower limits of leakage through the manway and top fittings. The first model fully sealed the manway and only allowed air flow through the PRV. This model was expected to represent the lower-bound of leakage (i.e., a tightly sealed tank car), which would represent an upper-bound for tank car stiffness. The second post-test model removed the pneumatic cavity representation of the outage, resulting in an outage unable to increase in pressure during the impact. This second model was expected to represent the upper-bound of leakage (i.e., a tank that was completely open to atmosphere), which would represent a lower-bound for tank car stiffness. These models were expected to bound the response measured during the test, when the tank was imperfectly sealed.

12.3 Comparison of Test and Analysis Results

A limited set of results are discussed in this report, while the complete set of model and test results can be found in the report for Test 9 (Eshraghi, S., Trevithick, S., Carolan, M., Rakoczy, P., & Wilson, N., 2020). These results include comparisons of test results to FEA results for force and energy versus impactor travel. [Figure 66](#) shows these comparisons. As expected, the two post-test FE results bounded the stiffness response and the energy response of the tank measured in Test 9. This provides strong evidence that the discrepancies between test and model can be attributed to the leakage observed through the manway and other top fittings during the test.

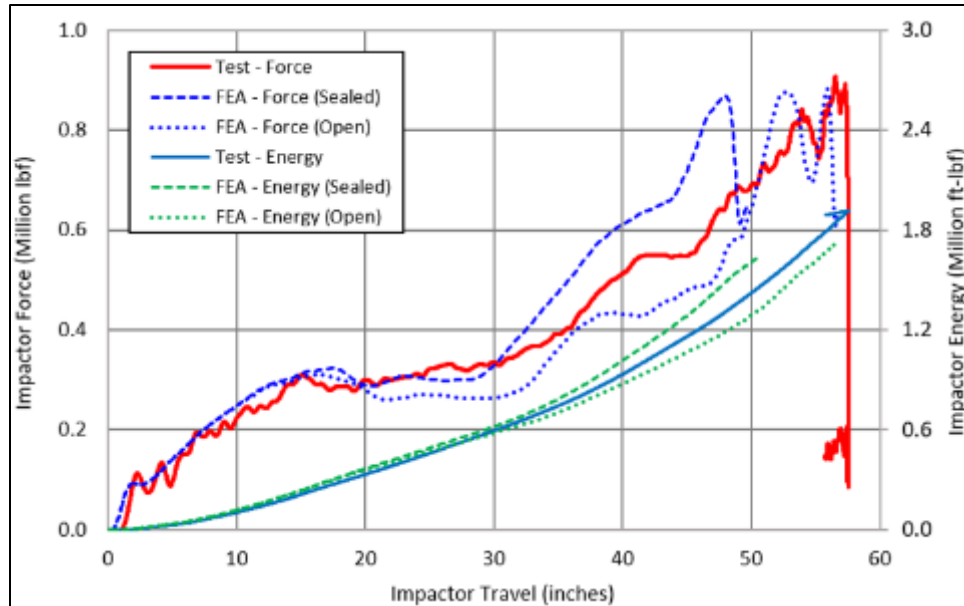


Figure 66. Test 9 – Test vs. Analysis Comparison of Impactor Force-Travel Plot

12.4 Discussion and Lessons Learned

Test 9 was the first test of a non-jacketed tank car. It also featured a ruggedized camera on board the impactor car, focused on the tip of the impactor. The camera effectively captured the initiation and propagation of the tear in the tank. This view allowed the onset of tank puncture to be visually observed for the first time. The tear was observed to initiate underneath a corner of the impactor. As the impactor continued forward and the tear propagated, it encountered a circumferential weld at the center of the tank car. Once the tear reached this weld, it continued to propagate along the weld. Thus, while the presence of a weld in the impact zone did not appear to influence the initiation of puncture, the propagation of puncture did follow a path along the weld.

Review of the test videos indicated that before the tank was punctured by the impactor, water leaked out of the manway seal on the top of the tank car due to increased internal pressure as the impactor compressed the tank. While it was expected that air and water could escape from the PRV if sufficient pressure developed during the test, leakage from around the manway was unexpected and undesired. This leakage effectively softened the force-indentation response of the tank car. Rather than building pressure of the air within the outage, the air simply escaped the tank. For future tests, it is important that all the necessary steps are taken to ensure correct operating conditions.

The DOT111 tank car was equipped with a bottom valve protection structure. The steel skid plates were placed on several plywood sheets to increase the clearance at the bottom center of the tank during the physical test. Additionally, the bottom outlet valve extension that projected past the bottom of the protective housing was removed before the test. Finally, the concrete “pit” at the base of the impact wall was expanded to provide additional clearance between the bottom outlet housing and the concrete. Post-test examination of the videos, the housing, and the concrete showed no evidence of contact between the housing and the concrete. This check should be performed before and after an impact test.

Accurate modeling of material properties in the FE model as well as the actual speed at which the test was performed are important to have good agreement between test and FEA results. The FE properties for TC128 material in the post-test model were updated based on the results of tensile tests performed on specimens extracted from the tested car. The post-test model was run at the measured test speed of 13.9 mph with the measured weight of the impactor car. The material properties for water were adjusted in the post-test model to match the properties at the temperature of the water in the test. The differences between pre-test and post-test behaviors were small for the water properties used in the model. Results from previous tests of unpressurized tank cars having a small outage (i.e., DOT112 [Test 5] and DOT117 [Test 7]) indicate the need to model the lading in such a way that sloshing and pressure increase of the outage can be accurately captured. Thus, water was explicitly modeled with a Lagrangian mesh, rather than the hydraulic cavity simplification employed in other simulations. The maximum tensile stress that the water could support was set to 0 psi, effectively limiting the water from experiencing any tensile stresses. Because water leakage from the manway and pressure plate was observed during the test, post-test model was updated to bound the upper and lower limits of leakage with a fully closed tank and a fully open tank. No attempt was made to develop a pressure-flow relationship to explicitly model the escape of fluid through the imperfectly sealed openings, as the bounding case approaches provided reasonable limits on the response.

Like Test 8, post-test material characterization from Test 9's car used 2-inch rectangular, 8-inch rectangular, and 2-inch cylindrical coupon geometries to investigate the effects of coupon geometry on the material model development process. It was concluded that while all geometries are suitable for determining the mechanical properties of the steel, cylindrical coupons are best suited for calibrating a material model for use in puncture simulations. The Eshraghi et al. (2020) report documents the coupon tests and material model development.

The repaired section of the tank car did not influence the outcome of the test. The successful repair of a cutout in the shell of the tank before the test opens the possibility of removing material from the tank car's shell before a future test to allow pre-test material characterization. It is important to select an area of the tank's shell that is unlikely to experience a significant amount of permanent deformation.

13. Test 10 – DOT113C120W (November 19, 2019)

Test 10 featured a DOT113 tank car struck by a 12-inch by 12-inch impactor. [Table 29](#) summarizes the specifications for the tested tank car.

Table 29. Test 10 – DOT113C120W Tank Car Specifications

DOT113	Pressurized tank car for transporting products at cryogenic temperatures
C	Inner tank design service temperature of -260 °F (110 °K)
120	120 psig test pressure
W	Fusion welded tank

Test 10 was the first test of a DOT113 tank car, which is a specialized tank car used to transport specified cryogenic liquids. The DOT113 featured a “tank-within-a-tank” design, with an inner tank made of stainless steel and an outer tank made of carbon steel. The annular space between the two tanks is typically filled with insulation (i.e., in this case, granular perlite) and is under a vacuum to further reduce heat transfer between the inner and outer tanks. [Figure 67](#) shows the test setup.



Figure 67. Test 10 – Test Setup Showing DOT113 Tank Car and Impactor

13.1 Summary of Test 10

The objective of Test 10 was to quantify the deformation mode, impact load-time history, and puncture resistance of an existing DOT113 tank car in a shell impact. A secondary objective of this test was to understand how the impact response, including puncture resistance, of the DOT113 tank car compared to the other tank cars from previous tests. The results of this test would be used to help in the development and validation of an FE model. It was anticipated that

additional tests and analyses of DOT113 tank cars would follow this test in the future. [Table 30](#) summarizes Test 10 test conditions and results.

Table 30. Test 10 – Test Conditions and Results Summary

Outage	17.6%
Target Speed	16.5 mph
Actual Speed	16.7 mph
Pressure	50 psig
Product	Water
Indenter Dimensions	12 in. ×12 in.
Impactor Weight	297,000 lbs.
Tank Car Weight (estimated)	345,500 lbs.
Nominal Thickness Inner/Outer	0.44 in. / 0.25 in.
Actual Thickness Inner/Outer	0.46 in. / 0.28 in.
Insulation and Thermal Protection	Vacuum and perlite
Nominal Insulation Thickness	6 in.
Test Outcomes	Inner and outer tanks punctured; impactor car continued into tank

The tank car used in Test 10 and the test setup itself are different from the previous tests in several ways. The DOT113 is a tank car intended for transporting products at cryogenic temperatures in pressurized conditions. It has two tanks with construction such that there is a tank surrounding another tank. The inner tank is designed to support the load of the product being carried at cryogenic temperatures, and the outer tank is designed to support the in-train forces. The specific DOT113 tank car tested in Test 10 featured two steel alloys that had not previously been encountered in other tested tank cars. Test 10’s tank car outer tank was made of A516 Grade 70 carbon steel and its inner tank was made of ASTM A240 Type 304 stainless steel. This tank car also featured an insulation material, granular perlite, which had not been encountered within previous tests. In addition to holding granular perlite, the annular space between the two tanks was under a vacuum. This was the first test of a tank car under a vacuum condition.

Finally, while the DOT113 tank car is designed to carry a cryogenic liquid at a cryogenic temperature, this test was performed using water at ambient temperature. At the time Test 10 was being planned, FRA and PHMSA had announced a Notice of Proposed Rulemaking (NPRM) to authorize the transportation of liquefied natural gas (LNG) in DOT113 tank cars (Pipeline and Hazardous Materials Safety Administration, 2019). The target outage pressure and volume used in Test 10 was based off the filling densities and pressures published in this NPRM, as there was no service condition data for LNG transport in DOT113 tank cars at the time.

Regarding the test setup, the impact point was not at the longitudinal center of the tank as [Figure 67](#) shows. A centered impact would have resulted in the DOT113 tank car fouling a right-of-way adjacent to the impact wall due to its substantial length (see [Figure 67](#)), and it would have

resulted in striking the tank car at a location with an internal structure between the two tanks. The horizontal offset from the longitudinal center of the tank is about 11 feet. Note that the impact point was still centered vertically with respect to the tank car.

Typically, the interior of the tested tank car is instrumented with pressure transducers along the length of the car and at the 0-, 90-, 180-, and 270-degree locations around the circumference of the inner tank. The interior is also typically instrumented with longitudinal (i.e., parallel to the direction of impact) and vertical string potentiometers in the vicinity of the point of impact. All these instruments require access to the interior of the inner tank. While the DOT113 tank car used in this test featured a manway, this manway was much smaller than those encountered in previous tank cars. There was no access to the inside of the tank to install string potentiometers, and all pressure transducers had to be installed within arm's reach of the manway opening. To attempt to measure the indentation of the outer tank, Test 10 used a new laser-based displacement measurement technique. Longitudinally oriented lasers were installed on the impactor car across its width. Four of these laser transducers reflected off the tank car, and a fifth transducer was located high above the impactor, reflecting off the impact wall. Additional laser transducers were installed in cutouts on the impact wall itself to measure any displacements of the side of the tank car opposite the point of impact.

13.2 Summary of Analyses

Volpe performed the pre- and post-test FEA. The pre-test model for Test 10 was developed from the ground-up due to the differences between the DOT113 tank car and the other, previously tested tank cars. As a result of the offset in the test setup, a full-length FE model was used. The simulation techniques used in the DOT113 tank car models included modeling tanks with elastic-plastic material responses, ductile failure implementation of multiple damage initiation models, and modeling of the water and air phases within the tank. In the post-test model, the perlite insulation was also modeled. The water phase was modeled as a hydraulic cavity. A pneumatic cavity was defined for the pressurized air phase. The hydraulic cavity approach was used to help reduce the considerable runtime of the full-length FE model having two patches of solid elements and was deemed to be suitable for an outage pressure (50 psig) and a relatively high outage volume (17.6 percent).

Pre-test, the stainless-steel inner tank was modeled using a Modified Mohr-Coulomb (MMC) triaxiality and Lode angle-based failure criterion. In the post-test FE models, the stainless steel was modeled using a B-W triaxiality-based failure criterion. Additionally, the post-test FE model was used to examine the influence of strain rate effects on the stress-strain and on the puncture behaviors of the stainless-steel inner tank. Unlike models of previous tests, the post-test FE models for Test 10 were updated to incorporate the actual thickness of the inner and outer tank shell materials, as they deviated significantly from the nominal thicknesses (see [Table 3](#)).

As a part of the pre-test and post-test modeling studies, non-puncture models and puncture-capable models were developed. The non-puncture models were mainly developed to reduce model solution time and to examine modeling techniques before their implementation in the puncture-capable model.

13.3 Comparison of Test and Analysis Results

A limited set of results are discussed in this report, while the complete set of model and test results can be found in the report for Test 10 (Wilson, N., Carolan, M., Trevithick, S., & Eshragi, S., 2021). These results include comparisons of test results to FEA results for force and energy versus impactor travel. Figure 68 shows these comparisons.

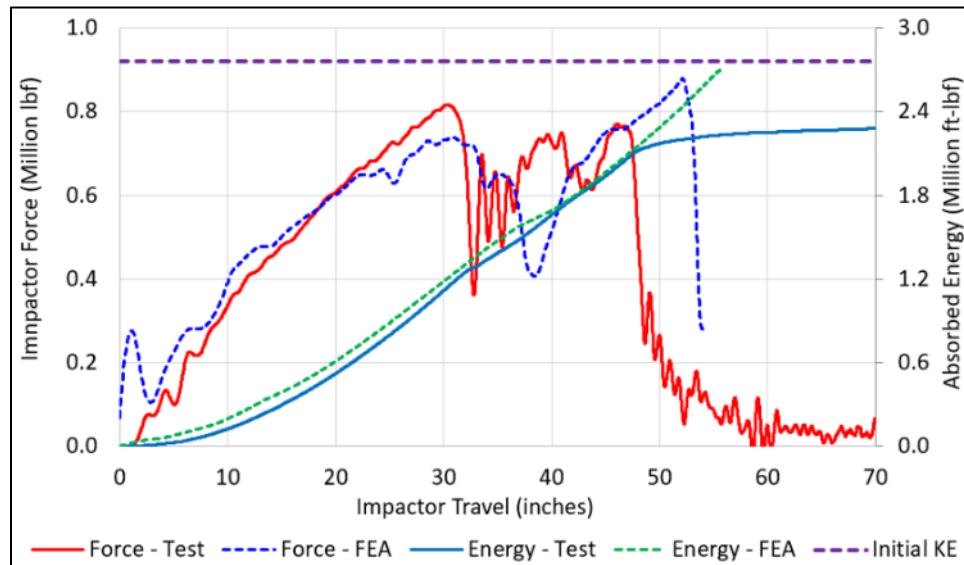


Figure 68. Test 10 – Test vs. Analysis Comparison of Impactor Force-Travel Plot

13.4 Discussion and Lessons Learned

Test 10 resulted in puncture of the inner and outer tanks of DOT113 tank car, with the impactor continuing to move forward after the impact. This indicated that the impactor had more kinetic energy than necessary to cause puncture of both tanks and to bring the impactor to a stop. Examination of the test measurements and comparison with the pre-test FE models revealed that the tank car exhibited a stiffer force-displacement response than estimated by the pre-test FE models. Further examination revealed that this apparent discrepancy was caused by the perlite insulation contributing more to the structural response of the tank car than expected. The perlite insulation is believed to have hastened the puncture of the outer tank, compared to a tank car without perlite, as the insulation was compacted and inhibited the outer tank from deforming in response to the impactor. This led to the need to develop a perlite material model in the post-test FE models to achieve better agreement. The role of perlite underscores the importance of understanding the condition of and potential structural behaviors of insulation in future tank car tests. Additionally, further examination of perlite mechanical behaviors may be appropriate if this material is to be used to insulate tank cars in the future.

The laser-based displacement transducers functioned as intended, but processing of the data proved to be challenging. For the displacement transducer at the center of the impactor car that reflected off the wall, this channel was found to be in excellent agreement with the impactor car displacement calculated off the onboard accelerometers and initial speed. Thus, using an onboard laser transducer aimed at the fixed impact wall provides a redundant, independent measurement of the impactor car's travel should there be a problem with the accelerometers in a future test. For the remaining four laser transducers reflecting off the outer tank of the DOT113, processing

the data was complicated due to the impactor car and the tank car in motion simultaneously. Initially, only the impactor car was in motion. As the impactor car makes contact with the tank car, the tank car begins to deform and to displace. When the point on the tank car that the laser is reflecting off begins to indent, the apparent distance measured by the laser transducer may grow larger even though the impactor car continues to move forward. The impactor car is slowing down, while the point on the tank car may be speeding up as the dent continues to grow deeper.

Pre-test and post-test LiDAR scanning of the inner and outer tanks were performed for Test 10. These measurements proved to be especially valuable in characterizing the dent of the tank car, since internal string potentiometer measurements could not be made in this test.

Post-test material characterization was performed on the outer tank and on the inner tank materials. While the inner tank's stainless steel had properties as expected, the outer tank was found to have a yield strength and ultimate strength that fell below the minimum values of specification ASTM A516 Grade 70 steel. To confirm this unexpected result, a second set of samples of the inner and outer tank steels were sent to a second testing laboratory, which confirmed the results of the first laboratory. Chemical analysis of the outer tank's steel indicated that the silicon and manganese content each fell below the minimum required by ASTM A516 Grade 70. This once again shows the importance of extracting samples from tested tanks and performing material testing on samples to be used in the FE models for analysis to obtain more accurate representation of the tanks.

Post-test FE modeling was challenged by the effects of the perlite insulation on the overall impact response of the DOT113 tank car. A new material model had to be estimated in the post-test FE model to account for the perlite. Even with this behavior, the post-test FE model over-estimated the energy to puncture the inner tank. While typical FE models of previously tested tank cars have attained reasonable agreement without including strain-rate effects in the carbon steel behaviors, review of available literature suggested that ASTM A240 Type 304 stainless steel experienced more significant strain-rate effects than typical carbon steels used in tank cars. Thus, post-test FE models examined the effects of strain rate on the overall impact response. However, no elevated strain-rate tensile testing was performed on the stainless steel removed from the Test 10 DOT113 tank car. This testing should be considered in the future, especially if additional tests of stainless-steel tanks are planned.

14. Discussion Across Multiple Tests

The tests conducted during this program can be categorized in several different ways. For example, all the tank cars tested to-date have been intended to carry one of three categories of commodity: TIH materials, flammable liquids or cryogenic liquids. The tank cars could also be categorized as unpressurized cars, pressure cars or cryogenic cars based on the condition of the lading in typical service conditions. Additionally, tank cars could be grouped by the outcome of the test, either puncture or non-puncture. This section contains comparisons between test results from different tests, organized in different ways.

Tank cars of different specifications are typically constructed to carry a particular commodity, under conditions particular to that commodity. Thus, the design pressure, tank thickness, tank capacity, and typical outage volume can vary significantly from one specification tank car to another, depending on the intended service. However, it might indicate relative behaviors of various tank cars by comparing their responses under the substantially similar impact test setup used in the shell impact testing program.¹² This section of this report compares measured behaviors from various tank cars subjected to the shell impact test scenario.

Figure 69 shows the naming convention used in the data series plotted in the graphs throughout this section of the report.

DOTxxx, y.y%, ZZxZZ, AA.Amph, BB, (Q)

where,

"xxx" is the three-number specification of the tank car;
"y.y" is the outage volume of the tank car;
"ZZxZZ" is the cross-sectional dimensions of the impactor;
"AA.A" is the measured test speed;
"BB" is either "NP" for non-puncture outcomes, or "P"
for puncture outcomes;
"Q" is the test number

Figure 69. Naming Convention Used to Distinguish Tests

A series identified as “DOT111, 2.5%, 12"×12", 14.0mph, P (4)” represents a DOT111 tank car with a 2.5 percent outage, struck with a 12-inch by 12-inch impactor at 14.0 mph, resulting in a puncture with a test ID of 4 referring to Test 4. Also, Test 3 is marked with an asterisk to indicate its uniqueness (i.e., the use of a protective panel with the tank car).

One of the challenges in comparing results from different speed impacts is that each impact occurs on a separate timescale. Higher-speed impacts result in a shorter timescale than lower-speed impacts, which can make comparing force-time histories a challenge. One approach for allowing a comparison is to cross-plot the force-time history against the displacement-time history, leading to a force-displacement response. The force-displacement responses of different

¹²Since Test 10 is for a DOT113 tank car which is unique compared to the other tank cars that were tested, generalized statements are not applicable to this test.

tests can provide more insight than the force-time responses, particularly when the test speeds differ greatly. Further, the responses from the different tests can be normalized with respect to speed or any other variable that can be used to compare results. The following sections discuss comparisons within tank car types and between different tank car types with variables that were identified as logical. One normalization used in this section divides the instantaneous speed of the impactor to its initial speed. All tests would start at a normalized speed of 1.0 for graphs using this normalization.

14.1 Tests of Pressurized Tank Cars

Seven tests out of a total of 11 were performed in this series with the tank car sealed and initially pressurized above atmospheric pressure: Tests 0, 1, 2, 3, 6, 8, and 10. Figure 70 contains a plot of the impact force versus time for these seven tests. Pressurized DOT105 tank cars were tested in six of these tests. While the outage and pressure were approximately the same in all six tests of DOT105 tank cars, the impact speed and impactor size varied across tests. This allows the responses of the struck tank cars to be compared, to gain insights into how the impactor size and impact speed affected the outcome of a test. Note that all the initially pressurized tests used a DOT105 tank car at 100 psig, except for Test 10 which used a DOT113 tank car initially pressurized at 50 psig.

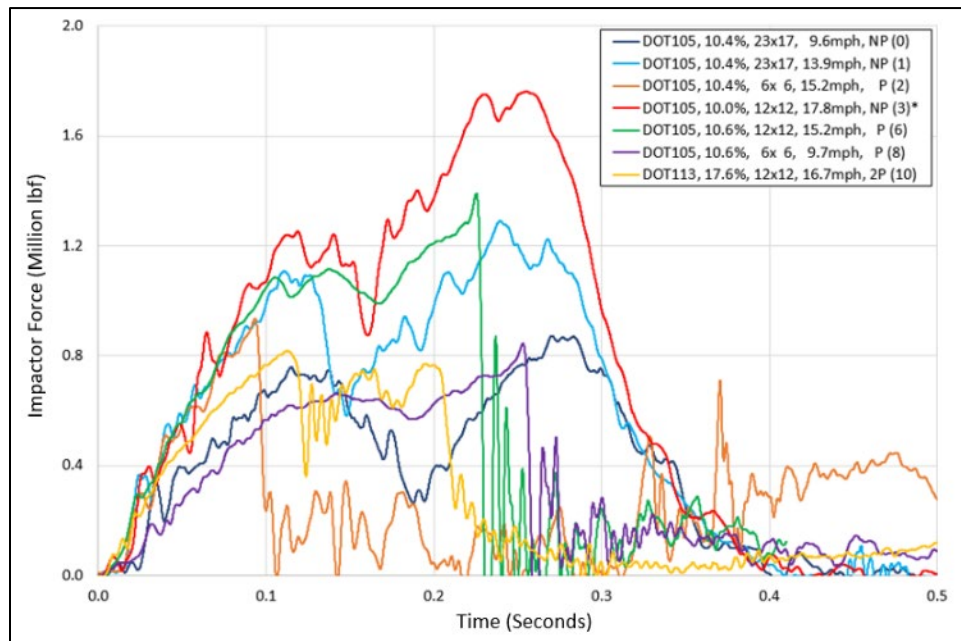


Figure 70. Force vs. Time for all Initially Pressurized Tank Cars

Figure 70 shows that DOT105 tank cars exhibit some similarities in force-time responses, regardless of impactor size or impact speed. In most tests, the force initially rises before reaching a plateau at several hundred thousand pounds of force. The one exception to this is Test 2, which punctured before reaching a plateau value. From all the other responses, the force then remains constant or drops slightly before beginning to climb again. The force then drops in all cases, which is a sudden drop in the case of a puncture test, or a more gradual decrease in the case of a non-puncture test.

Figure 71 contains a plot of the impactor force versus impactor displacement for the seven tests of initially pressurized tank cars conducted to-date.

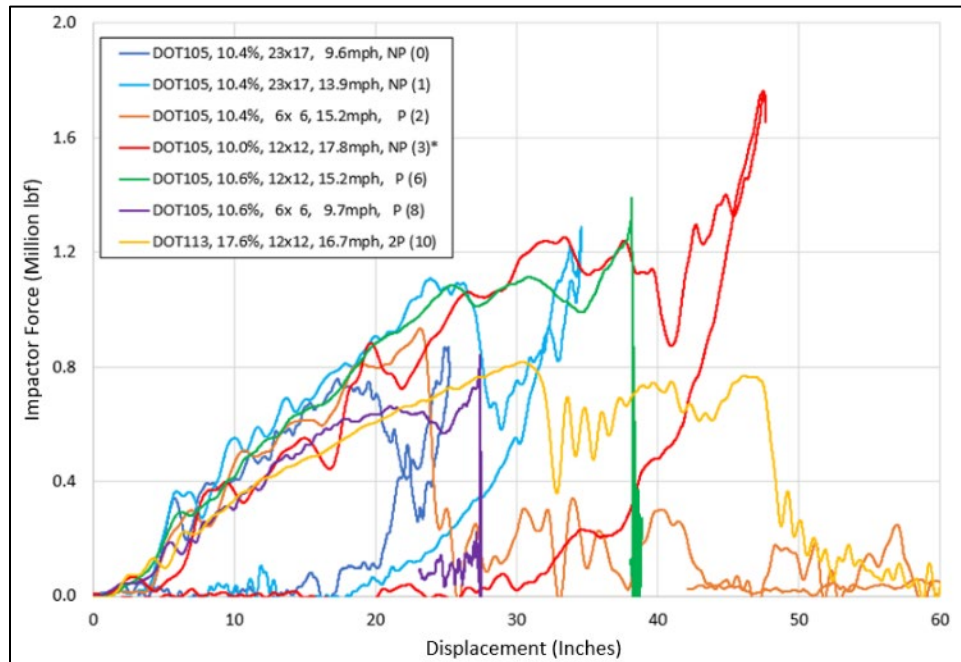


Figure 71. Force vs. Displacement for all Initially Pressurized Tank Cars

The force-displacement responses of the various DOT105 tank cars shown in Figure 70 exhibit certain similarities to the force-time responses shown in Figure 69. The initial force-displacement responses all follow a similar slope. Additionally, all the force-displacement histories feature approximately a 4-inch travel at a relatively low force before the force increases considerably. Each of the DOT105 tank cars tested in this program had 4 inches of insulation between the tank and the jacket. Thus, if the instrumentation triggered at the instant of contact between impactor and jacket, the 4 inches of relatively soft response corresponds to the insulation compressing before the impactor encountered the substantially stiffer commodity tank. Tests 1, 3, and 6 reach similar plateaus at approximately 1 to 1.1 million pounds of force.

Tests 0, 1, and 3 exhibit larger drops in force between the plateau and the subsequent rise in force compared to Tests 6 and 8. One probable explanation for this difference is attributable to the insulation in these tank cars. All these tank cars were DOT105 tank cars and featured insulation between the tank and its jacket. Tests 0, 1, and 3 featured ceramic blanket insulation, and Tests 6 and 8 featured a urethane foam insulation. Section 9 and 11 discussed the models for Tests 6 and 8, which exhibited better agreement with the test measurements when a simplified foam insulation was included. It is likely that the foam insulation offered more structural support for the commodity tank, which affected its dynamics as it was pushed up against the rigid impact wall. The insulation gets compressed in two regions as the impact occurs. Initially, the impactor compresses the foam between the jacket and tank in the impact zone. This is a localized deformation, and the presence of insulation may have only a minor effect on the initial stiffness necessary to move the jacket closer to the tank. As the impact continues, the forces acting on the tank want to move it closer to the wall, which is in contact with the jacket on the opposite side of the tank car as the impact. If the tanks for the DOT105 cars were uninsulated but were provided with a 4-inch gap between tank and wall, the tank could develop some relative speed before

coming to a sudden stop against the wall. With a relatively stiff insulation between tank and jacket, the commodity tank would not have been able to develop as much relative speed, as it would have had to crush the foam to get closer to the wall. The foam acts over a much larger area between the tank and jacket on the wall-side of the impact setup, as the entire tank is pushed toward the wall. Thus, the relative effect on the tank's response of a stiff insulation may be more substantial later in the impact event as the tank begins to move toward the wall, but it is resisted by compression of the stiff insulation. While the insulation itself absorbs some energy through plastic deformation, the insulation also increases the stiffness of the overall tank-wall system that is decelerating the impactor.

A subset of the pressurized tank cars includes all DOT105 tank cars that experienced puncture. [Figure 72](#) contains the force versus displacement responses from Tests 2, 6, and 8. These results are notable, as each of these three tests featured very similar impact parameters with another test in this subset. Test 2 featured a 6-inch by 6-inch impactor traveling at 15.2 mph. Test 6 used a 12-inch by 12-inch impactor traveling at approximately the same speed, which allows the influence of impactor size to be examined. Test 8 featured a 6-inch by 6-inch impactor traveling at 9.7 mph, which can be compared with Test 2 to assess the influence of impact speed when the same-sized impactor is used. Finally, Tests 6 and 8 each resulted in puncture of the tank car and rebound of the impactor car, indicating the tests occurred at approximately the threshold puncture speed. These two results can be compared to understand how the tank car response is affected by differently sized impactors when struck at approximately the threshold speed for that size of impactor under the given impact conditions.

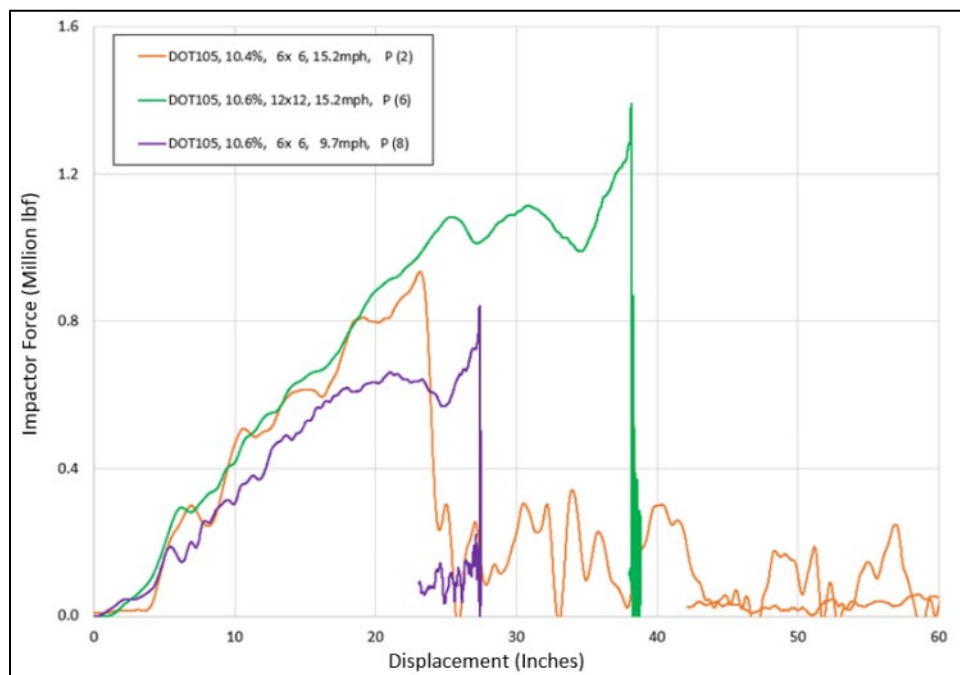


Figure 72. Force vs. Displacement – Tests 2, 6, and 8

Without any further normalization of the data, [Figure 71](#) shows Tests 2 and 6, which ran at 15.2 mph, have force-displacement curves that essentially overlay one another, up to the point of puncture of the tank car in Test 2. This result indicates that the overall stiffness of the tank car in the standardized impact scenario is independent of the impactor size. Effectively, the tank car's

impact response is independent of the impactor size (i.e., at least over the range examined), but the size of the impactor affects how far up the curve the response can travel before puncture occurs.

Focusing on Tests 6 and 8, it is apparent that the reduced impact speed of Test 8 (9.7 mph) results in a less stiff initial response than the other two tests (15.2 mph). As Tests 6 and 8 were run at speeds only slightly more than the threshold puncture speed for their respective test scenarios, these two responses provide a full picture of the DOT105 tank car's response up to puncture. Quantitatively, the Test 8 response experiences a lower force for a given displacement and punctures at a lower displacement than Test 6. Qualitatively, however, the force versus displacement curves for Tests 6 and 8 exhibit remarkable similarities. Each test featured an initial low force up to approximately 4 inches, which is likely when the crushing of the insulation between the jacket and tank occurs. Each response then stiffens up for a considerable distance, until reaching a plateau. Once on this plateau, the force remains roughly constant for increasing displacements, with some oscillations. At the end of the plateau, the force increases until a sharp spike in force is seen just before puncture. Puncture is marked by a near-instantaneous drop in force, with nearly no displacement change. Since Tests 6 and 8 caused the impactor car to rebound following puncture, the displacement response can be seen to begin recovering after puncture occurs.

To visualize how close a given test came to stopping the impactor car before puncture, the impact force can be plotted as a function of speed. Using this approach, the impact event starts with the impactor traveling at its closing speed and the impactor decreases in speed as the impact unfolds. If the impactor car is brought to a stop, the speed reaches zero and crosses into negative values. A negative impactor car speed indicates the impactor car is moving away from the tank. For a puncture outcome, the sudden drop in force associated with puncture occurs rapidly, at a near-constant speed. Thus, the residual speed of the impactor car can be determined from such a graph. [Figure 73](#) shows the force versus speed responses from the three puncture tests of DOT105 tank cars. Test 2 punctures when the impactor car speed is still moving at approximately 75 percent of the impact speed (i.e., 50 to 60 percent residual impact energy). Tests 6 and 8 puncture at low impactor car speeds (i.e., less than 1 mph), dissipating approximately 99 percent of the impact energy.

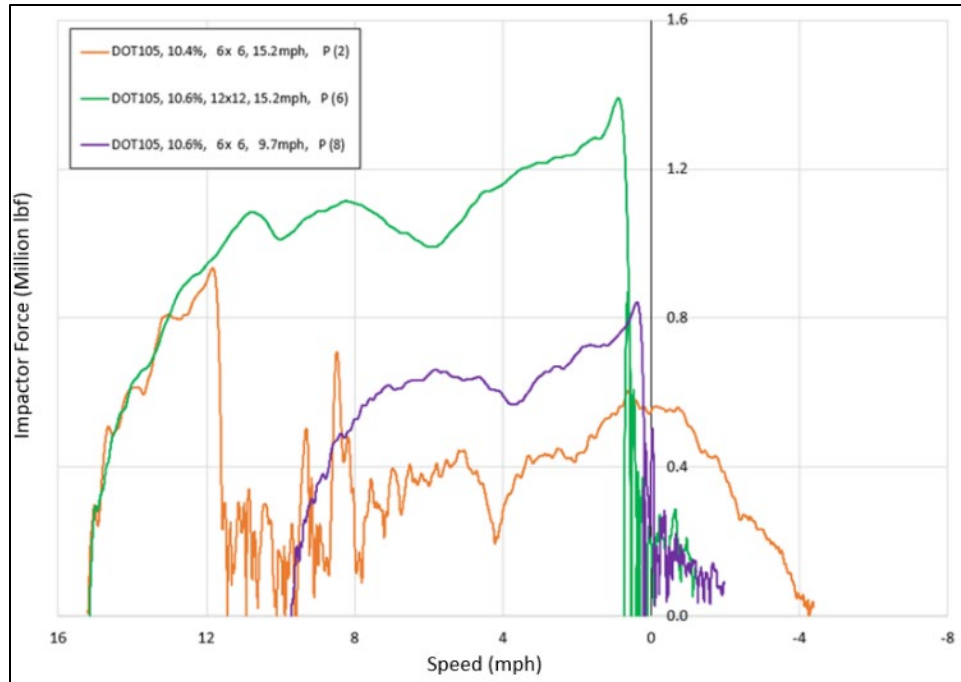


Figure 73. Force vs. Speed – Tests 2, 6, and 8

Another approach to normalizing the results divides the instantaneous forces and energies by the initial speed of the impactor car, resulting in speed normalized force (SNF) and speed normalized energy (SNE). A plot of SNF and/or SNE against normalized speed features all results starting at a normalized speed of 1 mph per mph and all force and energy values normalized to 1 mph speed of the impactor. Figure 74 contains a plot of SNF versus normalized speed for the three puncture tests of DOT105 tank cars. From this figure, it is more apparent that the DOT105 tank cars exhibit some typical behaviors across the range of impact speeds and impactor sizes used in this testing program. All three responses overlay each other up to the point of puncture in Test 2. As the normalized speed reduces, Tests 6 and 8's similarities are more pronounced qualitatively and quantitatively when the force and speed are each normalized. Irrespective of the size of the impactor and speed, when SNF is plotted against normalized speed, all three graphs have similar amplitudes up to the divergence point. Especially with Tests 6 and 8 that punctured with little energy left, both lines are like each other in terms of amplitude and of trend.

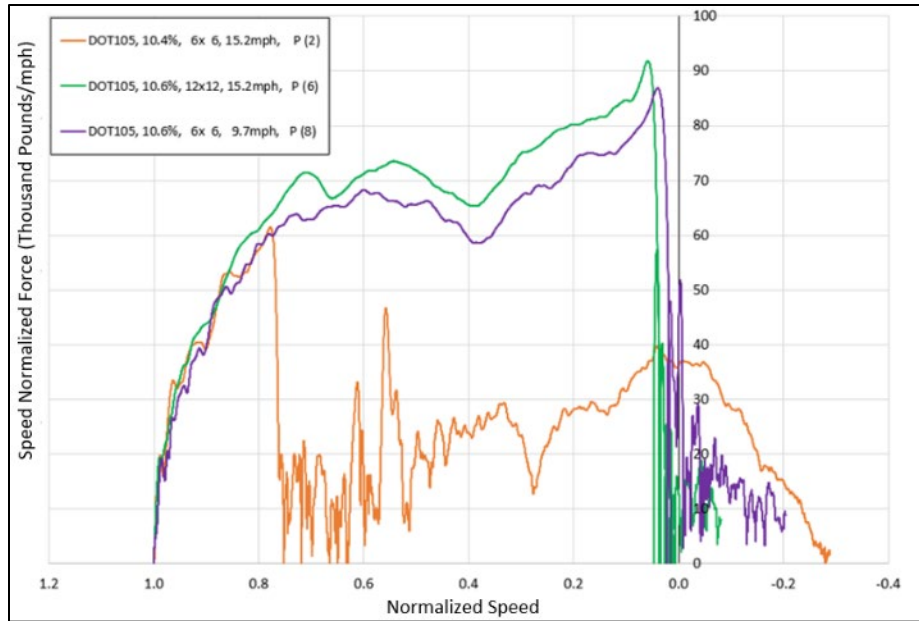


Figure 74. Speed Normalized Force vs. Normalized Speed – Tests 2, 6, and 8

Seeing the value in normalizing the test responses for the DOT105 puncture tests, the data results in Figure 74 have been extended to also include the non-puncture tests of DOT105 tank cars and plotted in Figure 75. The general trend is the same, although Tests 1 and 3 feature drops in force during the plateau phase not previously seen in the puncture results. These drops in force may be attributed to the use of a urethane foam insulation in the DOT105 tank cars used in Tests 6 and 8, which made a contribution to the two tank cars' structural responses and needed to be included in the FE models. The Test 2 tank car did not feature urethane foam, but it also punctured before reaching the plateau phase. The tank cars used in Tests 0 to 3 featured an insulation with less significant structural behavior, which may be responsible for additional dynamics in these tests.

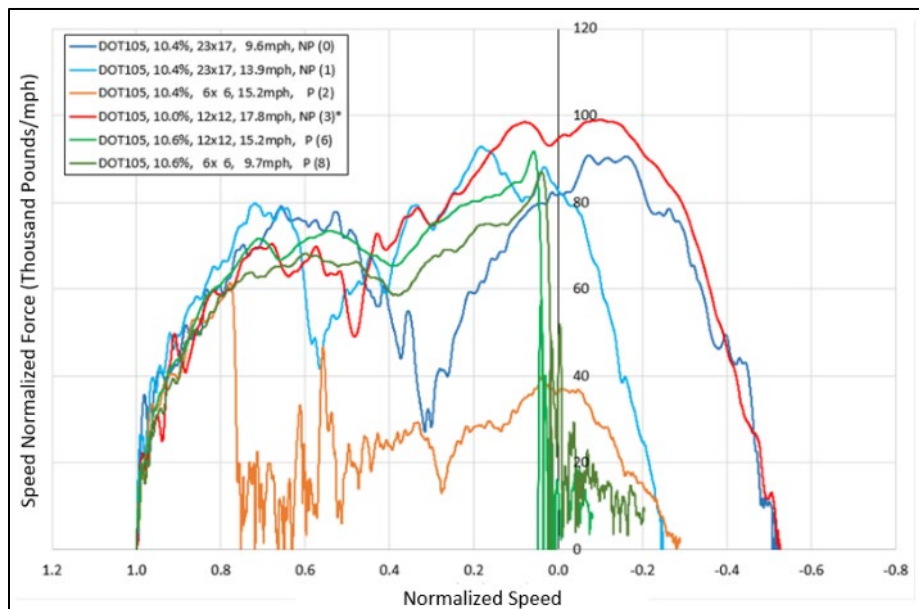


Figure 75. Speed Normalized Force vs. Normalized Speed – All DOT105 Tank Cars

14.2 Tests of Tank Cars Not Initially Pressurized

Four tests were performed in this testing series with the tank car sealed, but not initially pressurized above atmospheric pressure: Tests 4, 5, 7, and 9. Figure 76 contains a plot of the impact force versus time for the four tests that were performed with the outage initially at atmospheric pressure. Note that while a DOT112 tank car is typically operated at an elevated pressure, during Test 5, this tank car was tested at atmospheric pressure to represent an increased thickness unpressurized tank car. It should also be noted that the four impact tests were performed in a relatively narrow speed range, from 13.9 to 14.7 mph, using the 12-inch by 12-inch impactor. Thus, the primary differences among the unpressurized tank cars tested in this program are the thickness and the material used for the shell construction, initial outage volume, and absence or presence of a jacket.

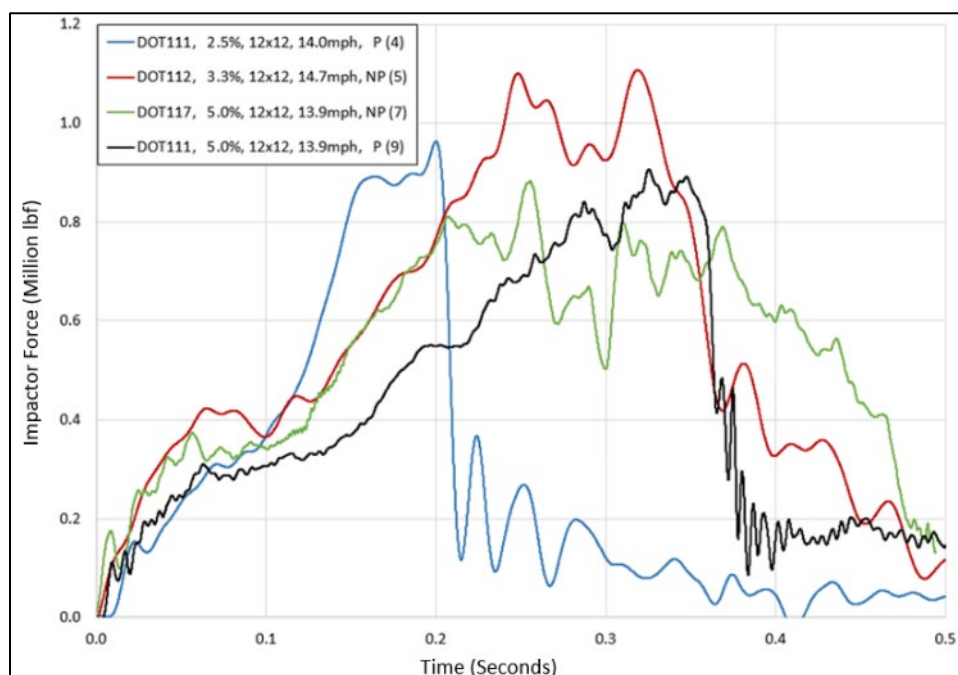


Figure 76. Force vs. Time – Unpressurized Tank Cars

Figure 77 contains a plot of the impact force versus the impactor displacement for the four tests of tank cars initially at atmospheric pressure. Figure 76 and Figure 77 show the unpressurized tank cars tested in this program exhibited some similar characteristics. Each tank car featured an initial rise in force that was followed by a plateau at approximately 300,000 to 400,000 pounds where the force remained nearly constant for increasing indentation. This is a much lower plateau force than observed for pressurized DOT105 tank cars. The ranges of time or displacement spanned by the plateau appear to be related to the outage volume. Test 4, with approximately 2.5 percent outage, has the shortest plateau phase. Tests 7 and 9, which each have a 5 percent outage, have comparatively longer plateau phases.

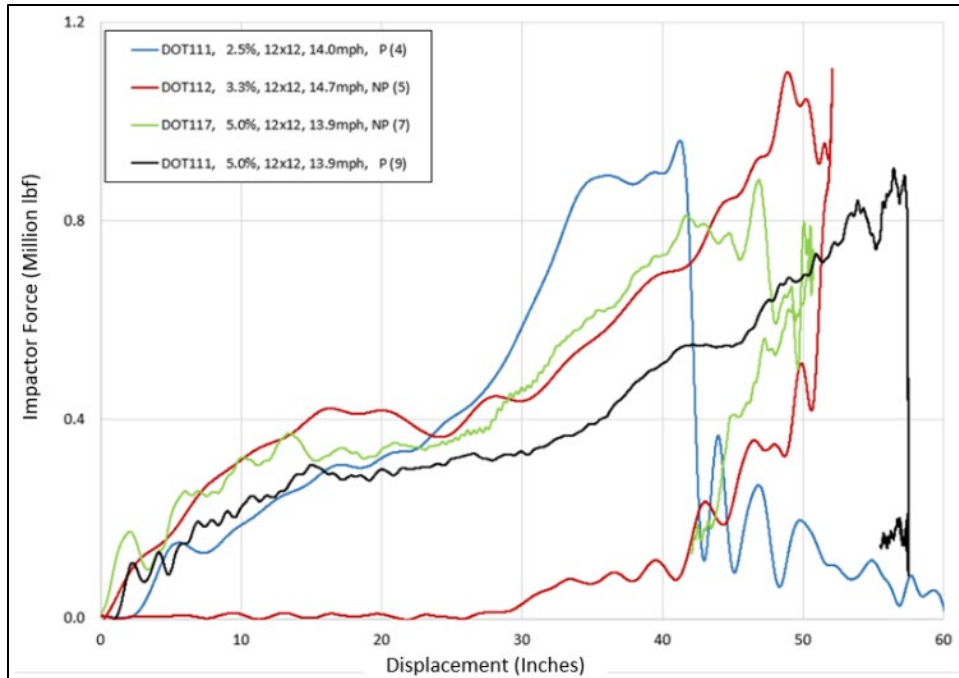


Figure 77. Force vs. Displacement – Unpressurized Tank Cars

Following the plateau phase, the force begins to rise again. This second rise occurs at a steeper slope than the initial rise for all the unpressurized tank cars. Near the peak load in each test, there is some noise and multiple localized peaks. This is believed to be caused by fluid motion in the decreased outage volume because of the large indentation of the tank car. Near the peak force a drop in force can be seen. The magnitude of the force drop varies greatly, with Test 4 exhibiting a relatively small force, whereas Test 7 exhibited a force of several hundred thousand pounds. Lastly, the force then drops in all cases; there is a sudden drop in the case of a puncture test, and a more gradual decrease in the case of a non-puncture test. In the case of a non-puncture outcome (Tests 5 and 7), the force gradually decreases as the displacement decreases, indicating the impactor car is now moving away from the tank car. In the case of a puncture outcomes (Tests 4 and 9), the force drops abruptly, with very little increase in impactor travel. Note that in Test 4, the impactor continued to move forward while in Test 9 the impactor began to rebound shortly after puncture. At least for these impact conditions, it is possible to say that the unpressurized tanks exhibit similar impact responses.

Figure 78 contains a plot of the impactor force versus the impactor speed for all tests conducted using an unpressurized tank car. Puncture of the tank cars of Tests 4 and 9 can be identified from the drop in force occurring while the impactor was still traveling forward. The drop in force during the non-puncture tests (Tests 5 and 7) occurred more gradually, with the impactor having a negative speed. A negative speed indicates the impactor was traveling backward, having come to a stop and rebounded from the tank car. Figure 79 shows speed normalized force versus normalized speed for all unpressurized tank cars in Tests 4, 5, 7, and 9.

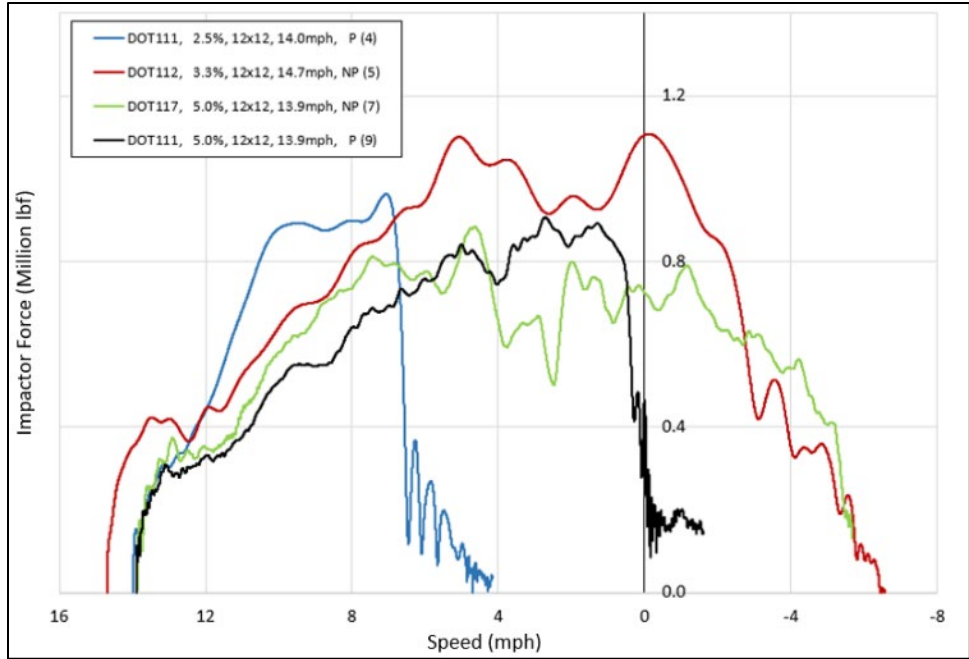


Figure 78. Force vs. Speed – Unpressurized Tank Cars

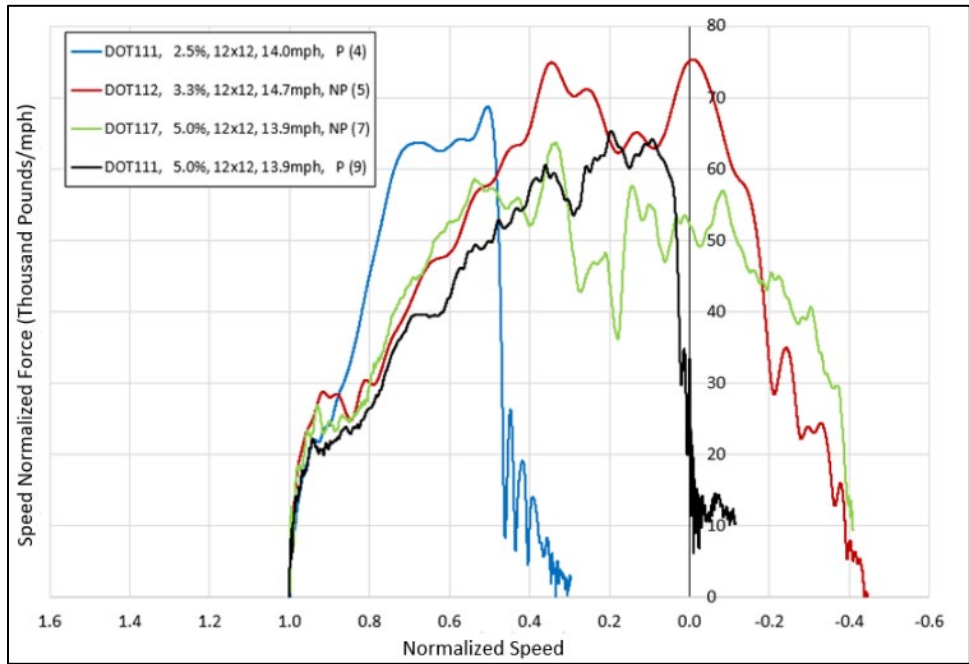


Figure 79. Speed Normalized Force vs. Normalized Speed – Unpressurized Tank Cars

14.3 Puncture Outcomes

Of the 11 tests performed to-date, 6 of the tests have resulted in puncture outcomes. The tank cars were punctured during Tests 2, 4, 6, 8, 9, and 10. These punctured tank cars include DOT105, DOT111, and DOT113 specification tank cars. Figure 80 contains a composite photograph of the puncture zones from each test that featured a punctured tank car. Note that for

Tests 2, 4, and 10 the impactor continued to travel toward the impact wall, and some of the damage observed in these photographs may be associated with removal of the impactor head following the test, not the puncture itself. In Tests 6 and 8, the outer jacket and insulation were removed from the impact zone to allow an inspection of the damage to the tank. Test 9 did not feature an outer jacket and the impactor rebounded, so the puncture of the tank was directly observable after the test without any further manipulation of the impactor car or tank car. The approximate “footprint” of the impactor’s face has been superimposed onto each photograph, except for the photograph from Test 2. Note that the individual photographs are from different angles and distances and are not to scale with one another.

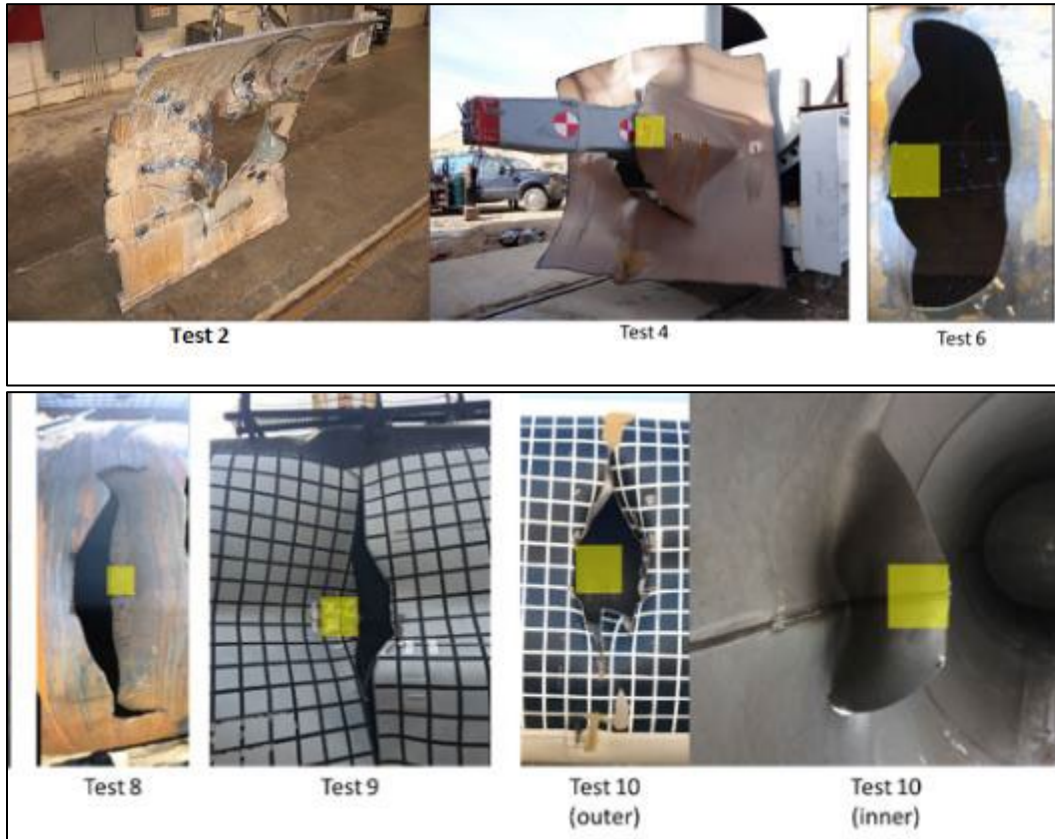


Figure 80. Photographs of Puncture Zone in All Tests with Puncture Outcomes (Not to scale)

From this composite image of [Figure 80](#), several observations can be made about puncture in general. The puncture zone initiates along an edge of the impactor face in every test. The supporting evidence for this result is the approximate vertical edge in each tear at approximately its mid-height, which corresponds with either the left or right-side edge of the impactor. In Tests 4 and 9, the tear initiated on the right-side edge of the impactor. In Tests 6 and 8, the tear initiated on the left side edge of the impactor. The outer tank in Test 10 punctured first and while it is not apparent from the figure, review of the video on board the impactor car showed the left side of the outer tank failed first. From the composite image, it is apparent that the inner tank in Test 10 also tore on the left side of the impactor.

Following the initiation of a puncture at the impactor, in each test the puncture propagated circumferentially around the tank (i.e., vertically above and below the point of impact). After propagating vertically for some distance, in each test the tear subsequently turned diagonally. The vertical tear continued to propagate in the direction it had originated (e.g., upward above the impactor and downward below the impactor). The horizontal component of the diagonal tear is always oriented toward the centerline of the impactor.

The force-time histories from the puncture tests are shown in [Figure 81](#). Two punctures are indicated for the DOT113 tank car, first for the outer shell, and approximately 0.09 seconds later for the inner shell. [Figure 80](#) shows one common indication of a puncture outcome is a rapid drop in the force occurring over a very short duration.

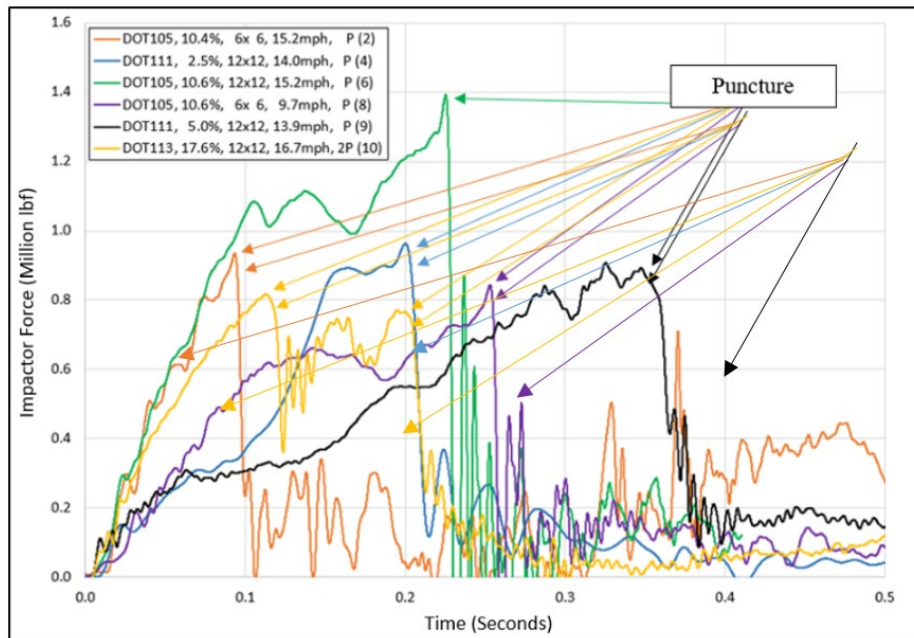


Figure 81. Force vs. Time – Punctured Tank Cars Only

[Figure 82](#) contains a plot of the impact force versus impactor travel for the six puncture tests. This presentation of the results provides some additional insight into whether the impactor continued to travel forward (increasing displacement) or rebounded (decreasing displacement) following puncture. Like the force-time response, the force-displacement response also features a near-vertical drop in force associated with puncture.

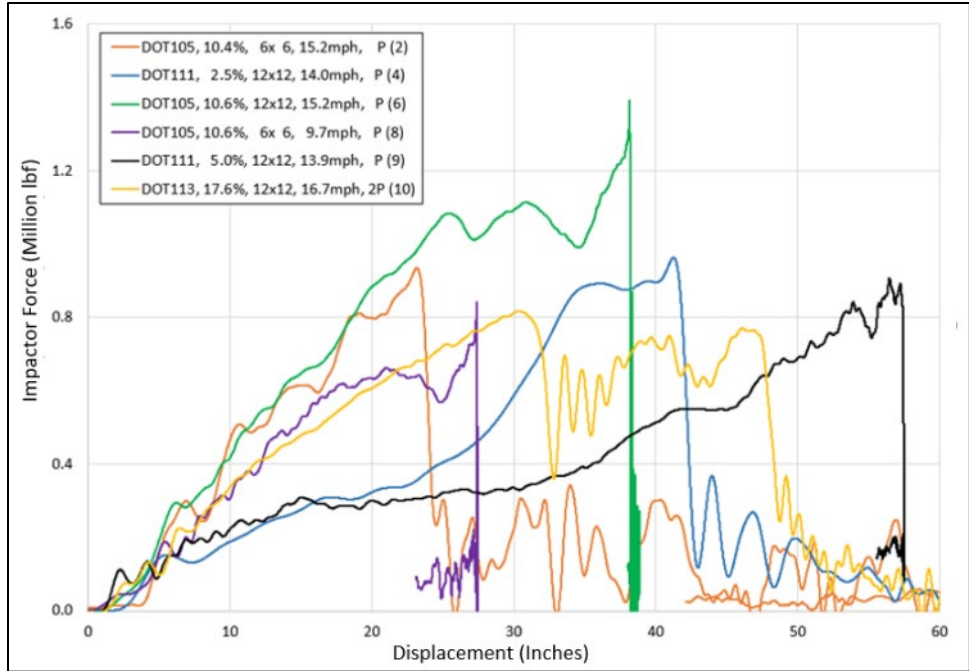


Figure 82. Force vs. Displacement – Punctured Tank Cars Only

Figure 83 contains a plot of the impactor force versus impactor speed for the tests that resulted in a puncture outcome. Note that in this figure, neither the force nor that speed has been normalized. This presentation of the data provides a clear indication of the residual speed of the impactor at the occurrence of puncture. As previously discussed in this section, a puncture outcome is often identifiable in force data by a sudden drop in force for a very small change in incremental speed or displacement. By plotting force versus speed for the puncture outcomes in Figure 83, one can visually estimate the residual speed at the time of puncture. Figure 82 shows Tests 6, 8, and 9 each experienced a puncture with a very small residual speed, while Tests 2, 4, and 10 experienced a puncture while the impactor was still moving with a substantial residual speed. Note that because of the highly nonlinear behavior of the tank car's impact response, the threshold puncture speed cannot simply be calculated by subtracting the residual speed from the initial impact speed.

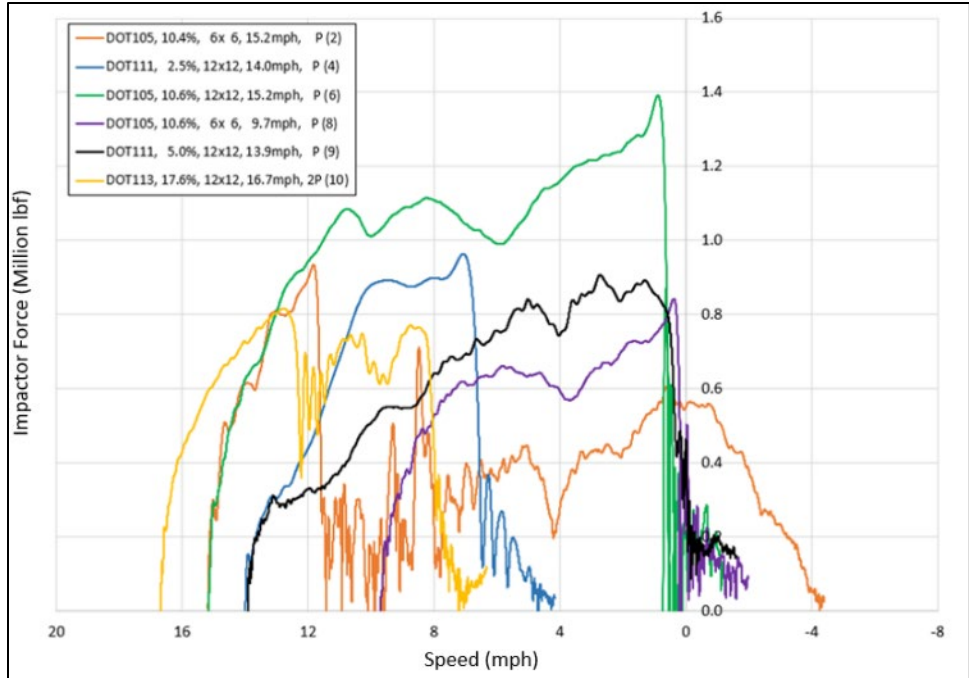


Figure 83. Force vs. Speed – Punctured Tank Cars Only

Also, [Figure 83](#) shows Tests 4 and 9 featured remarkable agreement initially, with the two responses diverging at the plateau phase. As previously discussed, the two tested tank cars featured very different outage volumes, which may be the reason for Test 4’s short plateau and rapid increase in force as the small outage volume rapidly increased in pressure. As previously discussed, Tests 2 and 6 also featured remarkable agreement up to the point of puncture of Test 2, despite these tests using different impactor sizes.

Finally, the SNF is plotted against the normalized speed for the puncture-outcome tests in [Figure 84](#). The three results from DOT105 tank cars follow a similar behavior up to the point of puncture from Test 2, and the two tests of DOT111 tank cars are similar up to the plateau phase. The initially pressurized DOT105 tank cars exhibit a different impact response from the initially unpressurized DOT111 tank cars. The DOT113 tank car, which was pressurized to a level between the atmospheric pressure of the unpressurized cars but less than the 100 psig of the DOT105 tank cars, exhibited an initial response that was somewhere between the pressurized and unpressurized tank cars. The DOT113 tank car punctured both of its tanks at SNF magnitudes that were substantially lower than the other tests.

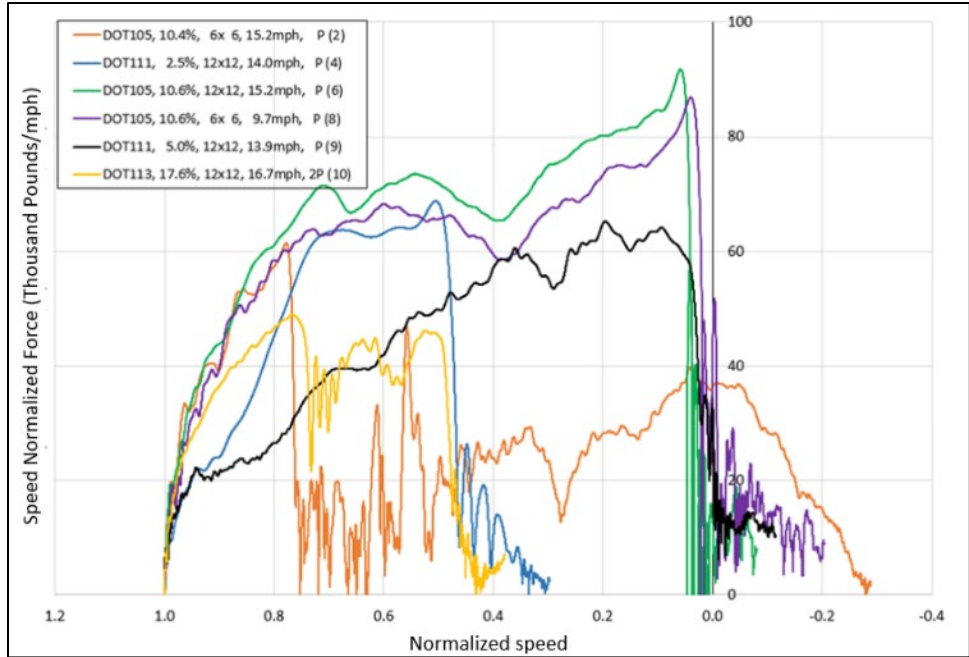


Figure 84. Speed Normalized Force vs. Normalized Speed – Punctured Tests Only

14.4 Non-puncture Outcomes

Of the 11 tests performed to-date, 5 have resulted in a non-puncture outcome: Tests 0, 1, 3, 5, and 7. These non-punctured tank cars included initially pressurized DOT105 and unpressurized DOT112 and DOT117 specification tank cars. Figure 85 contains a composite image showing photographs of the impact zone from each non-puncture test performed to-date. The impactor “footprint” has been superimposed onto the photographs for all tests except for Test 3, which included a protective panel between the impactor and the tank. Note that the individual photographs are from different angles and distances and are not to scale with one another.

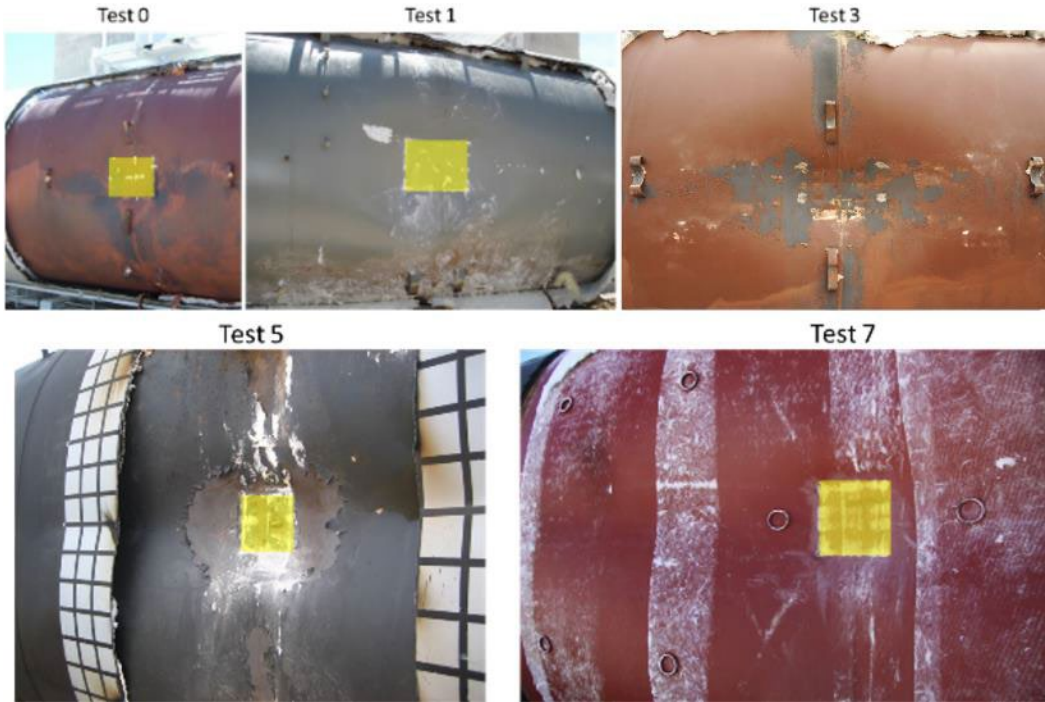


Figure 85. Photographs of Impact Zone in All Tests with Non-puncture Outcomes

Figure 86 contains a plot of the impact force versus time for each of the tests that resulted in a non-puncture outcome. As these tests span a range of speeds between 9.6 and 17.8 mph, it is difficult to compare the responses from different tests run at different speeds using a force versus time approach. However, it can be noted that by 0.5 seconds in all cases the force has dropped significantly compared to the peak value, which indicates the impact event of interest has ended. Also, Figure 85 plot shows the shapes of the force-time histories are distinctly different for the initially pressurized DOT105 tank cars (Tests 0, 1, and 3) and the initially unpressurized tank cars (Tests 5 and 7).

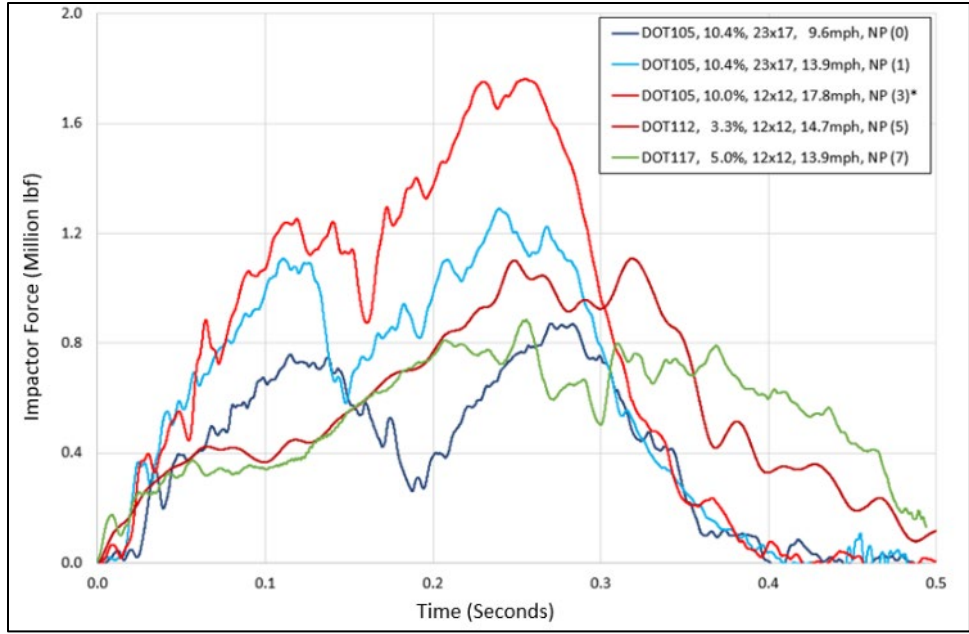


Figure 86. Force vs. Time – Non-Puncture Tests Only

Figure 87 contains a plot of impactor force versus impactor travel for the five non-puncture tests. In general, the DOT105 tank car tests exhibit similar responses to one another, which are distinctly different from the two tests of tank cars initially at atmospheric pressure. Notably, Figure 86 shows that the peak force and maximum indentation are not dependent solely on the energy of the impact. Test 3 featured the highest closing speed to-date (17.8 mph) and the highest impact force in a non-puncture outcome. However, Test 5 experienced the largest indentation of all the tests. The DOT112 tank car in Test 5 experienced a lower peak force than the DOT105 tank car in Test 1, despite Test 5 having a higher closing speed. These results underscore the importance of the differences between the tank car conditions during an impact test, including initial pressure, outage, and tank thickness. As all tests shown in Figure 86 resulted in a non-puncture outcome, the force level is not limited in any case based on failure of the tank car.

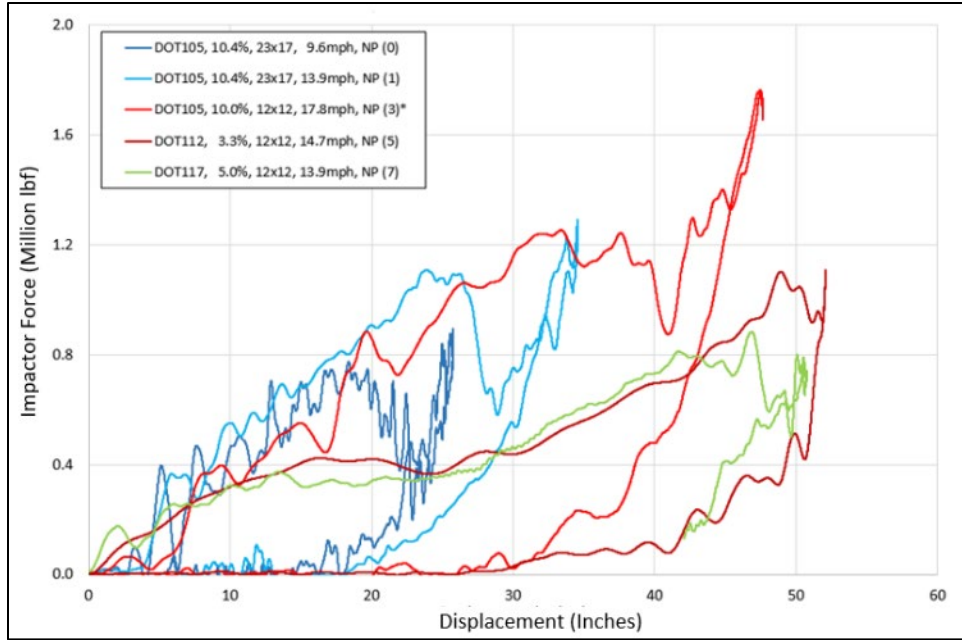


Figure 87. Force vs. Displacement – Non-puncture Tests Only

Figure 88 contains a plot of the impactor force versus impactor speed for the non-puncture tests. Note that in this figure neither the force nor the speed has been normalized. As all the tests in Figure 87 resulted in a non-puncture outcome, the impactor speed always slowed to zero and became negative as the impactor rebounded from the tank car.

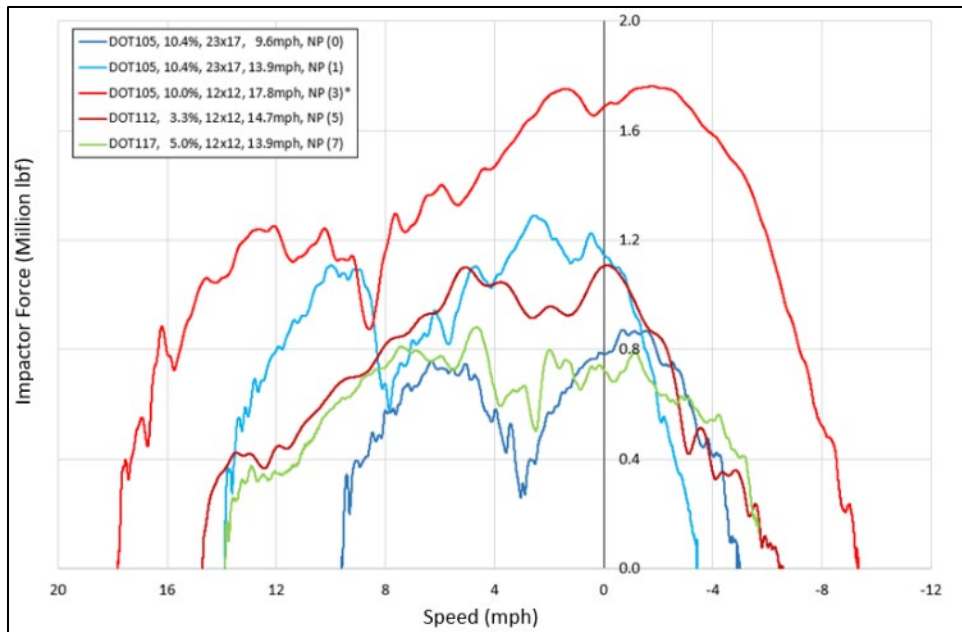


Figure 88. Force vs. Impactor Speed – Non-puncture Tests Only

Of particular interest in Figure 87 is the speed at which the final peak in force occurred. In several of the tests, a substantial peak force was measured while the impactor had a negative speed, meaning that the impactor was already rebounding. This indicates that while the impactor has successfully been brought to a stop, the impact event of interest may not have yet concluded.

Note that when the impactor car's speed is positive, the impactor car experiences deceleration (i.e., an acceleration pointed away from the rigid wall). After the impactor car has been brought to a stop, the impactor car experiences an acceleration from the tank car's attempt to recover energy (i.e., an acceleration pointed away from the rigid wall). Thus, the impactor force shown in figures throughout this report will have the same direction whether the impactor car is slowing down and moving toward the wall or speeding up and moving away from the wall.

The struck tank car will return some of the impact's energy to the impactor car in several ways. The tank car's steel will elastically recover some energy, pushing back directly on the impactor car. Elastic recovery against the rigid wall will also serve to propel the tank car away from the wall, which may result in the tank car pushing against the slow-moving impactor if the impactor has not moved far enough out of the way. Additionally, in all tests the outage's pressure increased during the impact because the tank car's volume decreased from the impact. Since these are non-puncture outcomes, that pressure was not relieved by puncturing the tank. Once the impactor's forward motion has stopped, the pressurized outage can begin to push back against the tank car's walls to return to the initial pressure. At the same time, the liquid phase of the lading may surge back toward the impactor, having pushed toward the wall during the impact. All these efforts by the tank car to deform or deflect can push against the impactor, which are measured as an acceleration.

For the three DOT105 tank car tests that resulted in a non-puncture outcome, [Figure 89](#) shows the similarities in the SNF and normalized speed. Additionally, this figure illustrates that the DOT112 and DOT117 tank cars, which were tested under unpressurized initial conditions, exhibited similar responses to one another. Further, the characteristic differences between tank cars initially at 100 psig (DOT105) and atmospheric pressure (DOT112 and DOT117) impact responses can be seen.

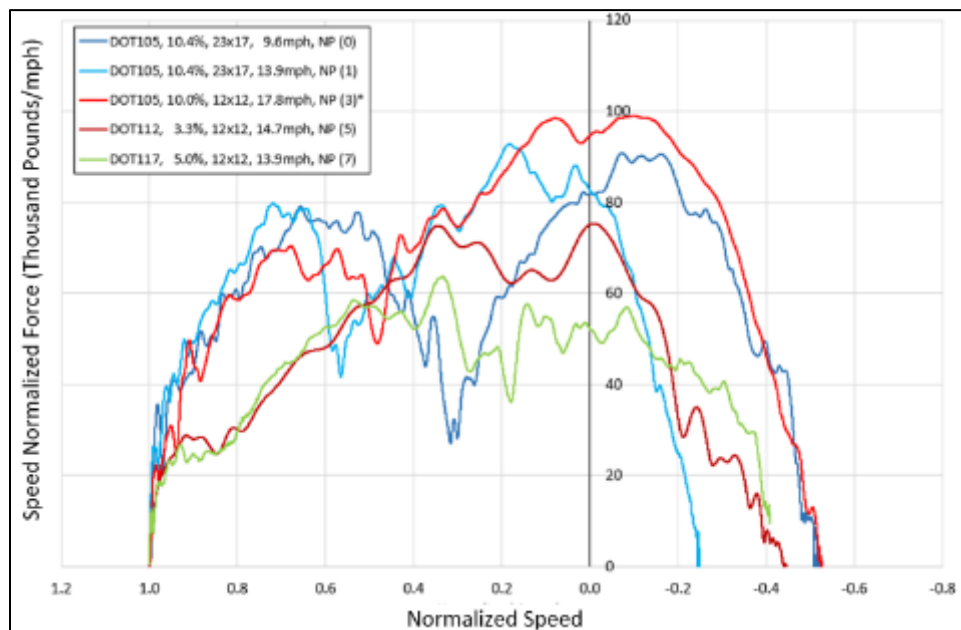
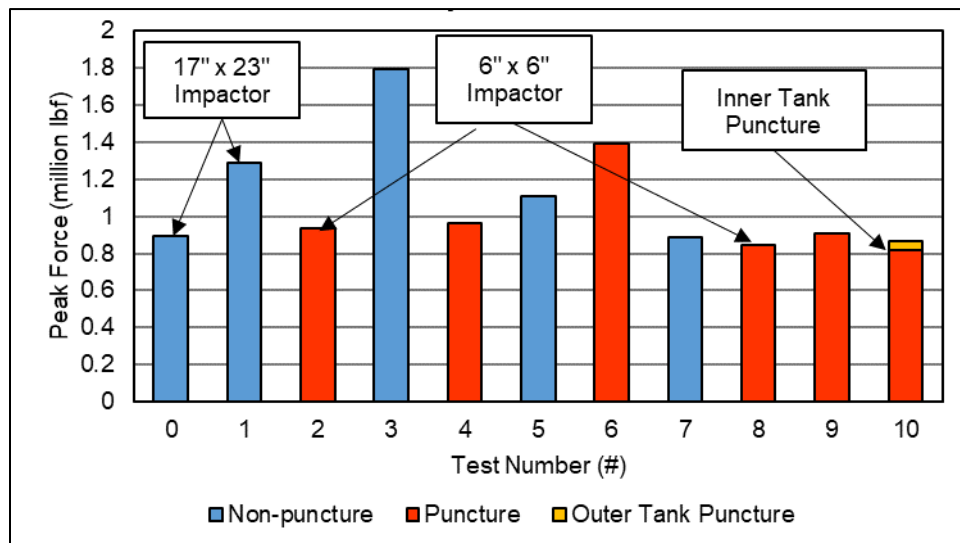


Figure 89. Normalized Force vs. Normalized Speed – Non-Puncture Tests Only

14.5 Comparison at Peak Force

This section compares all the tests using measured and calculated values at the time or displacement corresponding to peak force. The values of interest are relative displacement of the impactor and absorbed energy. The goal of comparing the values at peak force is to approximate the point in time corresponding to the point of puncture for puncture tests and maximum indentation for non-puncture tests. Finding the maximum of the force-time history is a straightforward and repeatable calculation across multiple tests. The only test that needed a slight modification of the procedure was the DOT113 tank car test (Test 10) which had two force peaks corresponding to puncture of the outer and inner tank (refer to [Figure 81](#)).

[Figure 90](#) shows peak force for each test with annotations for the impactor size and the inner tank puncture in Test 10. The tests that produced a non-puncture response are indicated with blue bars and the tests that punctured the commodity tank are indicated with red bars. Two peaks are shown for Test 10 for outer tank puncture (orange) and inner tank puncture (red). Another comparison is the relative difference in peak force between Tests 6 and 8, which were tests of similar DOT105 tank cars but with different impactor sizes and impact speeds. Recall that in both tests, the impact speed was only slightly above the minimum speed necessary to cause puncture.



**Figure 90. Summary of Peak Forces Across Tests
(12-inch by 12-inch impactor was used unless noted otherwise)**

[Figure 91](#) shows impactor displacement at peak force for each test. Two peaks are shown for Test 10 for outer tank puncture (orange) and inner tank puncture (red). Test 9 experienced the highest magnitude of displacement, but it should be noted that leakage of water through the manway cover was observed before puncture.

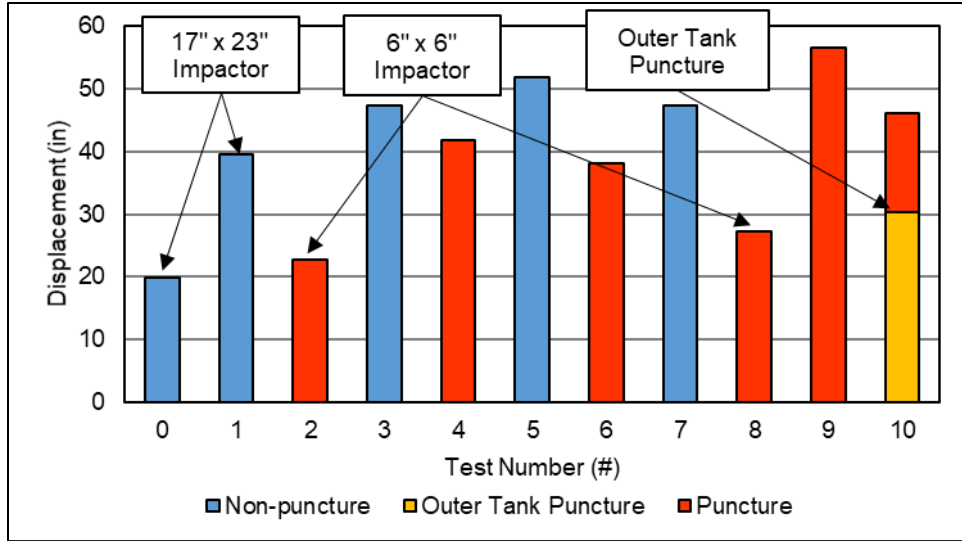


Figure 91. Summary of Displacements at Peak Forces Across Tests (12-inch by 12-inch impactor was used unless noted otherwise)

To make a more direct comparison of impactor displacement across tank cars with different diameters, the impactor displacement was divided by the initial diameter of the tank to calculate the reduction in diameter percentage, as depicted in Figure 92. In the case of the DOT113 tank car, the impactor displacement at the first peak force (i.e., outer tank puncture) was divided by the initial diameter of the outer tank, and the displacement at the second peak force (i.e., inner tank puncture) was divided by the initial diameter of the inner tank.

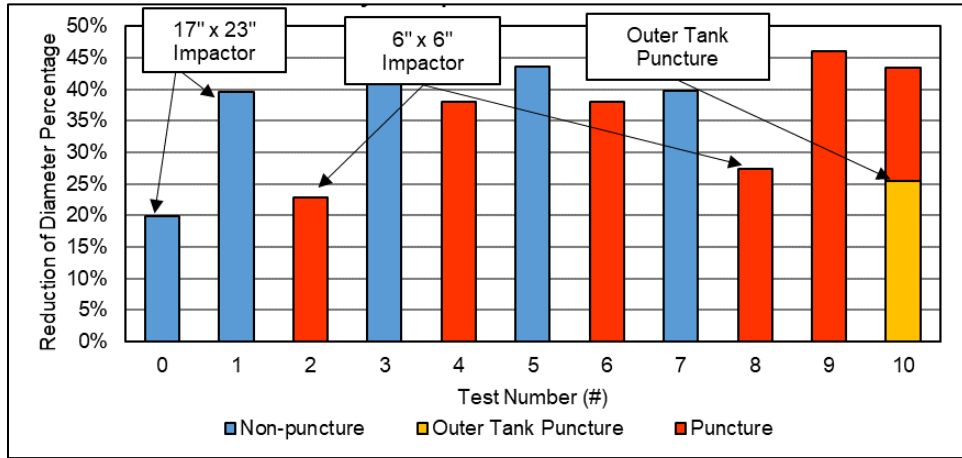


Figure 92. Summary of Reduction of Diameter Percentages at Peak Forces Across Tests (12-inch by 12-inch impactor was used unless noted otherwise)

Figure 93 shows absorbed energies at peak force for each test. Two peaks are shown for Test 10 (DOT113) for outer tank puncture (orange) and inner tank puncture (red). Test 3 (i.e., DOT105 equipped with a sandwich panel) had the highest energy absorption (non-puncture) and Test 6 (DOT105) achieved the next highest energy absorption (puncture). Note that Tests 0 and 1 may not have been close to the full energy absorption capacity of the DOT105 tank cars with a 17-inch by 23-inch impactor since caution was exercised with impact speed, as those were the first two tests in this series.

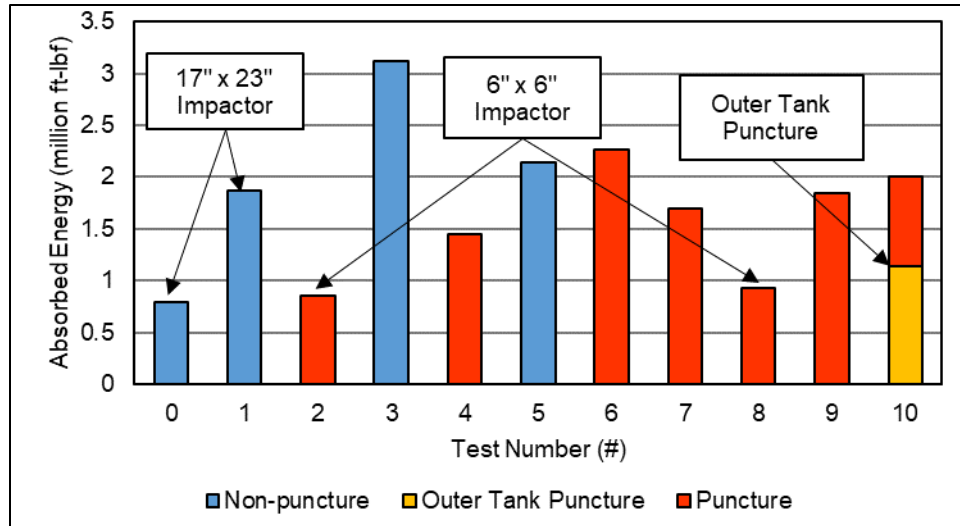


Figure 93. Summary of Absorbed Energies at Peak Forces Across Tests (12-inch by 12-inch impactor was used unless noted otherwise)

Figure 94 shows absorbed energy at peak force versus total tank thickness. Total tank thickness generally refers to the thickness of the commodity tank (not jacket) for Tests 0 through 9; for Test 10 (annotated), the thicknesses of the inner (commodity) tank and outer tank are added to calculate the total tank thickness. While other test conditions (e.g., initial pressure, initial outage volume, steel alloy[s] and/or quality used in tank shell, tank diameter) were not controlled while varying thickness, a positive correlation between tank thickness and absorbed energy can still be observed for the 12-inch by 12-inch impactor (blue circles).

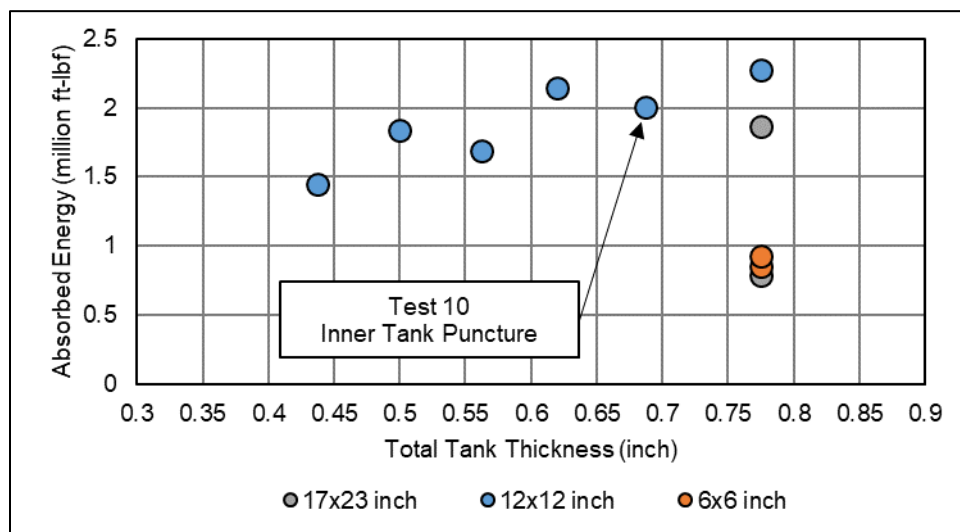


Figure 94. Absorbed Energy at Peak Force vs. Total Tank Thickness

Figure 95 shows absorbed energy at peak force versus initial volume percent outage. It should be noted that the smallest outage volume (corresponding to Test 4) is estimated, because the outage was not accurately measured before the test. A positive correlation between outage and absorbed energy for a given impactor size is expected but not easily observable due to other test variables, such as tank thickness and steel quality.

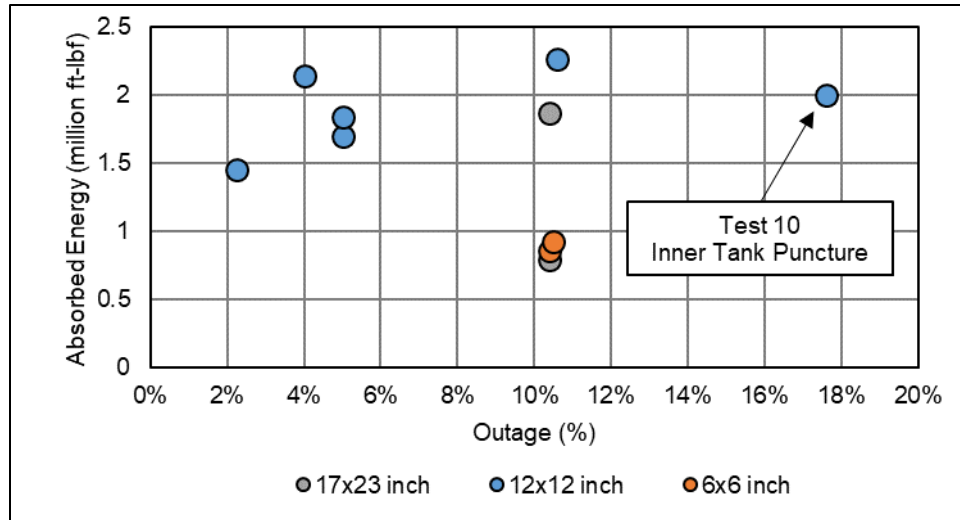


Figure 95. Absorbed Energy vs. Outage

14.5.1 Normalized Force to Puncture

The authors have attempted to account for the effects of the differences in the tank designs and impactor sizes on the peak forces using observations from previous research. Two methodologies were applied to estimate whether the peak force measured during the test was sufficient to puncture the tank based on simplified calculations.

The first methodology used to estimate puncture force normalizes the peak force by the “characteristic size” of the impactor multiplied by the combined thickness of the tank (Kirkpatrick, S. W., 2013). The characteristic size of the impactor in this work is defined as the square root of the area of the impactor face.

The second methodology used to estimate puncture force also considers the combined thickness of the tank but uses the perimeter of the impactor face instead of the square root of the area (Jeong, D. Y., Tang, Y. H., & Perlman, A. B., 2011). This methodology also considers the ultimate strength of the material. Note that these two methodologies were developed before Test 4, the first test to use a tank car other than a DOT105.

Figure 96 shows the comparison of normalized puncture forces using Kirkpatrick (2013)’s methodology. After applying this normalization, a normalized force threshold of 125,000 lbs./in.² was determined to segment the puncture outcomes from non-puncture outcomes. The force threshold was used to normalize the puncture force such that a normalized force greater than one should indicate a puncture result and a normalized force less than one should indicate a non-puncture result. Test 3 has been omitted from these normalizations, because the thickness of the protective panel is difficult to express as a single equivalent thickness.

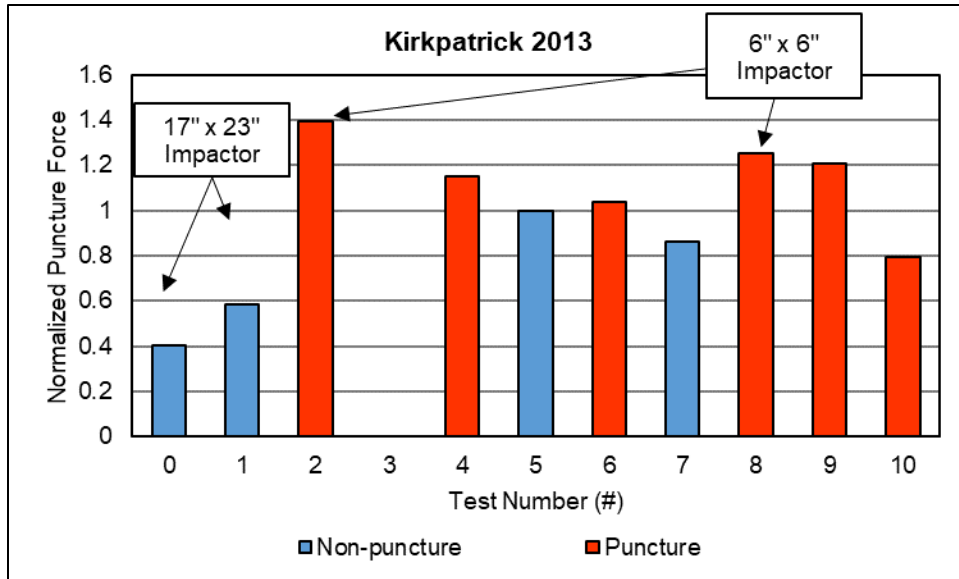


Figure 96. Normalized Force to Puncture Using Kirkpatrick’s Methodology

Using Jeong’s methodology, the peak forces across tests were normalized such that a normalized force greater than one should indicate a puncture result, and a normalized puncture force less than one should indicate a non-puncture result. Figure 97 shows the normalized forces using Jeong’s methodology. Test 3 has been omitted from these normalizations, because the thickness of the protective panel is difficult to express as a single equivalent thickness.

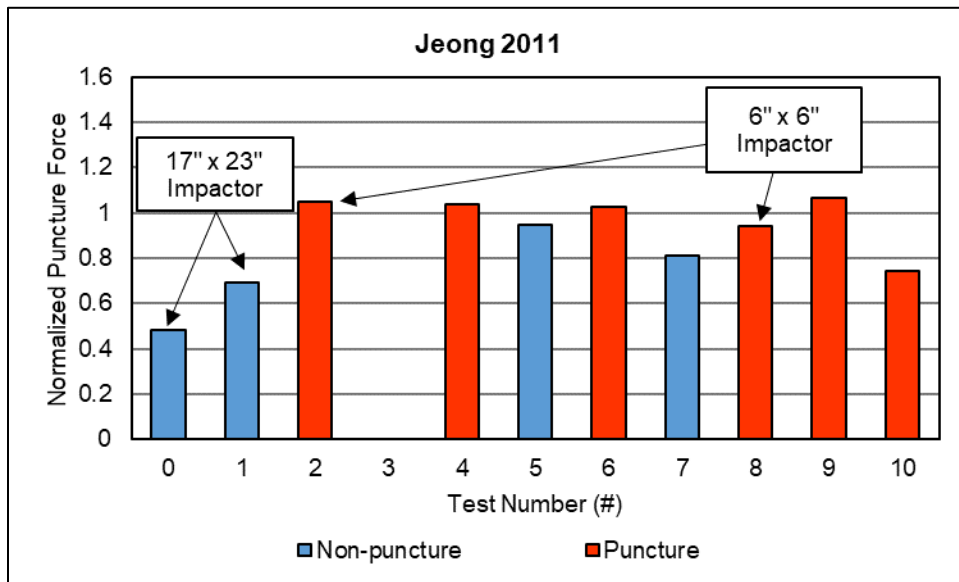


Figure 97. Normalized Force to Puncture Using Jeong’s Methodology

Both methodologies successfully segmented puncture results from non-puncture results, which indicates that there is a relationship between peak force and puncture. However, it should be noted that these methodologies cannot be used to predict a puncture versus a non-puncture result before a test.

The one significant outlier using both methodologies was Test 10 with a DOT113 tank car. However, the tank structure and insulation for Test 10 were significantly different from the other tests, and the punctures of the inner and outer tanks were more independent events rather than a puncture of the combined tank walls working as a unit. A simplified methodology capable of predicting puncture for unpressurized, pressurized, and cryogenic tank cars will require additional parameters beyond those included in the two methodologies applied here.

14.6 Discussion of Results Only Obtainable from FE Results

As discussed throughout this report, full-scale shell impact tests typically include measurements of impact speed, acceleration, pressure, and displacement. Additional results, including impactor force and impactor displacement, use the acceleration measurements to calculate these results. For an FE analysis of the same test, there are several other variables of interest that can be easily calculated, which may be impractical or impossible to measure during a test. For example, the reaction force acting on the rigid impact wall behind the tank car can be easily calculated in an FE analysis while it might be difficult to measure during testing. Similarly, total energy calculations can be performed using analysis which may not be readily available or easily calculated using test measurements.

14.6.1 Reaction Wall Loads

One quantity that can be readily obtained from the FE model but not easily measured in a test is the reaction force acting on the wall behind the tank car. Additional insights into the behavior of the tank car under the standardized impact scenario can be made by reviewing the impactor force and the reaction wall force for a given test, plotted on a common time scale. [Figure 98](#) shows an example of the force-time histories of the impactor and of the reaction wall from Test 8.

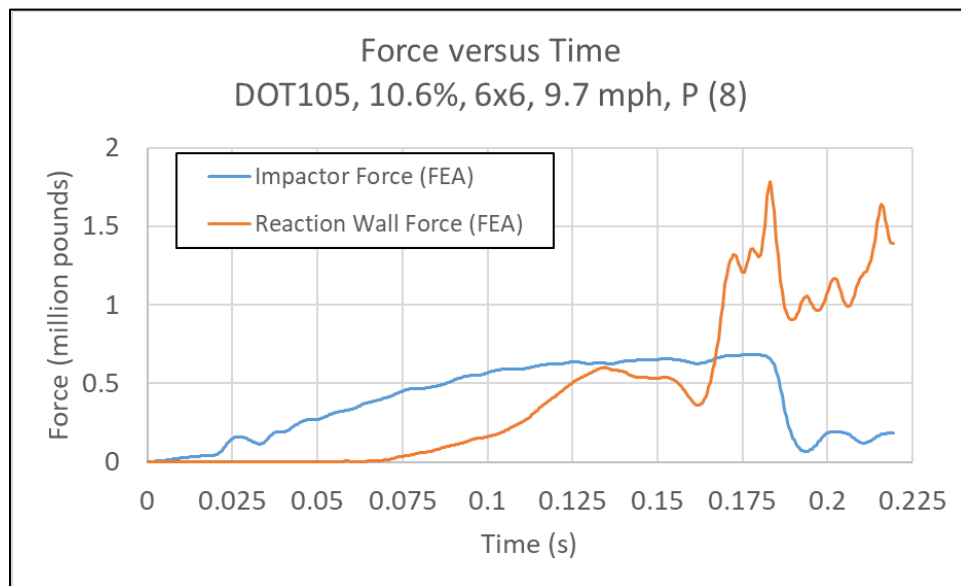


Figure 98. Impactor and Wall Forces vs. Time, Test 8 FEA

[Figure 98](#) shows that while the impactor force begins to rise almost immediately following contact between the impactor and the tank car, the wall reaction force lags behind the impactor force. While a quasi-static load application from the impactor through the tank car and into the wall may be expected to show an equal applied (impactor) and reaction (wall) force, the tank car

impact scenario is clearly dynamic. This apparent lag in reaction wall force may be attributed to the tank car's own inertia and the effects of friction between its skids and the ground. While the impactor is deforming the tank car from the point of first contact, the tank car does not immediately transfer an appreciable amount of that force into the rigid wall behind it.

The impact force leveled off at approximately 600,000 pounds, and the reaction wall force leveled off at approximately 1,000,000 pounds. While the impact force stays near constant, however, the wall reaction force continued to climb. The wall reaction force peaks at a higher force than the impactor force. While the tank car only sees a dynamic load from the approximately 297,000-pound impactor, the wall is seeing a dynamic load from the impactor and from the moving tank car with its considerable fluid mass. This may explain why the reaction force at the wall is substantially higher than the reaction force at the impactor.

Figure 99 shows a second example from a test using an unpressurized tank car with the force versus time responses from the impactor and the wall from the post-test FE model. Note that due to leakage from the top fittings during the test, the post-test FE model was run fully sealed and fully opened, and these outage conditions are represented in Figure 98.

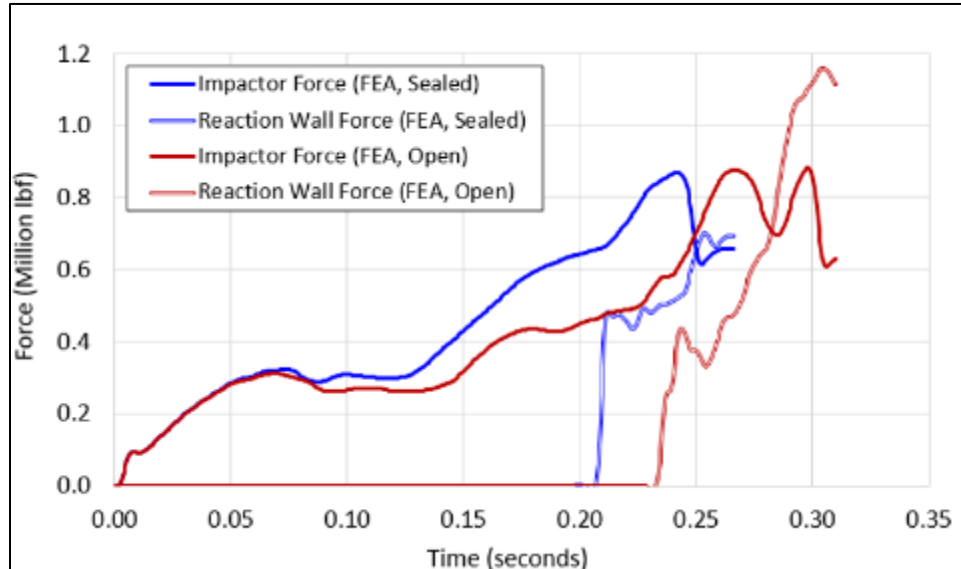


Figure 99. Impactor and Wall Forces vs. Time, Test 9 FEA

The results from Test 9's FE models exhibit some similarities and some differences from the Test 6 FE model results. In terms of similarities, Test 6 and Test 9's models show a clear delay between the rise in force on the impactor and the rise in force on the rigid wall. The delay is more pronounced in Test 9's FE model, with a longer delay and a more sudden increase in force once the tank car makes contact with the wall. Test 9's FE results also indicate that the softer, open tank car experiences a longer delay in an appreciable wall force developing than the stiffer, perfectly sealed tank car. This is consistent with the results seen from Test 6, in which an initially pressurized tank car sees an earlier and more gradual increase in force on its backing wall.

Examination of the FE model results showed that part of the reason for this delay in wall force is caused by the ovalization of the tank car during the impact. The tank car starts off initially in contact with the wall at its 3 o'clock position. The impactor contacts the tank at its 9 o'clock

position and begins to indent the tank car. This indentation causes the 12 o'clock position of the tank car to move vertically upward and the 6 o'clock position of the tank car to move downward. However, the ovalization also causes the 3 o'clock position to pull inward because of the vertical ovalization, temporarily creating a gap between the 3 o'clock position of the tank and the wall. As the impactor continues to travel forward, the tank car is simultaneously deforming and displacing as a rigid body to close the gap between the tank car and the wall.

In contrast, the peak wall force calculated in the Test 6 FE model was larger than the peak force measured on the impactor. In the Test 9 FE models, the perfectly sealed model was punctured by the impactor before the wall reaction force could exceed the impactor force. In the softer, open Test 9 model, the peak wall force exceeds the impactor force before puncture of the tank car.

14.6.2 Energy Balances

Another type of result that is easily obtained from the FE models is the energy balance during the impact. During the impact test, initially the moving impactor car contains kinetic energy which is readily calculated in the test and in the model. The standing tank car should not have any initial kinetic energy right before impact, but it will have some stored strain energy from supporting its own weight and the weight of the lading. Additionally, if the outage has been pressurized at the start of the test, the tank car also possesses stored energy in the compressed gas, plus the additional strain energy in the tank shell associated with containing the pressurized gas.

As the impact unfolds, energy is redistributed between the impactor car, the tank car, and the test setup (i.e., the reaction wall and ground). The impactor car's kinetic energy decreases as the impactor car slows down. The impactor car slows down because the tank car is offering resistance to the impactor car's continued motion. The tank car experiences displacement and deformation because of the impact. The entire tank car moves on its skids while simultaneously experiencing elastic and plastic strains. This motion is impeded by static and kinetic friction between the skids and the ground, as well as by contact forces between the tank car and the impact wall. The liquid phase of the lading accelerates from rest and can continue to slosh even after the impactor has come to a stop and begun to rebound. Indentation of the tank car will reduce the volume of the tank car, which in turn will increase the pressure of the outage. If the tank car punctures, the pressure in the gas phase will be relieved down to atmospheric pressure. If the tank car does not puncture, the post-test pressure in the outage will be higher than the pre-test pressure as the plastic portion of the tank deformation will not be recovered. Finally, the act of fracturing the jacket and/or tank will itself dissipate some energy.

The balance of energies at each point in time during an impact event is a straightforward output to request from an FE model. The energy totals can be reported for the entire model, or they could be broken down by component if desired. The various energy totals are defined in the Abaqus documentation found in Dassault Systèmes Simulia Corp. (2017) and are summarized in [Table 31](#). Note that several available energy outputs are listed in this table that are not typically requested for tank car FE simulations, but they are included for completeness.

Table 31. Description of Energy Totals from FE Models

Energy Quantity	Description from Abaqus Documentation (Dassault Systèmes Simulia Corp., 2017)
ALLAE	“Artificial” strain energy associated with constraints used to remove singular modes (e.g., hourglass control) and with constraints used to make the drill rotation follow the in-plane rotation of the shell elements
ALLCD*	Energy dissipated by viscoelasticity
ALLFD	Total energy dissipated through frictional effects (i.e., available only for the whole model)
ALLIE	Total strain energy (ALLIE=ALLSE + ALLPD + ALLCD + ALLAE + ALLDMD+ ALLDC+ ALLFC)
ALLKE	Kinetic energy
ALLPD	Energy dissipated by rate-independent and rate-dependent plastic deformation
ALLSE	Recoverable strain energy
ALLVD	Energy dissipated by viscous effects
ALLWK	External work (available only for the whole model)
ALLIHE*	Internal heat energy
ALLHF*	External heat energy through external fluxes
ALLDMD	Energy dissipated by damage
ALLDC	Energy dissipated by distortion control
ALLFC*	Fluid cavity energy, defined as the negative of the work done by all fluid cavities (i.e., available only for the whole model)
ALLPW*	Work done by contact penalties, including general contact and penalty/kinematic contact pairs (i.e., available only for the whole model)
ALLCW*	Work done by constraint penalties (i.e., available only for the whole model)
ALLMW*	Work done in propelling mass added in mass scaling (available only for the whole model)
ETOTAL	Energy balance defined as: ALLKE + ALLIE + ALLVD + ALLFD + ALLIHE – ALLWK – ALLPW – ALLCW – ALLMW – ALLHF (i.e., available only for the whole model)

*Quantity not typically requested for tank car FE models.

Figure 100 shows an example of the energy balance from the Test 5 FE model. The energy totals shown in Figure 99 are the total magnitudes of each energy in the whole model and are not broken down by individual components. As this test did not result in a puncture, the energy balance does not include any contributions from simulating puncture and element failure.

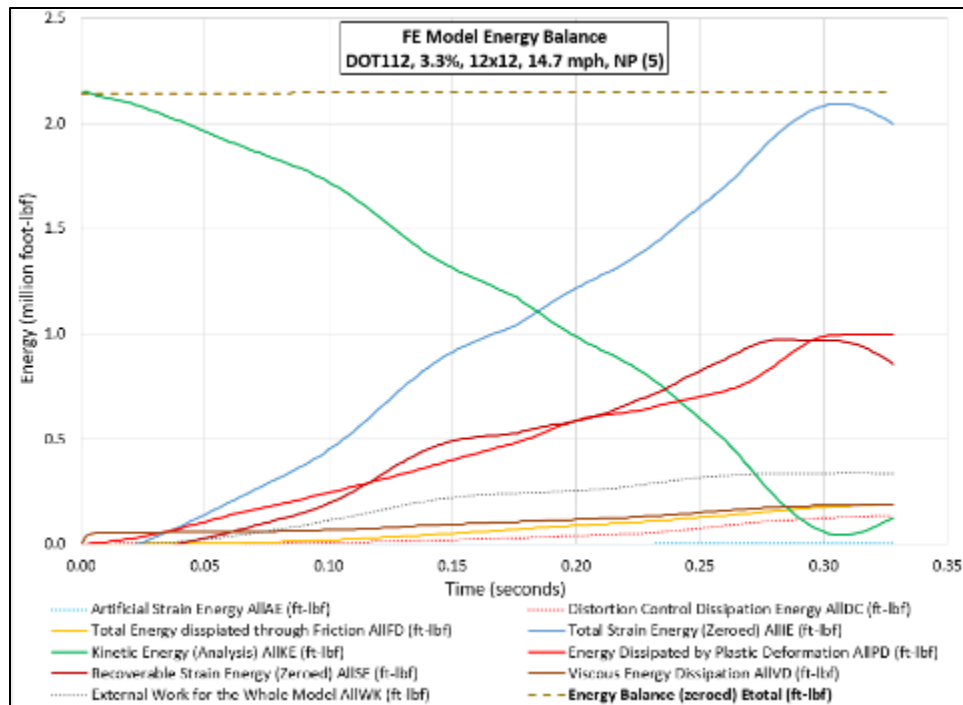


Figure 100. Energy vs. Time from Test 5 FE Model

Some quantities (e.g., artificial strain energy and distortion control energy) are unique to the FE model and have no “real-world” analogue. The initial value of internal energy has been set to zero as the model contains air at atmospheric pressure and the initial energy is nonzero. Figure 99 shows most of the initial kinetic energy is transferred into elastic and plastic strain energies. Note that for the Abaqus energy balance shown above, the P-V work from the compression of the air inside the tank is included in the recoverable strain energy (ALLSE). The elastic energy in the tank and jacket is a small fraction of this recoverable strain energy. The recoverable and plastic deformation energies of the DOT112 FE model each account for similar quantities of strain energy. Note that the recoverable energy decreases after reaching a global maximum value, indicating the stored P-V and elastic energy is being recovered as the impactor begins to rebound. The plastic energy reaches a plateau, as this energy is unrecoverable even as the external load (i.e., the impactor) is removed.

As the kinetic energy reported below is for the full model and not just the impactor, the kinetic energy does not reach zero in spite of the impactor car stopping during the analysis. The minimum value of kinetic energy is an indicator of the kinetic energy of the tank car and its lading at the point of the impactor car’s maximum travel.

The contributions of viscous dissipation through water motion and frictional losses are small compared to the elastic and plastic strain energies. Note that from Section 8.2 that this FE model used an SPH technique to model the air inside the outage and a Lagrangian technique to model the water in the tank. As modeling a gas explicitly (i.e., as opposed to using a cavity) requires definition of pressures in absolute terms, the DOT112 FE model also included a 1 atmosphere external pressure acting on the outside surfaces of the tank. This external force is the source of the external work energy, as the external air pressure remained constant even as the tank deformed during the analysis.

Strain energy accounts for the largest portion of energy compared with viscous and frictional energy. Although the lading and friction at the skids plays an important role in the tank car's behavior during side impact, the deformable tank and jacket have the greatest importance when considering energy absorption and dissipation. Thus, strengthening or thickening the tank and jacket will increase the energy absorption capabilities of the tank car and result in improved performance when involved in a side impact. This observation further underscores the importance of mechanical and thickness testing on the material(s) of construction of the tank to developing a credible FE model of the tank car.

15. Conclusion

The tank car shell impact testing and modeling program initially began to study and improve the crashworthiness of tank cars transporting TIH material in potential future derailments. Building on the knowledge gained from the study of such tank cars, the program extended to the study of the impact responses of tank cars transporting flammable liquids and cryogenic liquids. The testing and modeling approaches were improved and refined with each successive test. The improved modeling techniques provided a foundation for future tests and FE analyses. The standardized test approach facilitated capturing the critical responses of a tank car during impact and this impact event could then be accurately modeled.

The standardized impact scenario has remained fairly fixed, with the tank car placed against a rigid barrier in all tests. Note that some preliminary head impact tests were performed in the NGRTC program and are described in Kirkpatrick (2010)'s final report. Similarly, analyses of other impact conditions such as the effects of an angled or oblique impact or a tank without the rigid wall constraint were performed and documented as part of the ATCCRP program (Kirkpatrick, S. W., 2013).

To have a successful and repeatable impact test, it was found that the trucks needed to be replaced with skids to limit the body roll on the freight trucks. Additionally, the impactor needed to be aligned with the CG of the tank car to minimize the roll of the tank car during impact. Using a fill-empty approach to loading the tank car has been found to provide an accurate calculation of outage.

The instrumentation layouts used in typical tests have also changed somewhat, but they have become fairly standardized in recent tests. While strain gauges were investigated in early tests, they have largely been abandoned in more recent tests. The use of accelerometers and a laser-based speed trap has been satisfactory to allow for calculation of impactor car force and displacement histories throughout all the tests. In the most recent test, laser-based displacement transducers on the front of the impactor car have also had some success, more notably in providing a redundant measurement of the displacement-time history independent of the accelerometers on the impactor car. Internal pressure transducers and internal and external string potentiometers have also been successful, though these instruments have been the most common to experience a problem during a test (e.g., string potentiometer reaching its travel limit, spurious pressure readings associated with tank motion, etc.). One way of adapting to this has been to include more redundant pressure and displacement transducers on the tank car to increase the success of obtaining meaningful data.

Advances in camera technology and accessibility of LiDAR-based measurement systems have also enhanced the data collected during more recent tests. A camera has been successfully mounted on the impactor car providing an up-close view of the impact zone for several tests, which allowed the puncture of the Test 9 tank car to be directly observed for the first time. LiDAR maps of the tank car made pre- and post-test are useful for quantifying the indentation of the tank car and also for making a comparison to the deformed shape of each test's FE model.

To obtain a representative pre-test FE model and have a reasonably accurate prediction of the puncture threshold, it is necessary to have exact values for material properties and thickness of the tank car's shell to obtain the best correlation between test and FEA results. Material properties obtained from general material specifications were often not representative of a

specific tank car's material properties. Material properties obtained from material testing of coupons cut from the actual tank car are required to have the best chance of more closely predicting the threshold speed and impact response with an FEA model. This testing program has also led to improved understanding of the role of tank shell material properties on the overall impact response and the shell's puncture. Material samples were not always removed from the tested car as a matter of course. However, the variability in TC128 steel behaviors measured across the tank cars from which samples were removed and tested has led to material characterization becoming a standard part of the test plan since Test 6. The results of material characterization tests performed during the impact testing program have also led to further research into the effects of tank car fabrication processes on "as-built" material properties and into the suitability of different tensile coupon geometries for developing puncture-capable FE material models. While all geometries are suitable for determining the mechanical properties of the materials, cylindrical coupons are the best suited for calibrating a material model for use in puncture (B-W) simulations.

In Test 9, the test outcome was as expected, and results were not affected by the presence of a field-repaired area, which opens a possibility of getting material samples before testing far away from the impact point and using those actual material properties in the pre-test FE models. Further, the analysis will be able to use actual thickness measured compared to nominal thickness given in the drawings. This will help the pre-test FEA to predict the impact speed more accurately.

The role and representation of the two-phase lading was another important consideration. Various approaches to modeling liquid and pressurized gases were investigated during this testing program. Some techniques, such as Lagrangian meshing of fluid with an EOS material model, were found to be generally applicable over a wide range of outage volumes and pressures. Other techniques, such as the hydraulic cavity approach, offered a reduction in solution time but were only used successfully in models of tank cars initially having a larger outage (>10 percent) at an initially elevated (>50 psig) pressure. The accurate modeling of the air phase did not prove to be as sensitive as the water phase, and the pneumatic cavity approach was a reasonable representation of the air cavity in initially pressurized and in initially unpressurized conditions.

This testing program has shown that different types of insulation and thermal protection can have different effects on the structural response of the impacted tank car in the standardized impact scenario. Some types of insulation have been able to be neglected in FE models without affecting the level of agreement seen between test measurements and model calculations. Other types of insulation needed to be represented in the FE models to attain better agreement between the test and the model results. While structural behavior may not typically be a consideration in selecting a thermal protection or insulation material, this choice has been shown to affect the structural response of the tank car to an impact. This may lead to future investigations of whether there are materials or technologies that would offer benefits to the thermal performance of tank cars (e.g., insulation of lading, shielding of tank car from external fire effects) and to the structural impact response (e.g., energy-absorption, impactor blunting).

Comparisons across the different tests showed that no matter the outcome, the initial force-displacement responses of tank cars of the same specification were similar. Additionally, the lading of the tank car (e.g., clay slurry or water) did not appear to influence the tank car's initial force-displacement responses, since these were similar for all DOT105 tank cars. The likelihood

of puncture was strongly related to the size of the impactor that was used, the impactor car speed, the outage (i.e., pressure and volume), and the tank car construction (e.g., shell thickness, specification, and quality of shell material, etc.). While full-scale impact testing of future substantially different tank cars is recommended, multiple tests of similar impact conditions may not be necessary if the FE models can continue to evolve to address new impact conditions.

One of the trends is the need for testing to continually improve the modeling techniques. Of the 11 tests discussed in this report, Tests 2, 4, and 10 each exhibited a puncture outcome with a significant residual kinetic energy in the impactor car. This outcome is undesirable, as it makes determining the “true” amount of energy that would have been necessary to puncture the tank car difficult. Each of these tests was the first puncture test of a different specification tank car: Test 2 was the first puncture test of a DOT105, Test 4 was the first puncture test of an unpressurized tank car (DOT111), and Test 10 was the first puncture test of a DOT113 tank car. While modeling techniques have undoubtedly improved with the lessons learned from each test, there are obviously still new lessons to learn each time a substantially different tank car or set of test conditions are tested.

Two conclusions can be drawn from these observations. First, while the abilities to model tank car impact responses and puncture have improved through knowledge gained in each test, a substantially different test condition (e.g., new tank car material, design type, insulation type, lading condition, etc.) still presents a challenge to a predictive model. Second, while modeling can be used to support future test developments, the role of testing is still important to confirm or correct a model. The modeling supports testing and can extrapolate beyond the tested conditions within limits, but modeling is not yet a substitute for full-scale testing for sufficiently different impact conditions.

Note that throughout this program, the modeling improved quickly following a first test under substantially different conditions. The data collected from a first overspeed puncture test of a substantially different tank car design appeared to be adequate to improve the models enough that there was not a second overspeed impact of the same impact type. After Test 2, subsequent puncture tests of DOT105 tank cars (Tests 6 and 8) resulted in punctures with a small residual energy. After Test 4, Tests 5, and 7 resulted in non-puncture outcomes to tank cars under substantially similar impact conditions, and Test 9 resulted in a puncture with a small residual energy.

16. References

- Association of American Railroads. (2000). *AAR Manual of Standards and Recommended Practices, Section C-Part III, Specifications for Tank Cars, Specification M-1002*. M-1002, Washington, DC: Association of American Railroads.
- Carolan, M. E., Jeong, D. Y., Perlman, B., murty, Y. V., Namboodri, S., Kurtz, B., Elzey, R. K., Anankitpaiboon, S., Tunna, L., & Fries, R. (2013). [*Application of Welded Steel Sandwich Panels for Tank Car Shell Impact Protection*](#). Technical Report No. DOT/FRA/ORD-13/19, Washington, DC: U.S. Department of Transportation, Federal Railroad Administration.
- Carolan, M., & Rakoczy, P. (2019). [*Side Impact Test and Analyses of a DOT-105 Tank Car*](#). Technical Report No. DOT/FRA/ORD-19/12, Washington, DC: U.S. Department of Transportation, Federal Railroad Administration.
- Dassault Systèmes Simulia Corp. (2017). Abaqus 2017. Providence, RI.
- Eshraghi, S. (2020). [*Quick Calibration of Fracture Behaviors in TC128 Steel for Finite Element Modeling*](#). Technical Report No. DOT/FRA/ORD-20/46, Washington, DC: U.S. Department of Transportation, Federal Railroad Administration.
- Eshraghi, S., Trevithick, S., Carolan, M., Rakoczy, P., & Wilson, N. (2020). [*Side Impact Test and Analyses of a DOT-111 \(CPC-1232\) Tank Car*](#). Technical Report No. DOT/FRA/ORD/20-43, Washington, DC: U.S. Department of Transportation, Federal Railroad Administration. Retrieved from
- Jeong, D. Y., Tang, Y. H., & Perlman, A. B. (2011). [*Semi-Analytical Approach to Estimate Railroad Tank Car Shell Puncture*](#). *Proceedings of the ASME/ASCE/IEEE 2011 Joint Rail Conference* (p. 10). Paper No. JRC2011-56028, Pueblo, CO: Volpe National Transportation Systems Center.
- Kirkpatrick, S. W. (2010). [*Detailed Puncture Analyses of Various Tank Car Designs: Final Report - Revision 1*](#). Mountain View, CA: Applied Research Associates, Inc.
- Kirkpatrick, S. W. (2013). [*Detailed Puncture Analyses of Tank Cars: Analysis of Different Impactor Threats and Impact Conditions*](#). Technical Report No., DOT/FRA/ORD-13/17, Mountain View, CA: Applied Research Associates.
- Kirkpatrick, S. W., Rakoczy, P., MacNeill, R. A., & Anderson, A. (2015, October). [*Side Impact Test and Analyses of a DOT 111 Tank Car*](#). Technical Report No. DOT/FRA/ORD-15/30, Washington, DC: U.S. Department of Transportation, Federal Railroad Administration.
- National Transportation Safety Board. (2004). [*Derailment of Canadian Pacific Railway Freight Train 292-16 and Subsequent Release of Anhydrous Ammonia Near Minot, North Dakota January 18, 2002*](#). Railroad Accident Report No. NTSB/RAR-04/01, Washington, DC: U.S. Department of Transportation.

- National Transportation Safety Board. (2005). [*Collision of Norfolk Southern Freight Trains 192 with Standing Norfolk Southern Local Train P22 with Subsequent Hazardous Materials Release at Graniteville, South Carolina, January 6, 2005*](#). Railroad Accident Report No. NTSB/RAR-05/04, Washington, DC: U.S. Department of Transportation.
- National Transportation Safety Board. (2006). [*Collision of Union Pacific Railroad Train MHOTU-23 with BNSF Railway Company Train MEAP-TUL-126-D With Subsequent Derailment and Hazardous Materials Release, Macdona, Texas, June 28, 2004*](#). Railroad Accident Report No. NTSB/RAR-06/03, Washington, DC: U.S. Department of Transportation.
- Pipeline and Hazardous Materials Safety Administration. (2019, October 24). [*84 FR 56964. Hazardous Materials: Liquefied Natural Gas by Rail \(Notice of Proposed Rulemaking\)*](#). Washington, DC: U.S. Department of Transportation.
- Rakoczy, P., & Carolan, M. (2016). [*Side Impact Test and Analysis of a DOT-112 Tank Car*](#). Technical Report No. DOT/FRA/ORD-16-38, Washington, DC: U.S. Department of Transportation, Federal Railroad Administration.
- Rakoczy, P., Carolan, M., Eshraghi, S., & Gorhum, T. (2019). [*Side Impact Test and Analyses of a DOT-117 Tank Car*](#). Technical Report No. DOT/FRA/ORD-19/13, Washington, DC: U.S. Department of Transportation, Federal Railroad Administration.
- SAE International. (2007). *Instrumentation for Impact Test - Part 1: Electronic Instrumentation: SAE J211/1*. Warrendale, PA: SAE.
- Wilson, N., Carolan, M., Trevithick, S., & Eshragi, S. (2021). [*Side Impact Test and Analyses of a DOT-113 Tank Car with Water*](#). Technical Report No. DOT/FRA/ORD-21/35, Washington, DC: U.S. Department of Transportation, Federal Railroad Administration.
- Wilson, N., Eshraghi, S., Trevithick, S., Carolan, M., & Rakoczy, P. (2020). [*Side Impact Test and Analyses of a DOT-105 Tank Car – 6 X 6 Inch Indenter*](#). Technical Report No. DOT/FRA/ORD-20/38, Washington, DC: U.S. Department of Transportation, Federal Railroad Administration.
- Witte, M., & Anankitpaiboon, S. (2007). *Next Generation Rail Tank Car (NGRTC) Tank Baseline Side Impact Assurance Test Report*. Pueblo, CO: Transportation Technology Center, Inc.

Abbreviations and Acronyms

ACRONYMNS	EXPLANATIONS
ATCCRP	Advanced Tank Car Collaborative Research Program
ASTM	American Society for Testing and Materials (formerly)
ARA	Applied Research Associates, Inc.
ALE	Arbitrary Lagrangian-Eulerian
AAR	Association of American Railroads
B-W	Bao-Wierzbicki
CPC	Casualty Prevention Circular
CG	Center of Gravity
CFC	Channel Frequency Class
DAQ	Data Acquisition System
EOS	Equation-of-State
FRA	Federal Railroad Administration
FEA	Finite Element Analysis
FE	Finite Element
FSI	Fluid-Structure Interaction
HMR	Hazardous Materials Regulations
HAZ	Heat Affected Zone
LiDAR	Light Detection and Ranging
LNG	Liquefied Natural Gas
MTR	Material Test Report
MMC	Modified Mohr-Coulomb
NTSB	National Transportation Safety Board
NGRTC	Next Generation Rail Tank Car
NPRM	Notice of Proposed Rulemaking
PHMSA	Pipeline and Hazardous Materials Safety Administration
PRV	Pressure Relief Valve
P-V	Pressure-Volume

ACRONYMNS	EXPLANATIONS
SPH	Smoothed Particle Hydrodynamics
SAE	Society of Automotive Engineers
SNE	Speed Normalized Energy
SNF	Speed Normalized Force
STD	Start-to-discharge
TIH	Toxic by Inhalation
TTC	Transportation Technology Center (the site)
TTCI	Transportation Technology Center, Inc. (the company)
DOT	United States Department of Transportation
Volpe	Volpe National Transportation Systems Center